CHAPTER IV
RESULTS

1. Preparation of KP crude extract

KP rhizomes and crude extract were shown in Figure 27. Its rhizomes had dark purple color. The 95% ethanolic crude extract was characterized as crystal dark brown color with 5.71% yield. It contained 23.318 mg of PMF, 31.056 mg of TMF, and 21.103 mg of DMF/g of crude extract.

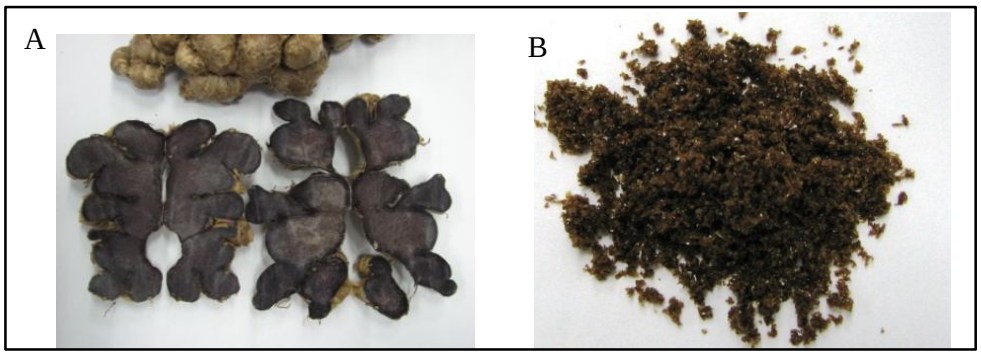

Figure 27 A: KP rhizomes, B: KP crude extract

2. Pharmacokinetics and bioavailability study

2.1 Animals

Male Wistar rats orally or intravenously received a single dose of 250 mg/kg of KP solution did not showed any clinical signs of toxicity.

2.2 Blood extraction

According to the optimization of blood extraction, it was found that acetonitrile with triplicate liquid-liquid extraction was the best method giving the highest %yield at 91.63±0.23%. Therefore, this extraction method was further used for blood extraction.

2.3 Optimization of chromatographic conditions

HPLC systems were successfully developed to analyze the methoxyflavones in KP crude extract with good linearity, precision, and high accuracy. The chromatogram of mixture of three major compounds of KP (PMF,

TMF, and DMF) and KP crude extract were presented in Figure 28 and 29, respectively. The method validation of optimized HPLC systems was shown in Table 7. Intra-day and inter-day precision of methoxyflavones in KP crude extract ranged 0.125-6.296 %RSD and 2.275-14.718% RSD, respectively. LOD and LOQ of the methoxyflavones in KP crude extract ranged from 0.093 to 0.930 µg/ml and 0.186 to 1.860 µg/ml, respectively. The linear regression equations of methoxyflavones, which were constructed by plotting the peak areas versus concentrations, showed good linear relationships as R^2 higher than 0.990. The accuracies of method at two concentrations (1 and 50 µg/ml) were less than 6.5% error.

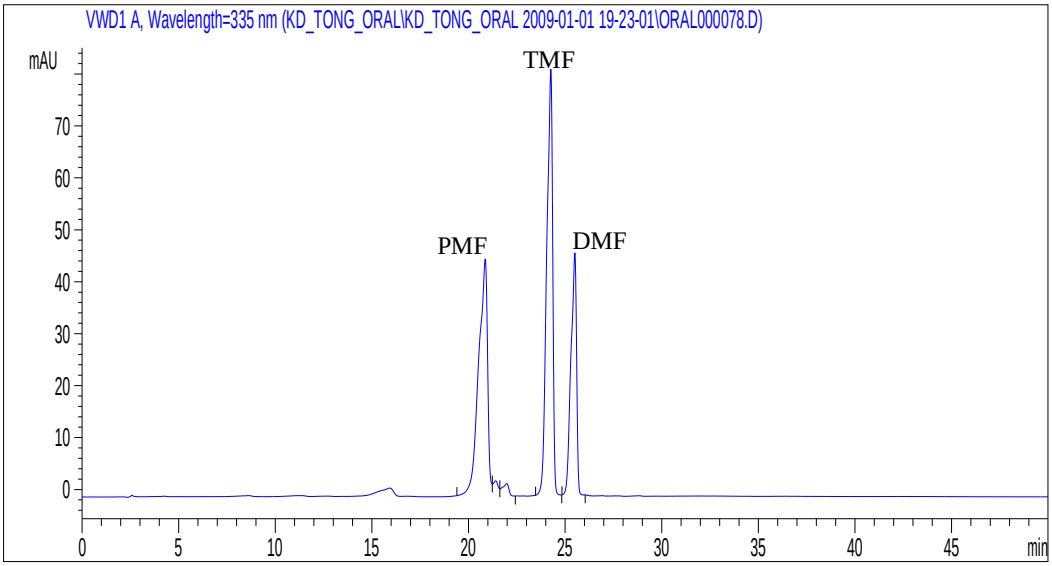

Figure 28 HPLC chromatogram of the mixture of PMF (0.0078 µg/ml), TMF (0.0113 µg/ml), and DMF (0.0094 µg/ml)

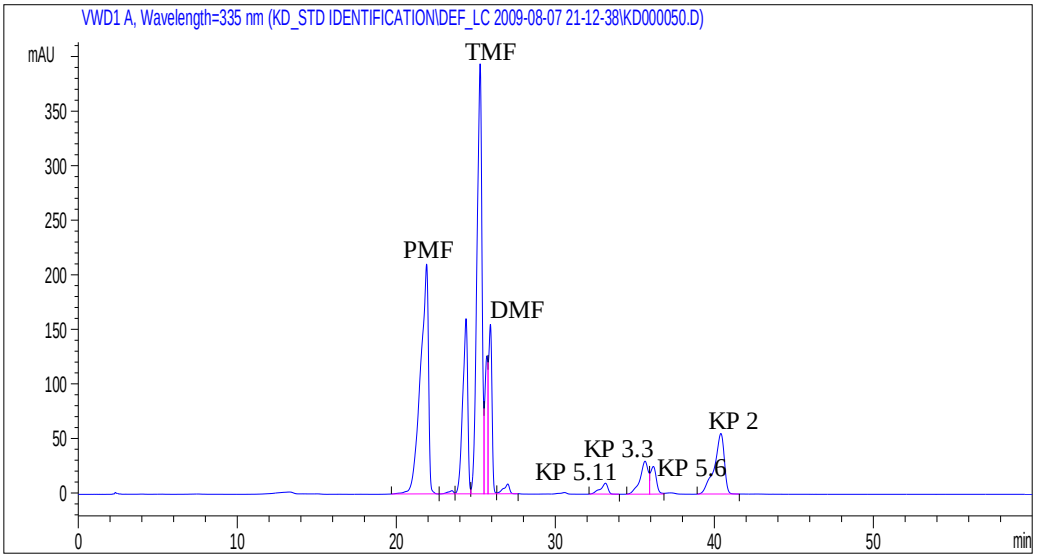

Figure 29 HPLC chromatogram of KP crude extract (0.400 mg/ml, KP5.11: 5-OH-3,7,3',4'-tetramethoxyflavone, KP3.3: 5 -OH-7-methoxyflavone, KP5.6: 5-OH-3,7,4'-trimethoxyflavone, KP2: 5-OH-3,7-dimethoxyflavone)

Table 7 Method validation of HPLC method

Flavonoids	Precision (%RSD)			LOD	LOQ	Linearity	Accuracy (% error)	
	Conc. (µg/ml)	Intra -day	Inter- day	(µg/ml)	(µg/ml)	(R^2)	1 µg/ml	50 µg/ml
5-OH-3,7-dimethoxy flavone	2	3.483	6.964	0.186	0.372	y = 17.757x + 17.541 (R^2 = 0.994)	4.152	2.083
	5	3.129	2.952					
	10	4.946	7.266					
	20	0.385	8.646					
	40	0.125	5.102					
5-OH-7-methoxyflavone	2	0.348	10.154	0.151	0.302	y = 64.818x – 47.936 (R^2 = 0.990)	1.027	3.033
	5	1.405	6.755					
	10	1.129	9.785					
	20	3.552	14.718					
	40	1.001	10.866					
5-OH-3,7,4'-trimethoxy flavone	2	6.296	5.573	0.174	0.349	y = 61.480x + 112.780 (R^2 = 0.990)	1.042	0.462
	5	4.939	4.886					
	10	0.664	7.655					
	20	3.667	9.999					
	40	1.073	6.779					
5-OH-3,7,3',4'-tetramethoxyflavone	5	1.988	4.714	0.186	0.372	y = 17.378x + 27.762 (R^2 = 0.994)	1.679	0.593
	10	1.331	7.414					
	20	0.602	9.598					
	40	0.303	4.523					
3,5,7,4'-tetramethoxyflavone	5	2.124	2.645	0.744	1.488	y = 14.88x– 1.715 (R^2 = 1.000)	1.035	2.138
	10	4.010	9.384					
	20	0.974	7.876					
	40	1.427	2.275					

Table 7 Method validation of HPLC method (Cont.)

Flavonoids	Precision (%RSD)			LOD	LOQ	Linearity	Accuracy (% error)	
	Conc. (μg/ml)	Intra -day	Inter -day	(μg/ml)	(μg/ml)	(R^2)	1 μg/ml	50 μg/ml
DMF	5	1.307	5.512	0.930	1.860	y = 9.027x + 3.646 (R^2 = 0.996)	6.115	0.426
	10	2.050	2.597					
	20	1.230	4.176					
	40	0.530	2.294					
PMF	2	3.849	5.003	0.186	0.372	y = 20.771x + 11.987 (R^2 = 0.993)	3.231	2.164
	5	0.856	3.661					
	10	1.394	6.380					
	20	1.400	7.466					
	40	0.317	3.548					
TMF	2	4.887	5.003	0.093	0.186	y = 74.471x + 56.212 (R^2 = 0.993)	2.802	2.489
	5	1.040	6.381					
	10	0.711	7.313					
	20	0.316	7.727					
	40	0.388	4.067					

2.4 Pharmacokinetic profiles and parameters

Methoxyflavones were found in blood samples. PMF, TMF and DMF, the major compounds in KP crude extract, were found at the high concentration in rat blood receiving 250 mg/kg of KP solution. HPLC chromatograms of blood samples after single orally and intravenously administrations of the extract were shown in Figure 30 and 32. The blood concentrations of PMF, TMF and DMF at several time points for oral and intravenous routes were illustrated in Figure 31 and 33. Pharmacokinetic parameters of two routes which were calculated from Phoenix® WinNonLin® program were presented in Table 8 and 9. The one-compartment oral and intravenous input models were the best fits.

In oral route, PMF, TMF and DMF concentrations were rapidly achieved the maximum concentration (0.55-0.88 μg/ml) within 0.76-1.71 h. After

that, the concentrations slowly dropped below the limit of detection at 24 h post-dosing with Ke of 0.284, 0.145, and 0.127 h^{-1} for PMF, TMF and DMF, respectively. Their half-lifes ($t_{1/2}$, h) were 3.115, 5,043, and 5,846 for PMF, TMF, and DMF, respectively. Cl (ml/h) of PMF was the highest value at 622.848 ± 114.861 ml/h, followed by DMF (367.275 ± 62.166 ml/h) and TMF (337.002 ± 82.353 ml/h). Vd (ml) of PMF, TMF and DMF ranged 2385 – 2951 ml. Bioavailability was calculated based on the AUC from oral and intravenous routes. The results showed that PMF (3.317%) showed the highest bioavailability following by DMF (2.097%) and TMF (1.749%), respectively.

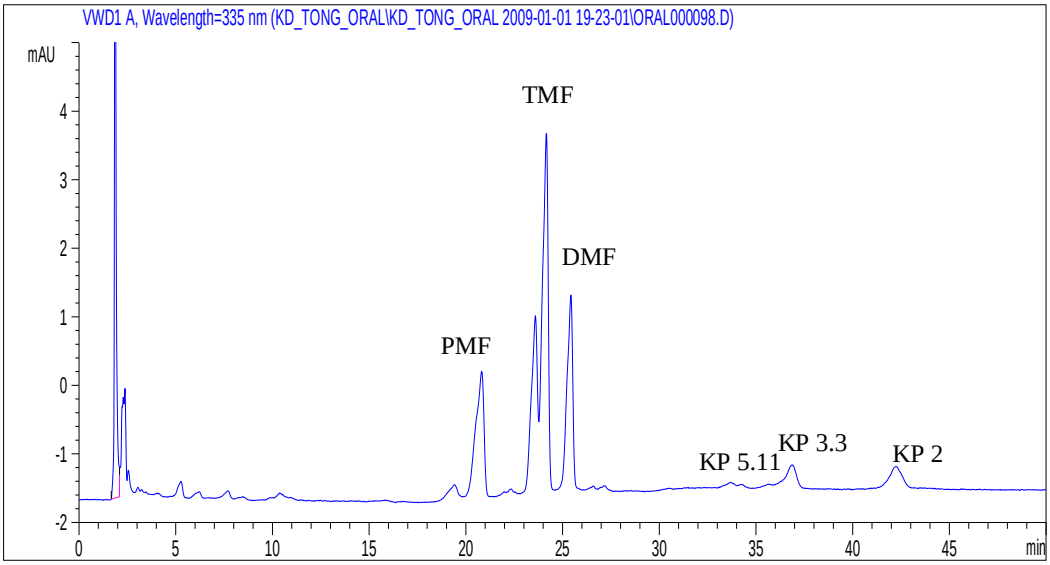

Figure 30 HPLC profile of rat blood after 30 min oral administration of 250 mg/kg KP solution (KP5.11: 5-OH-3,7,3',4'-tetramethoxyflavone, KP3.3: 5-OH-7-methoxyflavone, KP2: 5-OH-3,7-dimethoxyflavone)

.

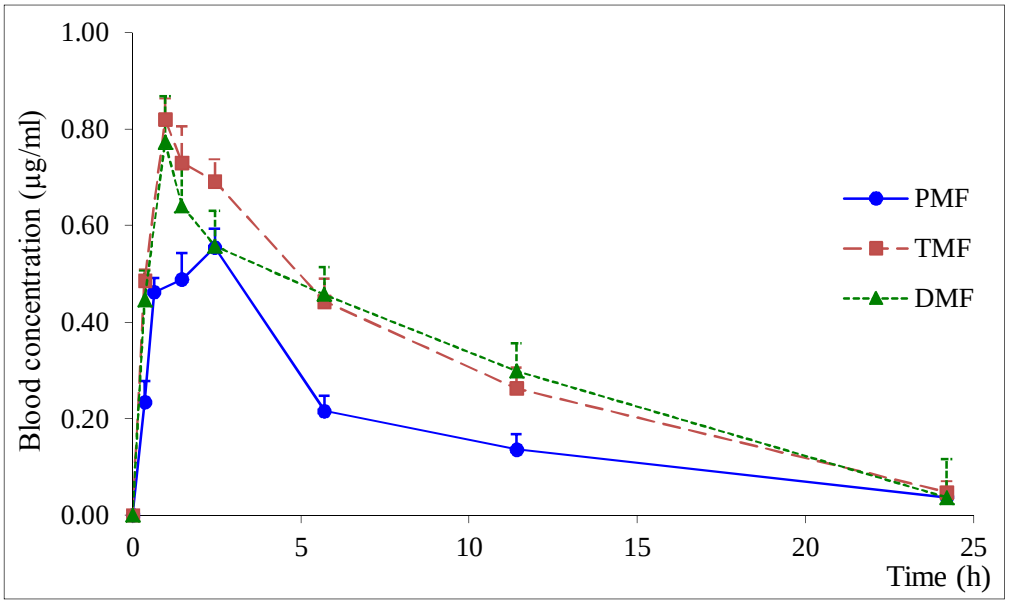

Figure 31 Blood concentration-time profile of methoxyflavones after a single oral administration of 250 mg/kg of KP solution to rats. Each data point represents the mean ± SD (n=10)

Table 8 Pharmacokinetic parameters and oral bioavailability of methoxyflavones after single oral administration of 250 mg/kg of KP solution in rats

PK parameters	PMF	TMF	DMF
AUC (h*μg/ml)	3.654 ± 0.631#	6.960 ± 1.105	7.007 ± 1.369
$t_{1/2}$ (h)	3.115 ± 1.337	5.043 ± 1.103	5.846 ± 1.721
Cl (ml/h)	622.848 ± 114.861*	337.002 ± 62.166	367.275 ± 82.353
Tmax (h)	1.710 ± 0.362*	0.848 ± 0.403	0.760 ± 0.404
Cmax (μg/ml)	0.550 ± 0.050#	0.883 ± 0.108	0.782 ± 0.112
Vd (ml)	2637.134 ± 846.592	2385.102 ± 364.367	2957.529 ± 458.189
Ke (1/h)	0.284 ± 0.172	0.145 ± 0.037	0.127 ± 0.034
F (%)	3.317	1.749	2.097

Note: Data are expressed as mean ± SD (n=10), *: significant higher than the others, $P < 0.05$, #: significant lowers than the others, $P < 0.05$, F, oral bioavailability

In intravenous route, methoxyflavones concentrations rapidly decreased and cleared out from the systemic within 24 h. PMF showed higher Cmax value (46.431 ± 18.387 μg/ml) than that of TMF and DMF. AUC value of PMF was found highest at 76.774 ± 19.499 h*μg/ml. Vd and Cl of PMF was 66.539 ± 16.548 ml and 21.562 ± 7.182 ml/h, respectively, that were the higher values than those of TMF and DMF. PMF possessed the highest value of Ke (0.606 ± 0.215 h^{-1}) following by TMF and DMF. The $t_{1/2}$ of methoxyflavones ranged from 2.36 to 4.19 h.

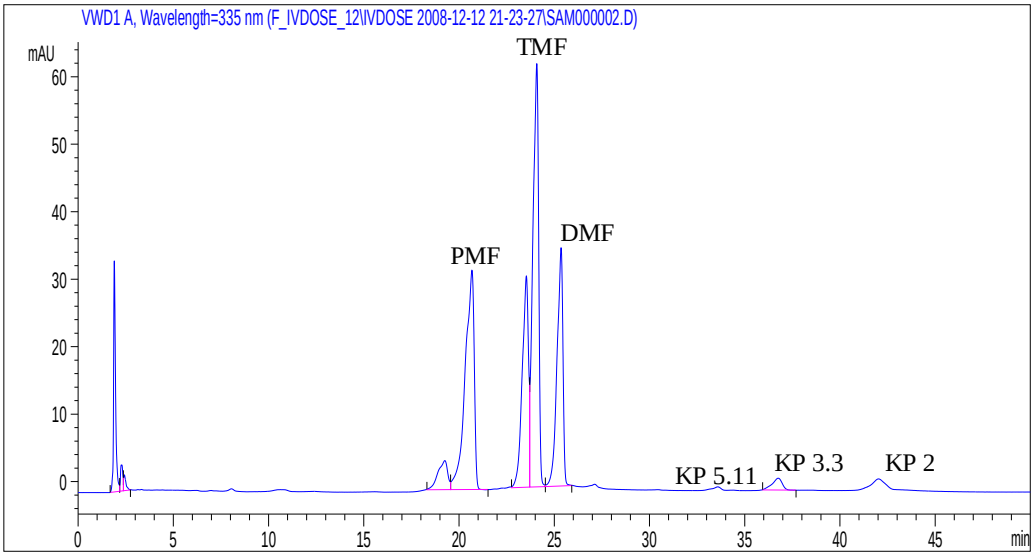

Figure 32 HPLC profile of rat blood after 30 min intravenous administration of 250 mg/kg of KP solution (KP5.11: 5-OH-3,7,3',4'-tetramethoxyflavone, KP3.3: 5 -OH-7-methoxyflavone, KP2: 5-OH-3,7-dimethoxyflavone)

.

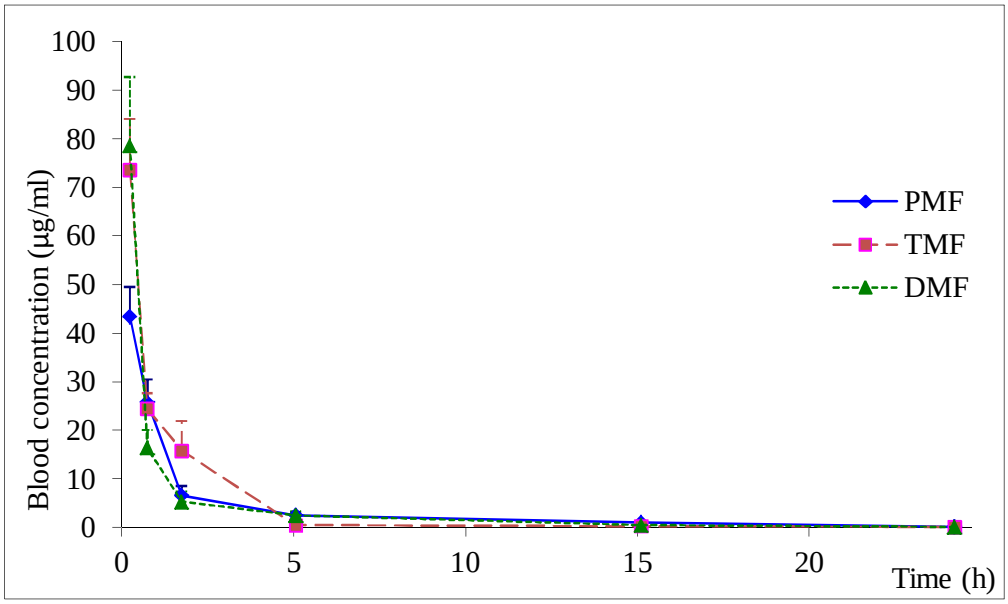

Figure 33 Blood concentration-time profile of methoxyflavones after a single intravenous administration of 250 mg/kg of KP solution to rats. Each data point represents the mean ± SD (n=10)

Table 9 Pharmacokinetic parameters of methoxyflavonoids after single intravenous administration of 250 mg/kg of KP solution in rats

PK parameters	PMF	TMF	DMF
AUC (h*µg/ml)	76.774 ± 19.499#	275.660 ± 86.057	233.476 ± 71.569
$t_{1/2}$ (h)	2.362 ± 1.887	4.191 ± 1.453	3.752 ± 1.009
Cmax (µg/ml)	46.431 ± 18.387#	68.288 ± 30.265	71.554 ± 16.317
Cl (ml/h)	21.562 ± 7.182*	6.305 ± 2.116	7.984 ± 2.338
Vd (ml)	66.539 ± 16.548*	30.369 ± 6.391	39.037 ± 12.446
Ke (1/h)	0.606 ± 0.215*	0.321 ± 0.119	0.323 ± 0.113

Note: Data are expressed as mean ± SD (n=10), *: significant higher than the others, $P < 0.05$, #: significant lowers than the others, $P < 0.05$

3. Organ distribution study

3.1 Animals

The male Wistar rats received 750 mg/kg of KP solution did not show any signs of toxicity. The HPLC chromatogram of 750 mg/kg of KP solution used in this study was presented in Figure 34.

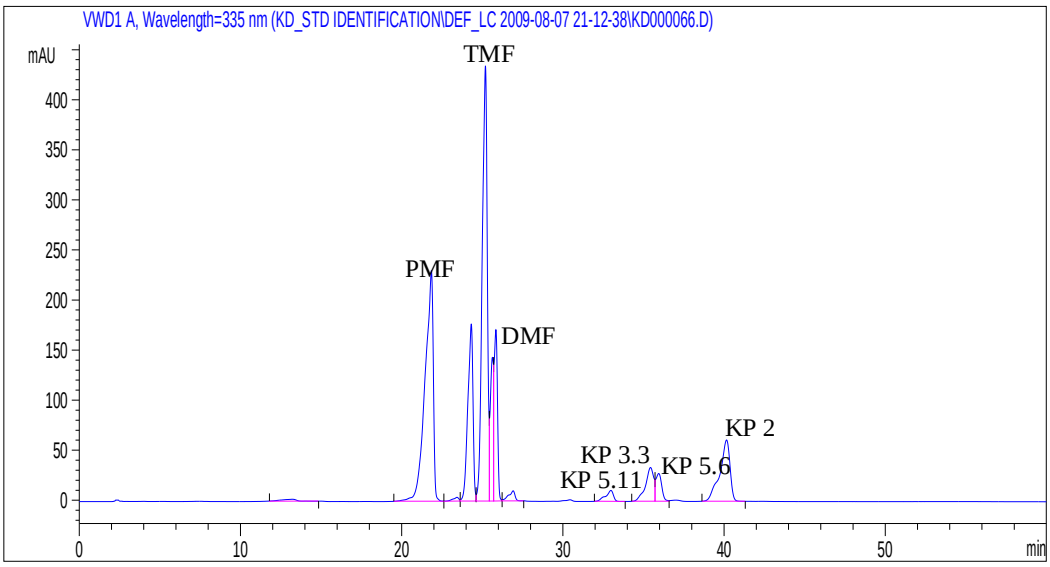

Figure 34 HPLC chromatogram of KP solution (0.75 mg/ml, KP5.11: 5-OH-3,7,3',4'-tetramethoxyflavone, KP3.3: 5 -OH-7-methoxyflavone, KP5.6: 5-OH-3,7,4'-trimethoxyflavone, KP2: 5-OH-3,7-dimethoxyflavone)

3.2 Organ extraction

The optimization method by liquid-liquid extraction using acetonitrile by pre-treated with PBS pH 7.4 showed high recoveries at 90-92%. In addition, the results showed that the blank organs were not containing methoxyflavones.

3.3 Organ distribution

The HPLC profiles of rat organs after receiving 750 mg/kg of KP solution were illustrated in Figure 35-39 for liver, kidney, lung, brain, and testes, respectively. The quantitative data of methoxyflavonoids, PMF, TMF and DMF in KP crude extract were presented in Table 10. The highest levels of PMF, TMF and DMF were found in liver following by kidney. PMF and DMF were also detected in lung,

testes, and brain. For TMF, the highest concentrations showed in liver followed by kidney, brain, testes, and lung, respectively. In term of amounts among methoxyflavones, the concentrations of PMF, TMF and DMF in liver were not significant difference (P-value = 0.05). TMF and DMF concentrations in kidney, lung, brain, and testes samples were similar (P-value > 0.05). For PMF, the concentrations in kidney and lung were lower than those of TMF and DMF, respectively (P-value < 0.05). In brain and testes, TMF and DMF concentrations were significantly higher than those of PMF (P-value < 0.05).

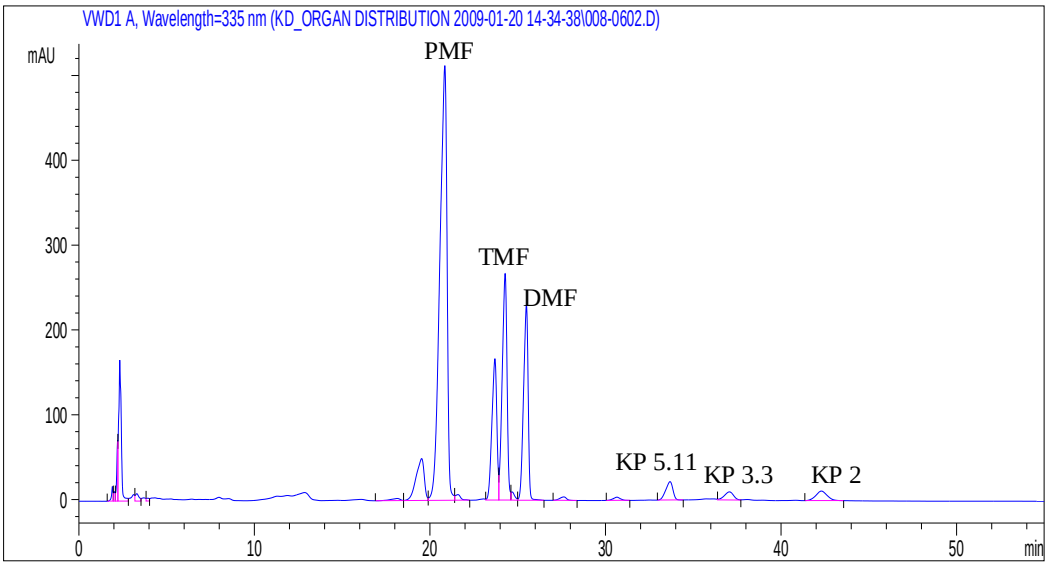

Figure 35 HPLC profile of rat liver after 30 min oral administration of 750 mg/kg of KP solution (KP5.11: 5-OH-3,7,3',4'-tetramethoxyflavone, KP3.3: 5-OH-7-methoxyflavone, KP2: 5-OH-3,7-dimethoxyflavone)

.

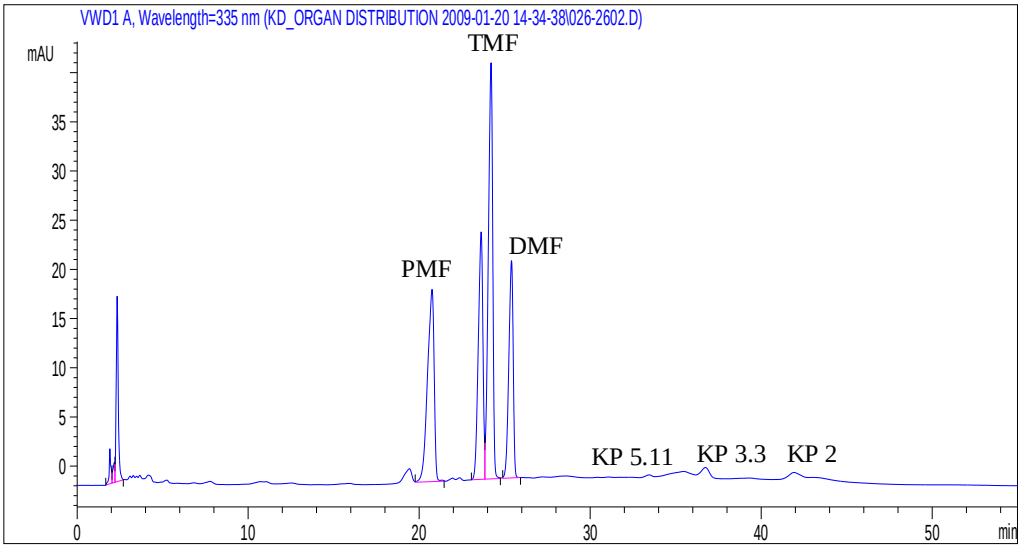

Figure 36 HPLC profile of rat kidney after 30 min oral administration of 750 mg/kg of KP solution (KP5.11: 5-OH-3,7,3',4'-tetramethoxyflavone, KP3.3: 5-OH-7-methoxyflavone, KP2: 5-OH-3,7-dimethoxyflavone)

.

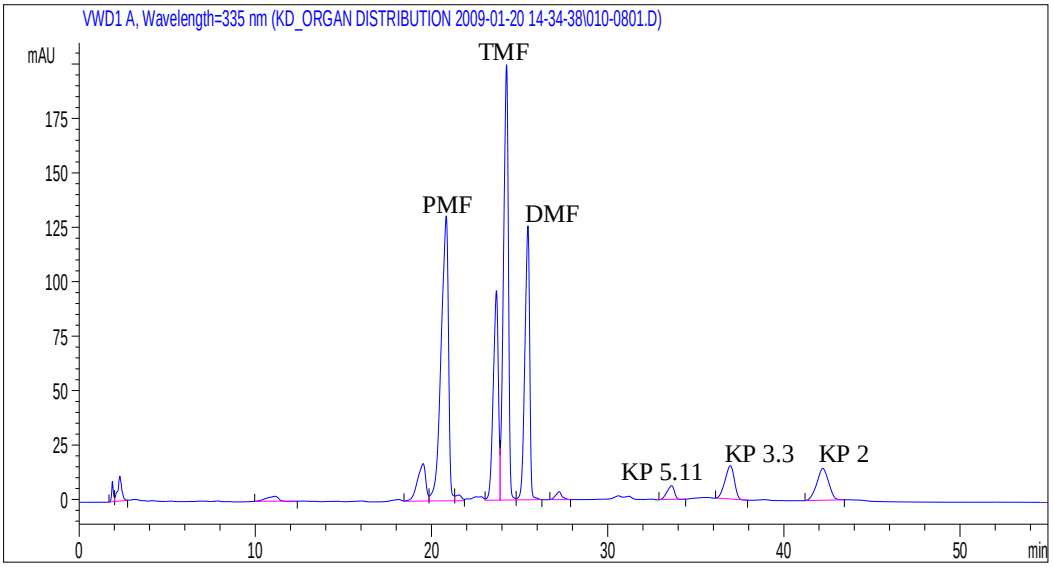

Figure 37 HPLC profile of rat lung after 30 min oral administration of 750 mg/kg of KP solution (KP5.11: 5-OH-3,7,3',4'-tetramethoxyflavone, KP3.3: 5-OH-7-methoxyflavone, KP2: 5-OH-3,7-dimethoxyflavone)

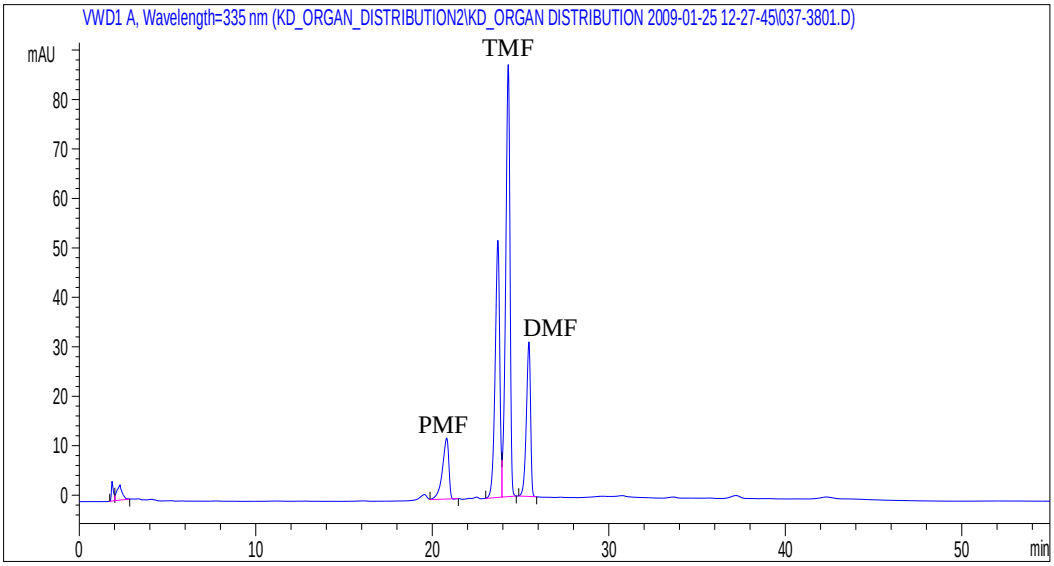

Figure 38 HPLC profile of rat brain after 2 h oral administration of 750 mg/kg of KP solution

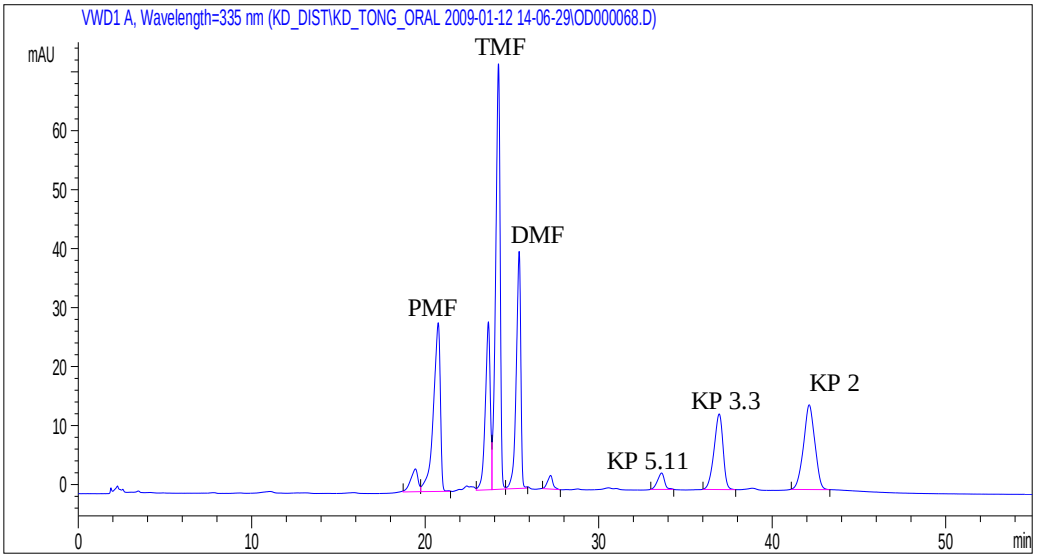

Figure 39 HPLC profile of rat testes after 10 min oral administration of 750 mg/kg of KP solution ((KP5.11: 5-OH-3,7,3',4'-tetramethoxyflavone, KP3.3: 5-OH-7-methoxyflavone, KP2: 5-OH-3,7-dimethoxyflavone)

.

Table 10 Tissue accumulative of PMF, TMF, and DMF in various organs after oral administration of 750 mg/kg of KP solution for 4 h

Organ	**$AUC_{5\text{-}240min}$** (µg.min/g of organ)		
	PMF	TMF	DMF
Liver	543.875 ± 82.248	469.784 ± 19.651	515.894 ± 117.965
Kidney	121.818 ± 40.178*	180.390 ± 50.929	150.700 ± 40.763
Lung	96.200 ± 22.147$^{\#}$	112.691 ± 20.938	130.320 ± 18.520
Brain	45.846 ± 7.541†	149.850 ± 21.890	114.509 ± 33.681
Testes	60.679 ± 14.417†	117.322 ± 40.216	113.863 ± 37.209

Values are mean ± SD of seven rats, *: Significance lowers than TMF, $P < 0.05$, #: Significance lowers than DMF, $P < 0.05$, †: Significance lowers than the others, $P < 0.05$

4. Effect of KP crude extract on cytochrome P450 enzymes

4.1 Animals

Mice receiving 250 mg/kg of KP crude extract which dispersed in CMC for long-term (14- and 21- consecutive days) showed hyperactivity. Nevertheless, the others behaviors and organs appearances of KP groups were similar to untreated group. For other groups, mice did not show any manifests of toxicity. Moreover, mouse liver of ethanol (35% in DI water) treated group was bigger than that of the other groups.

4.2 *In vivo* effect of KP crude extract on CYP450 enzymes activities

CYP contents and enzymatic activity of *in vivo* KP crude extract on mouse hepatic microsome are shown in Table 11. CMC did not have any effect on CYP450 contents, CYP1A1, and CYP3A activities in all durations of treatment, and CYP1A2, CYP2B and CYP3A activity in 7- and 14-day of treatments. Nevertheless, the vehicle slightly changed CYP1A2, CYP2B, and CYP2E1 activities at 21-day of treatment. The CYP450 contents in hepatic microsomes of mice that were administered KP crude extract for 7, 14, and 21 days were not significant different from those observed in negative controls. The induction of CYP1A1, CYP1A2, CYP2B, CYP2E1, and CYP3A activated by each specific inducer (3-methylchrolanthrene, β-naphthoflavone, phenobarbital, ethanol, and dexamethasone, respectively) raised the CYP450 content significantly greater than that of untreated controls.

The CYP1A1 activity of mice that had been administered KP crude extract for 7 and 14 days were significantly greater than that of vehicle groups at the same duration of treatment and the untreated group. However; after 21 days of treatment, these activities returned to that observed in the vehicle group and the untreated groups. Nevertheless, the induction effect of KP crude extract on CYP1A1 activity was significantly lower than that of 3-methylchrolanthrene.

Administration of KP crude extract for 7 and 14 days markedly elevated mouse microsome CYP1A2 and CYP2B activities. However; the activities were lower than that following treatment with β-naphthoflavone or phenobarbital. After 21 days of treatment with the KP crude extract, CYP1A2 activity returned to the

same level as observed in the vehicle control groups. In contrast, CYP2B activity continued to increase 21 days after KP crude extract treatment.

The activity of CYP2E1 was slightly reduced at 7 and 14 days after treatment with the KP crude extract when compared to the untreated control group but were not significant different from the vehicle control group. However, 21 days after treatment with the KP crude extract, CYP2E1 activity was greater than that observed in the vehicle control group.

The mouse hepatic microsomal CYP3A activity of KP crude extract treatment after 7, 14, and 21 days was not different from the vehicle and untreated control groups.

Table 11 Effect of KP on CYP450 content and enzymes activities in rat liver microsomes (*In vivo*)

Treatment	Duration of treatment (days)	CYP450 content (nmole/mg protein)	CYP1A1 activity (pmole/min/mg protein)	CYP1A2 activity (pmole/min/mg protein)	CYP2B activity (pmole/min/mg protein)	CYP2E1 activity (mmole/min/mg protein)	CYP3A activity (µmole/min/mg protein)
KP crude extract	7	0.617 ± 0.210	11.021 ± 1.056^{a,b,c}	9.588 ± 2.124^{a,b,c}	7.043 ± 1.161^{a,b,c}	5.650 ± 0.437^{a,b}	3.5 ± 0.4^{b}
	14	0.704 ± 0.108^{c}	10.313 ± 3.732^{a,b,c}	9.774 ± 2.789^{a,b,c}	5.762 ± 1.982^{a,b,c}	5.025 ± 1.432^{a,b}	3.2 ± 0.4^{b}
	21	0.574 ± 0.148	6.930 ± 1.962^{b}	6.898 ± 1.862^{a,b}	6.169 ± 1.708^{a,b,c}	6.088 ± 1.160^{b,c}	3.2 ± 0.1^{b}
Vehicle (2% CMC)	7	0.538 ± 0.125	6.389 ± 1.449	4.629 ± 1.261	1.462 ± 0.283	4.950 ± 0.918	3.0 ± 0.3
	14	0.545 ± 0.114	6.326 ± 1.734	5.093 ± 0.765	1.860 ± 0.297	5.469 ± 1.609	3.2 ± 0.2
	21	0.507 ± 0.120	5.541 ± 1.341	6.043 ± 1.227^{a}	2.572 ± 0.321^{a}	4.144 ± 1.001^{a}	3.3 ± 0.3
3-MC	3	0.734 ± 0.115^{a}	121.081 ± 35.823^{a}	ND	ND	ND	ND
β-NF	7	0.817 ± 0.274^{a}	ND	20.943 ± 8.976^{a}	ND	ND	ND
PB	7	0.979 ± 0.176^{a}	ND	ND	47.030 ± 4.109^{a}	ND	ND
Ethanol	7	0.352 ± 0.128^{a}	ND	ND	ND	11.061 ± 2.073^{a}	ND
Dexa	7	1.179 ± 0.210^{a}	ND	ND	ND	ND	5.2 ± 0.1^{a}
Untreated	21	0.595 ± 0.169	6.730 ± 1.659	3.046 ± 0.849	1.036 ± 0.320	7.606 ± 1.898	3.2 ± 0.2

Note: The results are expressed as mean ± SD (n=10), ND: not determine, a,b,c Significant difference when compared to untreated group, control group and vehicle group at the same duration of treatment, respectively at P-value < 0.05, 3-MC: 3- methylchrolanthrene, β-NF: β-naphthoflavone, PB: phenobarbital, Dexa: dexamethasone

4.3 *In vitro* effect of KP crude extract on CYP450

From the Lineweaver-Burk plots as shown in Figure 40 provided Vmax and Km (Table 12). Ki, % maximum inhibition, and IC_{50} values were presented in Table 13. KP crude extract significantly inhibited CYP1A1 activity causing a lower Vmax (2.739 ± 0.042 nmole/min) than that of the control group (4.939 ± 0.886 nmole/min). However, the Km of CYP1A1 in the presence of KP crude extract (50.985 ± 2.513 pmole) was not significant different from the control group (63.155 ± 18.138 pmole). The results indicated that the KP crude extract inhibited CYP1A1 activity based on a non-competitive mechanism with an IC_{50} value of 0.439 ± 0.009 µg/ml and a Ki of 0.623 ± 0.001 µg/ml. The Michaelis-Menten parameters of CYP1A2 in the presence of KP crude extract were higher than that of control group (Vmax = 15.276 ± 0.206 nmole/min versus 13.754 ± 0.081 nmole/min, and Km = 27.848 ± 0.725 pmole versus 11.382 ± 0.255 pmole), suggesting a mixed-type inhibition. The highest amount of KP crude extract used in this study (5.682 µg/ml) showed the greatest inhibition of CYP1A2 (6.42 ± 0.14% of maximum activity) with a Ki of 0.008 ± 0.002 µg/ml. The KP crude extract did not change the Vmax of CYP2B but increased its Km (1.599 ± 0.147 pmole versus 0.488 ± 0.151 pmole), suggesting a competitive mechanism of inhibition (Ki of 0.699 ± 0.001 µg/ml; 10.33 ± 0.36 % inhibition of maximum activity). Compared to the control, the Km and Vmax values of CYP2E1 and CYP3A were significantly lowered in the presence of KP crude extract, suggesting an uncompetitive mechanism of inhibition. The Ki and IC_{50} values of CYP2E1 in the presence of KP crude extract were 0.137 ± 0.003 and 0.613 ± 0.032 µg/ml, respectively. The KP crude extract also inhibited CYP3A (7.62 ± 0.82 % inhibition of maximum activity) with a Ki of 0.07 ± 0.03 µg/ml.

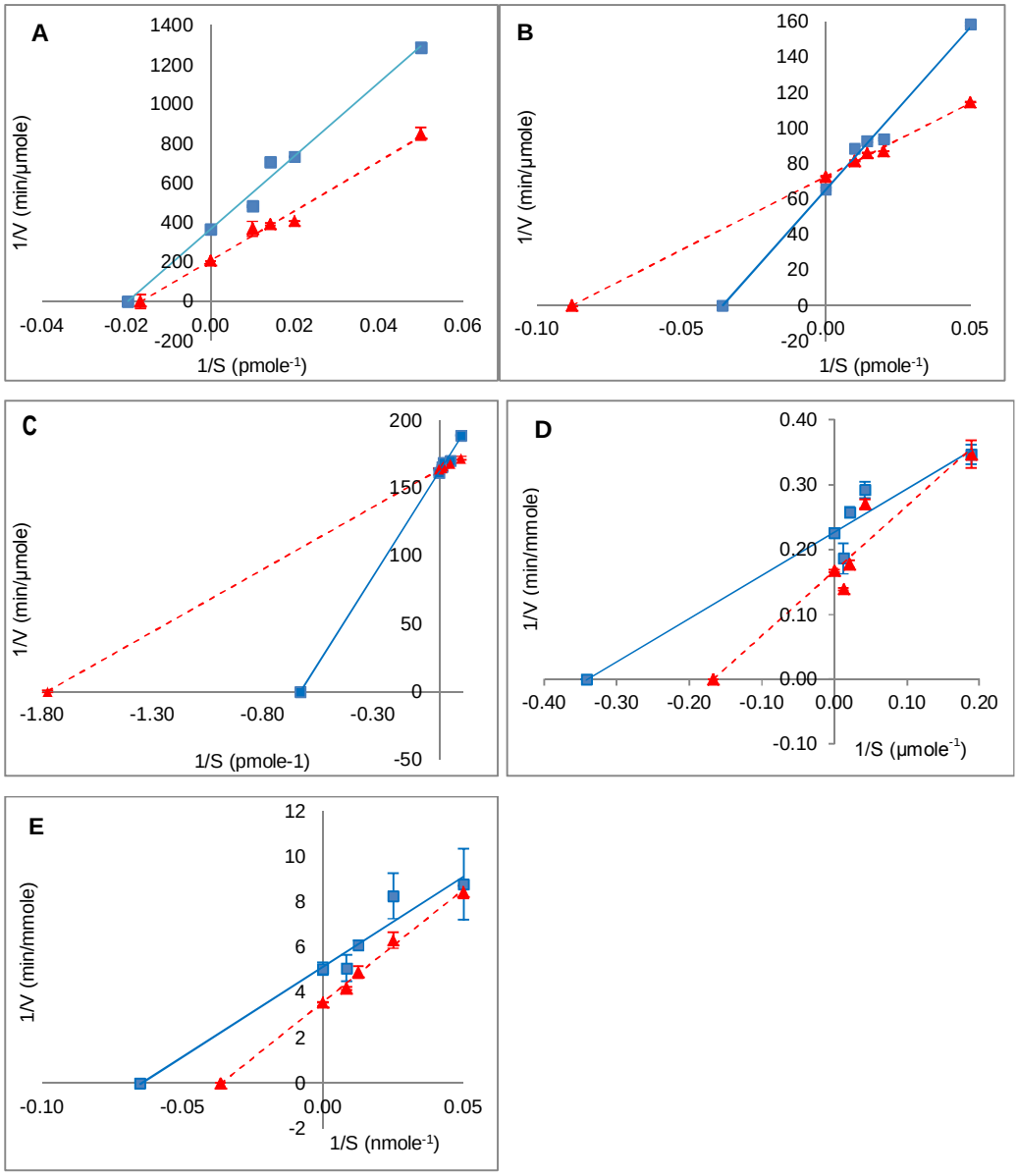

Figure 40 Lineweaver-Burk plots of CYP450 enzyme activities in non-induced mouse liver microsomes. A: CYP1A1, B: CYP1A2, C: CYP2B, D: CYP2E1, E: CYP3A (■:KP, ▲: Control)

Table 12 Effect of KP crude extract on Vmax, Km, and type of reaction of CYP enzyme of non-induced mouse liver microsomes

CYP isoforms	Vmax*		Km**		Type of reaction
	KP	Control	KP	Control	
CYP1A1	2.739 ± 0.042†	4.939 ± 0.886	50.985 ± 2.513	63.155 ± 18.138	Non-competitive
CYP1A2	15.276 ± 0.206†	13.754 ± 0.081	27.848± 0.725†	11.382 ± 0.255	Mixed-type
CYP2B	6.190 ± 0.070	6.095 ± 0.037	1.599 ± 0.147†	0.488 ± 0.151	Competitive
CYP2E1	4.433 ± 0.138†	5.985 ± 0.071	3.023 ± 0.672†	6.010 ± 0.544	Uncompetitive
CYP3A	0.198 ± 0.011†	0.281 ± 0.000	16.553 ± 5.935†	27.490 ± 0.667	Uncompetitive

The values are exposed as mean ± SD (n=3), *nmole/min for CYP1A1, CYP1A2, and CYP2B, mmole/min for CYP2E1 and CYP3A, **pmole for CYP1A1, CYP1A2, and CYP2B, µmole for CYP2E1, nmole for CYP3A, †: significant difference when compared to control group at P-value < 0.05

Table 13 Ki, % maximum inhibition, and IC_{50} values of CYP enzyme from non-induced mouse liver microsomes in the presence of KP crude extract

CYP isoform	Ki (µg/ml)	% Maximum inhibition	IC_{50} (µg/ml)
CYP1A1	0.623 ± 0.001	ND	0.439 ± 0.009
CYP1A2	0.008 ± 0.002	6.42 ± 0.14	ND
CYP2B	0.699 ± 0.001	10.33 ± 0.36*	ND
CYP2E1	0.137 ± 0.003	ND	0.613 ± 0.032#
CYP3A	0.07 ± 0.03	7.62 ± 0.82	ND

The values are expressed as mean ± SD (n=3), *: significance greatest at P-value < 0.001 by a one-way ANOVA, #: significant difference at P-value < 0.001 between CYP1A1 and CYP2E1, ND: not determined

5. Excretion study

5.1 Animals

The rats receiving 750 mg/kg of KP solution for 72 h in the excretion study look healthy and did not show any physical signs of toxicity.

5.2 Feces and urine extraction

The optimized method using liquid-liquid extraction by acetonitrile was selected. It showed the high recovery at 92-98%. The HPLC chromatograms of urine and feces samples that were added with KP crude extract similar to the chromatogram of KP solution (Figure 41-42, and 34).

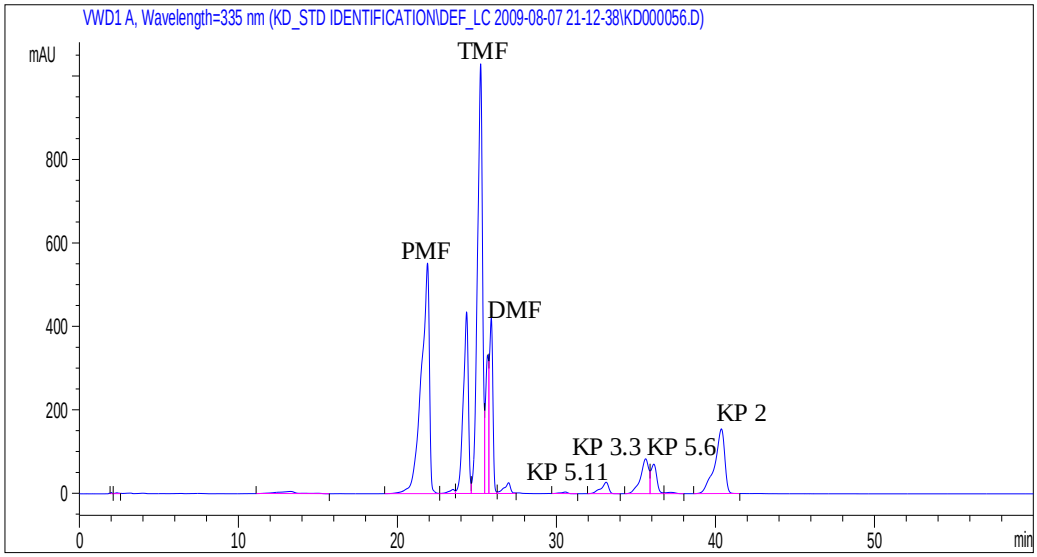

Figure 41 HPLC chromatogram of urine that was added with 0.06-0.11 g of KP crude extracts (KP5.11: 5-OH-3,7,3',4'-tetramethoxyflavone, KP3.3: 5-OH-7-methoxyflavone, KP5.6: 5-OH-3,7,4'-trimethoxyflavone, KP2: 5-OH-3,7-dimethoxyflavone)

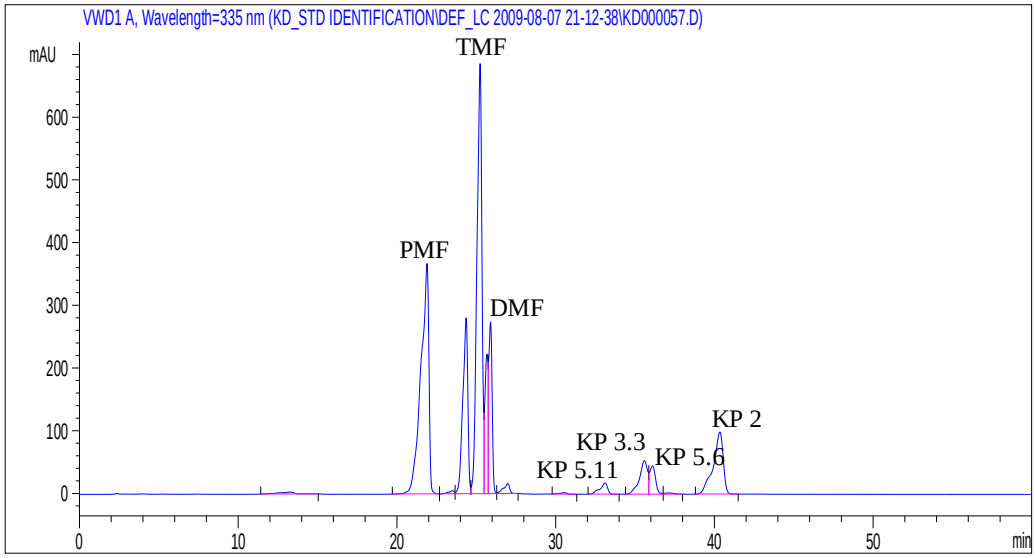

Figure 42 HPLC chromatogram of feces that was added with 0.06-0.11 g of KP crude extracts KP5.11: 5-OH-3,7,3',4'-tetramethoxyflavone, KP3.3: 5-OH-7-methoxyflavone, KP5.6: 5-OH-3,7,4'-trimethoxyflavone, KP2: 5-OH-3,7-dimethoxyflavone)

5.3 Quantitative analysis

HPLC chromatograms of urine and feces samples of rats receiving 750 mg/kg of KP solution as shown in Figure 43 and 45 demonstrated that the urine and feces samples contained the known (methoxyflavones) and unknown peaks. The unknown peaks presented earlier than the peak of methoxyflavones indicating the more polar in the samples. The profile of methoxyflavones concentrations with time in urine and feces were illustrated in Figure 44 and 46. The amounts of PMF, TMF and DMF in urine and feces samples at various times were presented in Table 14 and 15.

In urine samples of rats receiving KP crude extract, the amounts of PMF and TMF were highest at 24-30 h. After that, their amounts were rapidly declined within 72 h. For DMF, its urine concentration was highest at 18-24 h and then the levels slowly detected below limit of detection at 72 h. It was notice that DMF concentrations were markedly lower than those of PMF and TMF concentrations as observed at 0-6, 12-28, 18-24, 24-30, and 42-54 h. At 6-12 and 54-

66 h of collecting time, TMF levels were significantly higher than those of PMF and DMF. PMF concentration at 66-72 h was greater than that of TMF and DMF. However, the major parent compounds were found in urine with small amounts (0.027, 0.259, and 0.141% of giving dose of PMF, TMF, and DMF, respectively).

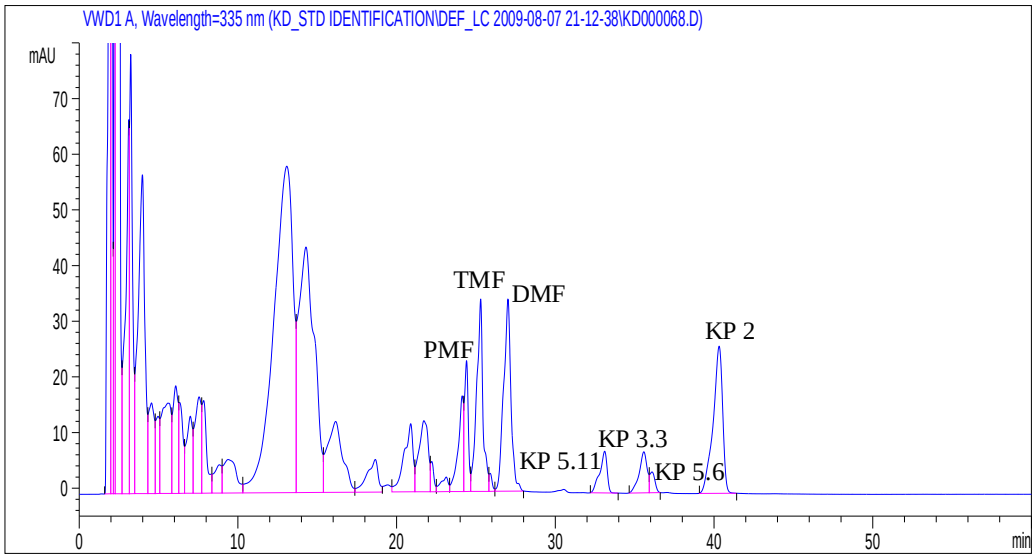

Figure 43 HPLC profile of rat urine after receiving 750 mg/kg of KP solution for 12 h (KP5.11: 5-OH-3,7,3',4'-tetramethoxyflavone, KP3.3: 5 -OH-7-methoxyflavone, KP5.6: 5-OH-3,7,4'-trimethoxyflavone, KP2: 5-OH-3,7-dimethoxyflavone)

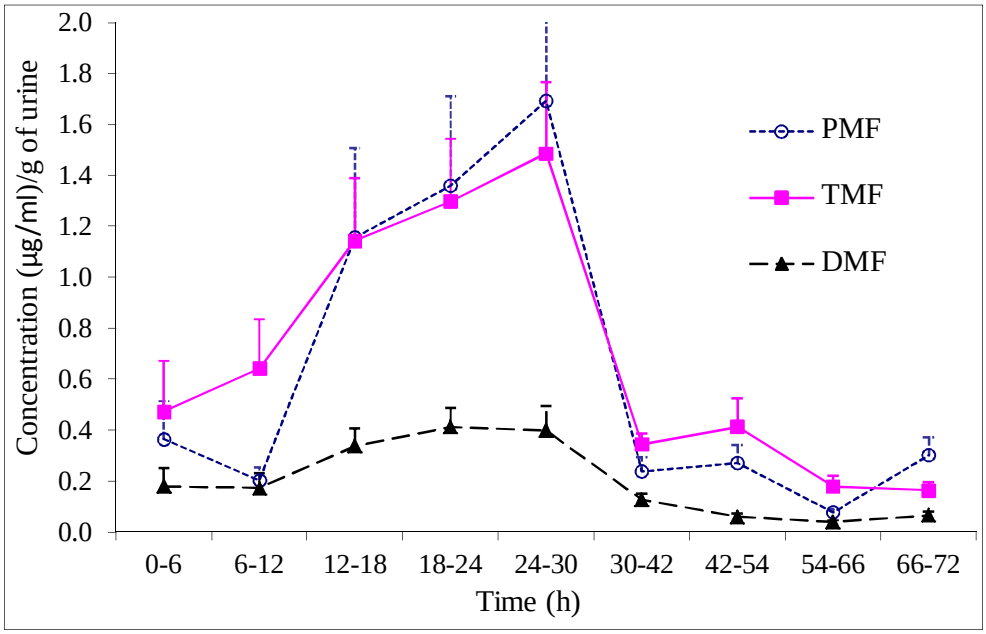

Figure 44 Profile of methoxyflavones concentrations with times of urine samples of rats after receiving 750 mg/kg of KP solution for 72 h

Table 14 Concentration of three methoxyflavones in urine samples of rats after receiving 750 mg/kg of KP solution

Time (h)	Amount of methoxyflavones (μg/g of urine)		
	PMF	TMF	DMF
0-6	0.364 ± 0.150	0.473 ± 0.200	0.179 ± 0.072*
6-12	0.203 ± 0.050	0.642 ± 0.194#	0.173 ± 0.058
12-18	1.157 ± 0.350	1.144 ± 0.245	0.337 ± 0.070*
18-24	1.360 ± 0.350	1.298 ± 0.245	0.413 ± 0.075*
24-30	1.693 ± 0.503	1.486 ± 0.279	0.399 ± 0.096*
30-42	0.238 ± 0.057	0.344 ± 0.042	0.127 ± 0.023
42-54	0.271 ± 0.071	0.413 ± 0.112	0.060 ± 0.012*
54-66	0.077 ± 0.014	0.179 ± 0.041#	0.040 ± 0.007
66-72	0.302 ± 0.070†	0.164 ± 0.032	0.066 ± 0.014

The values are expressed as mean ± SD (n=10), *: significant lower than PMF and TMF at P-value = 0.05, #: significant higher than PMF and DMF at P-value = 0.05, †: significant higher than TMF and DMF at P-value = 0.05

In feces samples of rats receiving 750 mg/kg of KP solution, PMF, TMF and DMF levels quickly reached the highest levels within 24 h and then the concentrations gradually decreased. The highest amounts of PMF and TMF were presented at 18-24 h collecting time. While, DMF concentration showed the highest levels at 12-18 h. In general, the patterns of these three methoxyflavones concentrations in feces were similar except the level of DMF at 0-6 h was significantly lower than that of PMF and TMF. Nevertheless, the amounts of parent compounds were detected at 0.89, 0.198, and 0.35% of giving dose of PMF, TMF, and DMF, respectively.

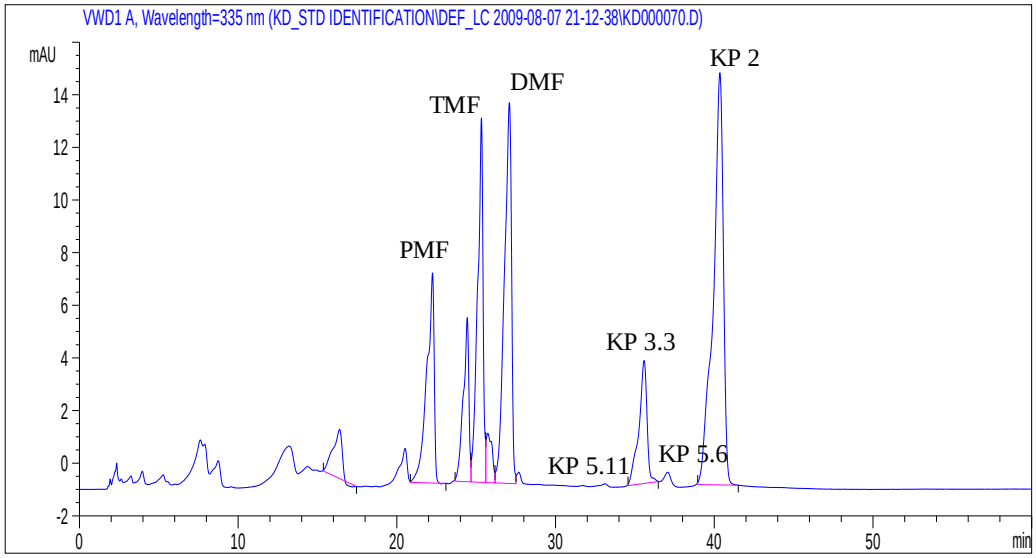

Figure 45 HPLC profile of rat feces after receiving 750 mg/kg of KP solution for 12 h (KP5.11: 5-OH-3,7,3',4'-tetramethoxyflavone, KP3.3: 5-OH-7-methoxyflavone, KP5.6: 5-OH-3,7,4'-trimethoxyflavone, KP2: 5-OH-3,7-methoxyflavone)

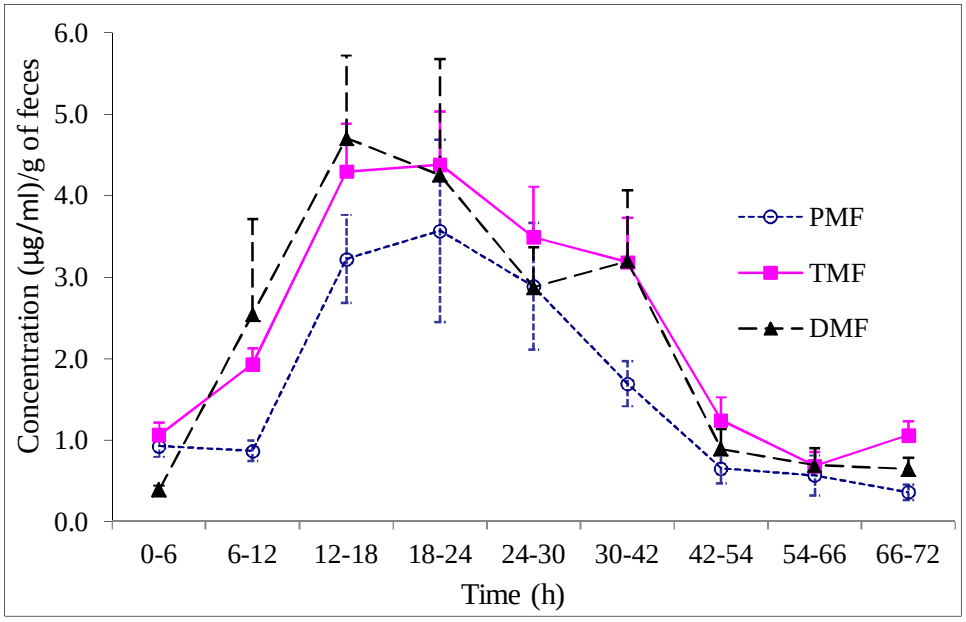

Figure 46 Profile of methoxyflavones concentrations of feces samples of rats after receiving 750 mg/kg of KP solution for 72 h

Table 15 Concentrations of three methoxyflavones in feces samples of rats after receiving 750 mg/kg of KP solution

Time	Amount of methoxyflavones (µg/g of feces)		
	PMF	TMF	DMF
0-6	0.926 ± 0.131	1.062 ± 0.158	0.392 ± 0.047*
6-12	0.868 ± 0.124	1.930 ± 0.195	2.544 ± 1.168
12-18	3.225 ± 0.541	4.298 ± 0.587	4.708 ± 1.011
18-24	3.572 ± 1.119	4.382 ± 0.655	4.254 ± 1.421
24-30	2.888 ± 0.780	3.492 ± 0.623	2.875 ± 0.488
30-42	1.693 ± 0.279	3.188 ± 0.541	3.197 ± 0.872
42-54	0.653 ± 0.185	1.246 ± 0.280	0.894 ± 0.239
54-66	0.568 ± 0.243	0.683 ± 0.171	0.690 ± 0.211
66-72	0.362 ± 0.097	1.059 ± 0.175	0.645 ± 0.137

The values are expressed as mean ± SD (n=10), *: significant lower than PMF and TMF at P-value = 0.05

5.5 Qualitative analysis

5.5.1 Collision energy optimization

In order to optimize the collision energy, one of major compound, TMF (m/z = 313), was used. Collision energy was varied from 10 to 70 eV. Total ion chromatogram of TMF and mass spectrum in various collision energies were showed in Figure 47 and 48, respectively. The optimum collision energy can make the fragments of metabolites in high relative abundance and show low abundance of parent compound. From Figure 48, the best collision energy ranged from 35 to 40 eV which were further used for urine and feces samples in MS/MS mode.

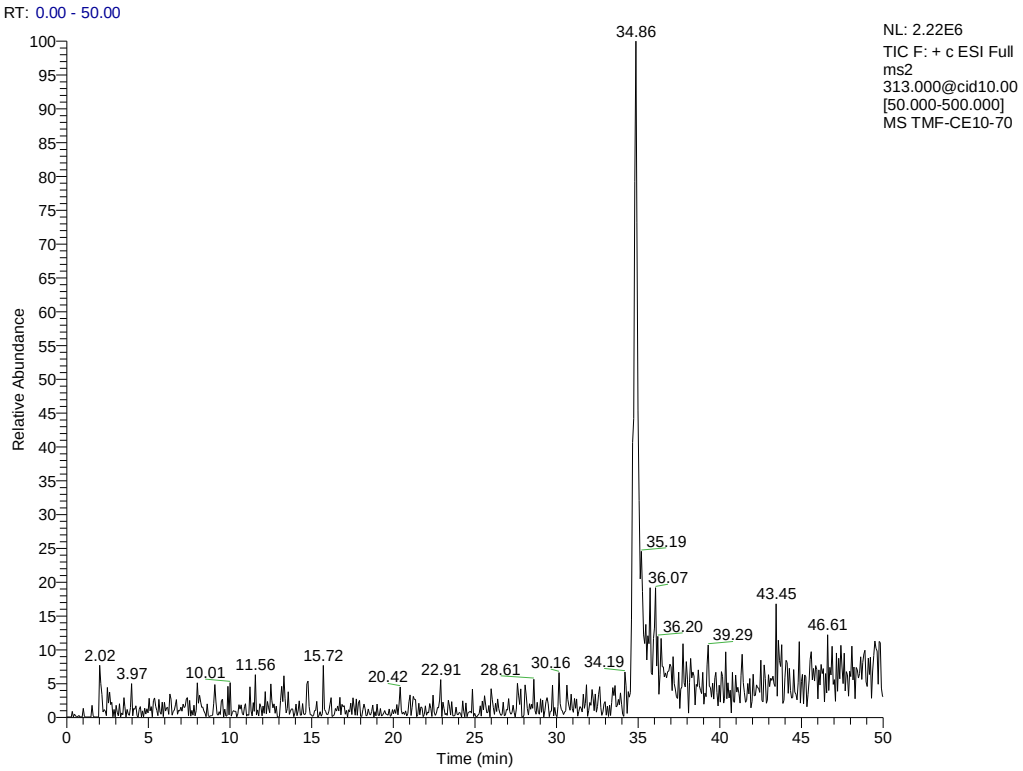

Figure 47 Total ion chromatogram of TMF for optimization the collision energy

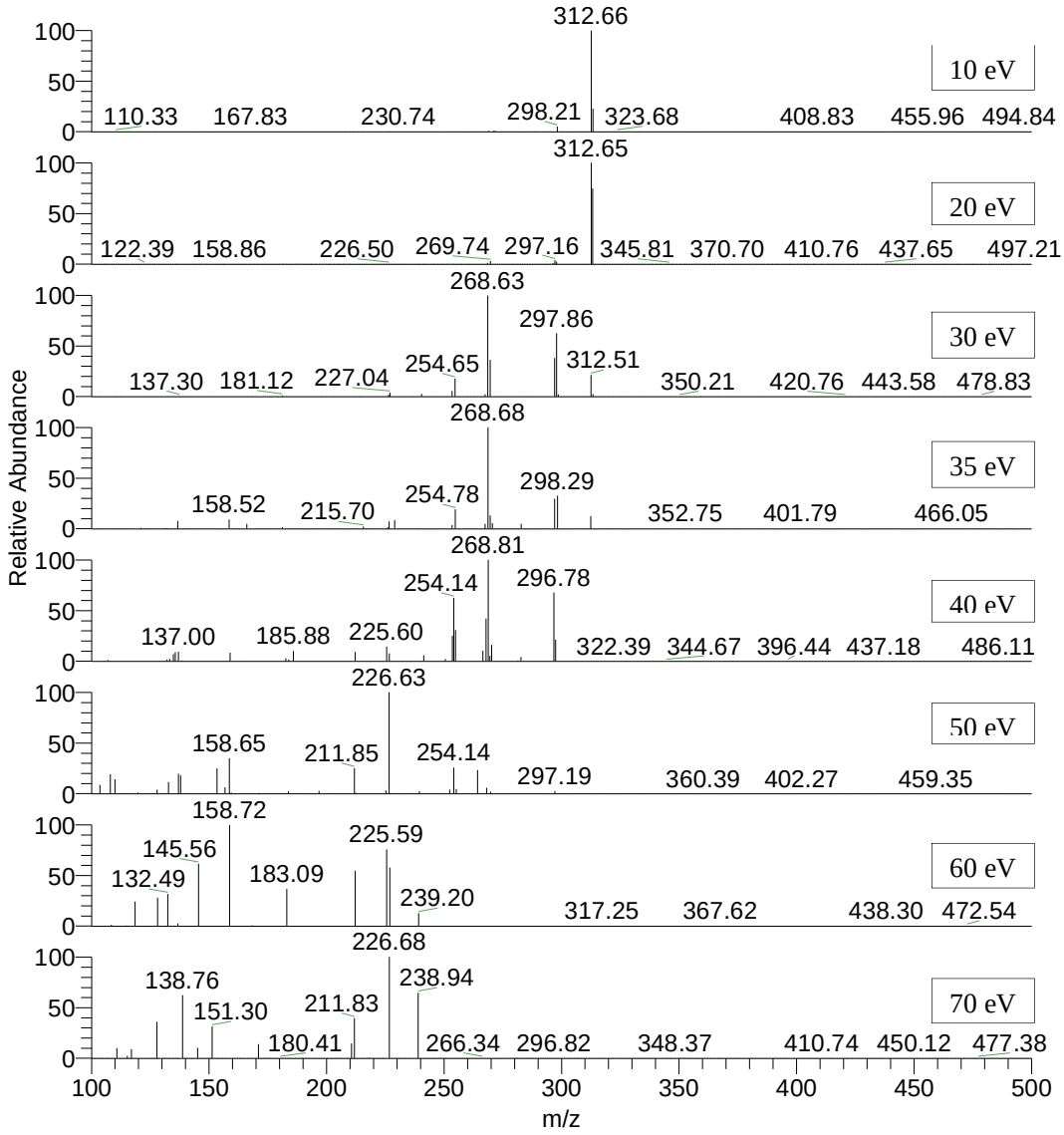

Figure 48 Mass spectrum of TMF (m/z = 313) at various collision energy (10-70 eV)

5.5.2 Identification of metabolites

The criteria to identify the metabolites were 1) difference retention time of known compound, 2) determination of unknown m/z ratios by LCMS, and 3) no detectable in KP extract formulation. The m/z ratios of metabolite in urine and feces samples were determined from full scan from m/z 30 to 1,000 as positive mode providing parent ions. Structural elucidation of metabolites in urine and feces samples were based on their fragmentation pathways of parent ion from MS/MS

mode at collision energy of 35-40 eV generating daughter ions. The m/z ratios of parent ions from full scan MS mode, the m/z ratios of daughter ions of each parent ion from MS/MS mode, fragment pathways, and proposed metabolic pathways for metabolites in urine were presented in Figure 49-66 and in feces were Figure 67-76, respectively. The metabolites in urine and feces after administration of KP crude extract were concluded in Table 16 and 17.

5.5.2.1 Metabolites in urine of rat receiving KP crude extract

1. $[M+H]^{+1}$ = 255 (M1)

The daughter ions spectrum from MS/MS mode at 35 eV collision energy contained major fragment ions at m/z 239 (loss O, 16 amu) (Figure 49B) and the fragment pattern (Figure 49C). It was suggested that demethylation occurred at C-5 and C-7 positions of DMF structure as illustrated in Figure 50.

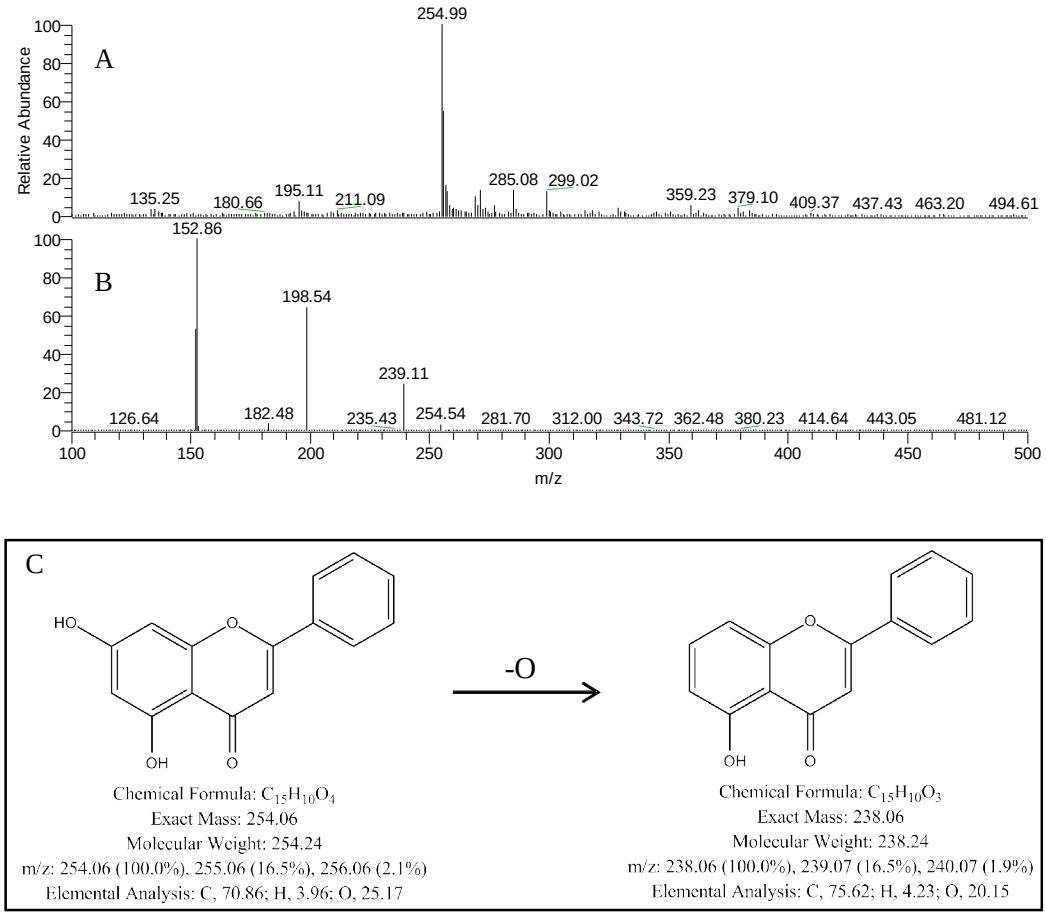

Figure 49 A: mass spectrum of metabolite in urine in full scan mode, B: product ions of the metabolite in MS/MS mode at m/z = 255 (M1), and C: fragmentation pathway of the metabolite in MS/MS mode

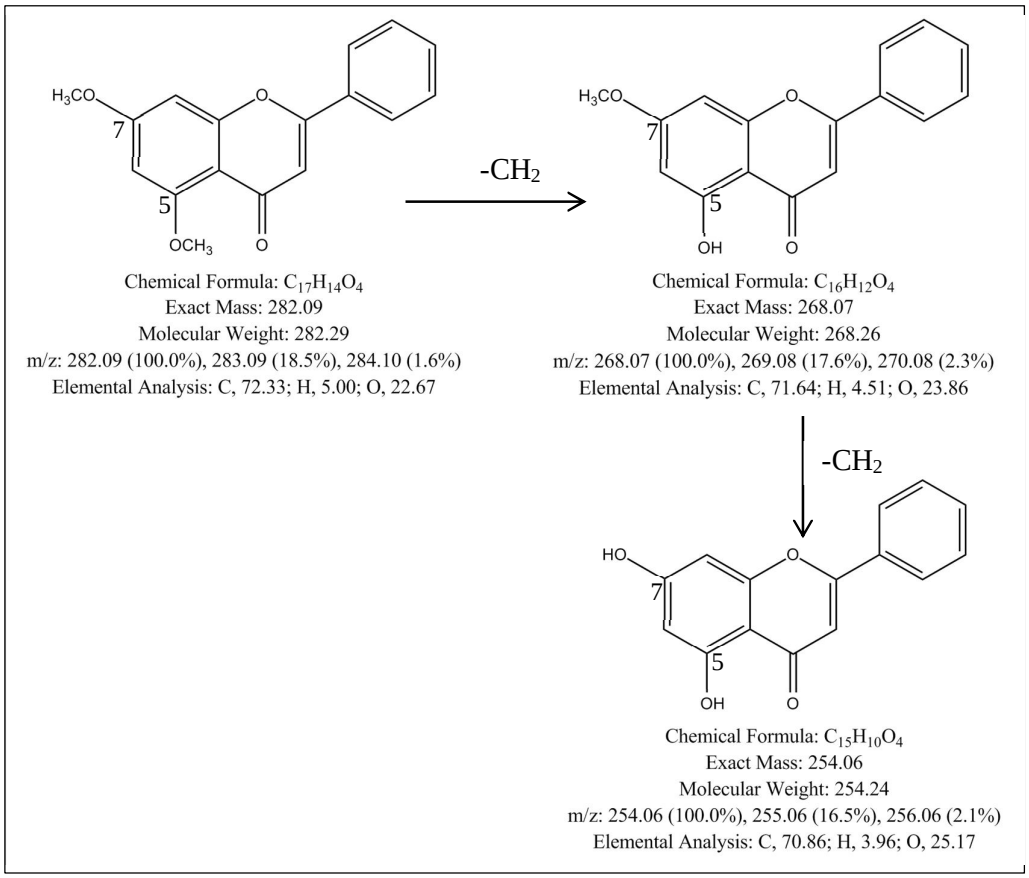

Figure 50 Proposed metabolic pathway of M1

2. $[M+H]^{+1}$ = 285 (M2)

The fragment ions of $[M+H]^{+1}$ signal at 269 and 255 resulted from loss of oxygen (16 amu) and methyl group (14 amu), respectively (Figure 51B and 51C). From the ions at $[M+H]^{+1}$ = 285, there were loss of methyl groups at C-5 and C-4' of TMF molecule (demethylation) led to formation of M2 (Figure 52).

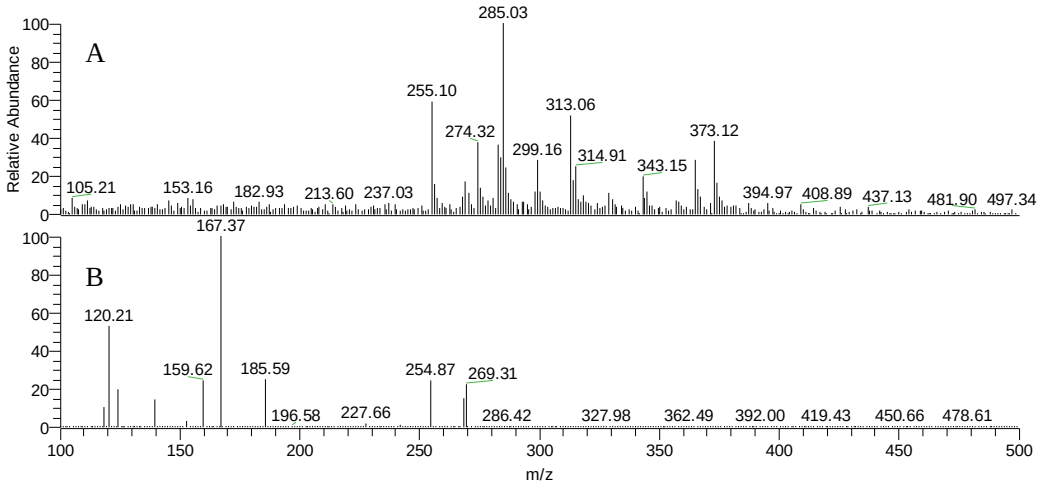

Figure 51 A: mass spectrum of metabolite in urine as full scan mode, B: product ions of the metabolite in MS/MS mode at m/z = 285 (M2), and C: fragmentation pathway of the metabolite in MS/MS mode

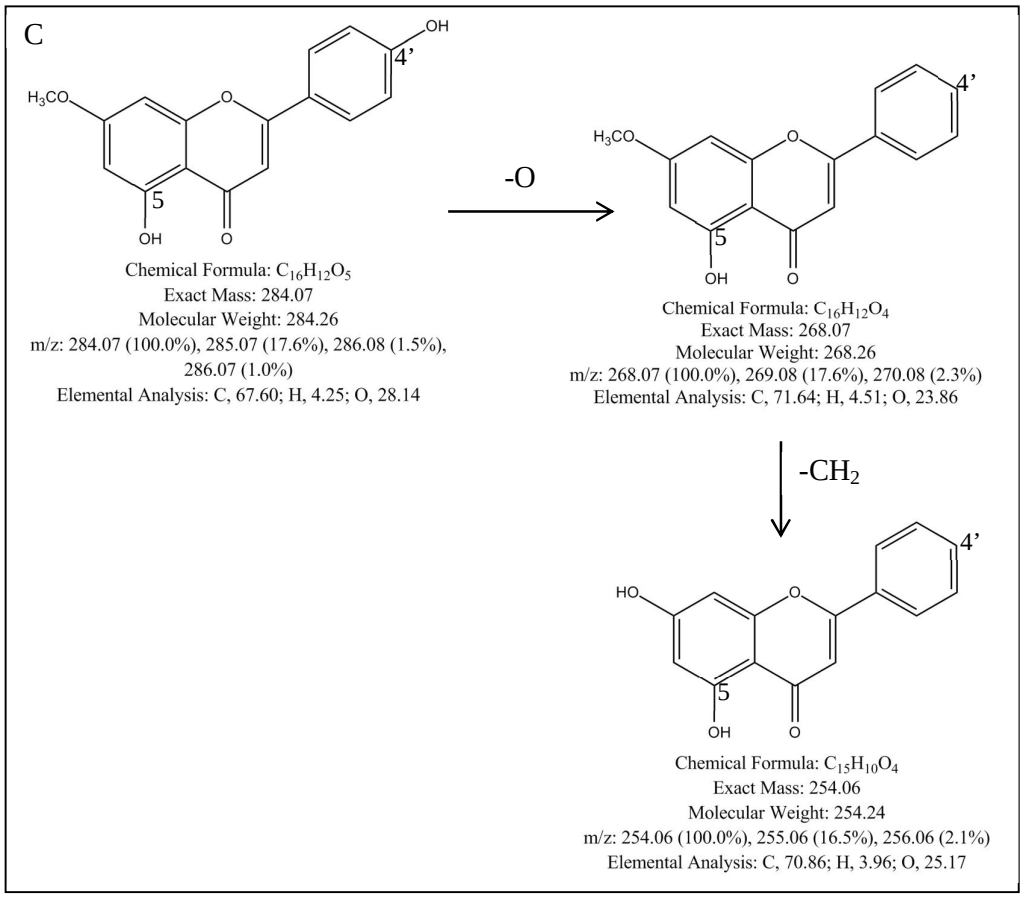

Figure 51 A: mass spectrum of metabolite in urine as full scan mode, B: product ions of the metabolite in MS/MS mode at m/z = 285 (M2), and C: fragmentation pathway of the metabolite in MS/MS mode (Cont.)

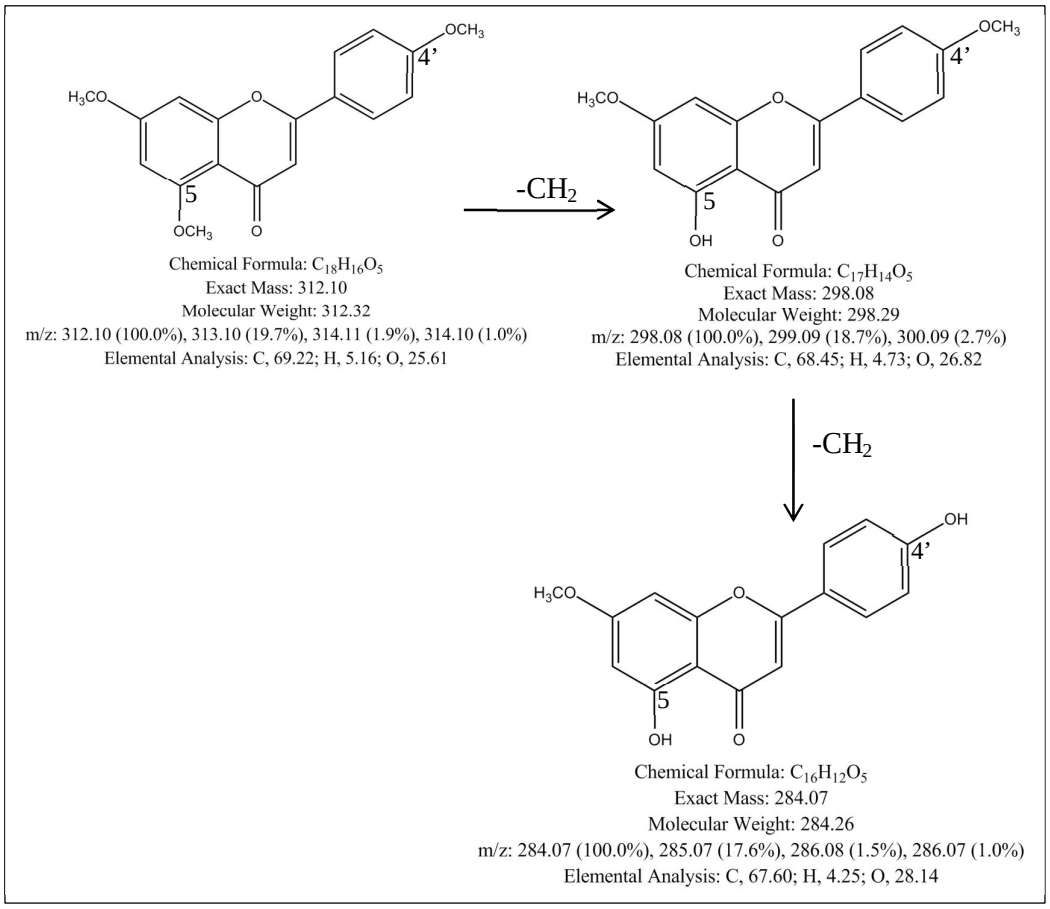

Figure 52 Proposed metabolic pathway of M2

3. $[M+H]^{+1}$ = 315 (M3)

The m/z ratios at 299, 269, and 255 were the fragment ions that found in MS/MS mode of M3 resulting from the loss of O, OCH_3, and CH_2 molecules, respectively (Figure 53B, and 53C). M3 had a $[M+H]^{+1}$ signal at 315, which it was metabolized from 3,5,7,4'-tetramethoxyflavone by demethylaton reaction at C-5 and C-3 as illustrated in Figure 54.

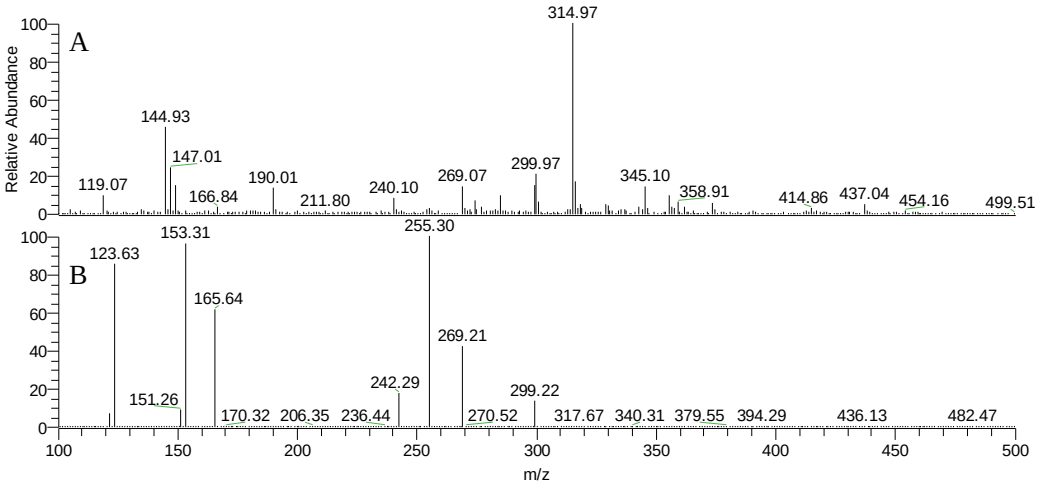

Figure 53 A: mass spectrum of metabolite in urine as full scan mode, B: product ions of the metabolite in MS/MS mode at m/z = 315 (M3), and C: fragmentation pathway of the metabolite in MS/MS mode

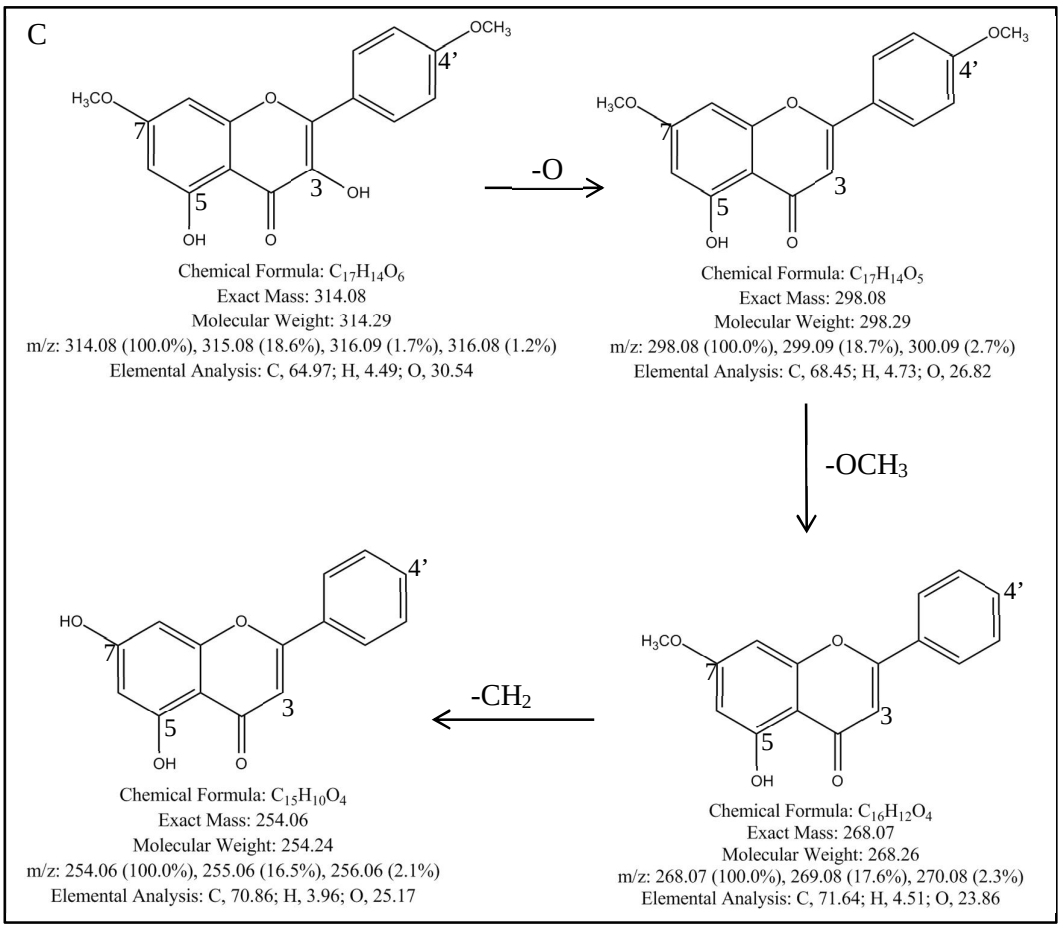

Figure 53 A: mass spectrum of metabolite in urine as full scan mode, B: product ions of the metabolite in MS/MS mode at m/z = 315 (M3), and C: fragmentation pathway of the metabolite in MS/MS mode (Cont.)

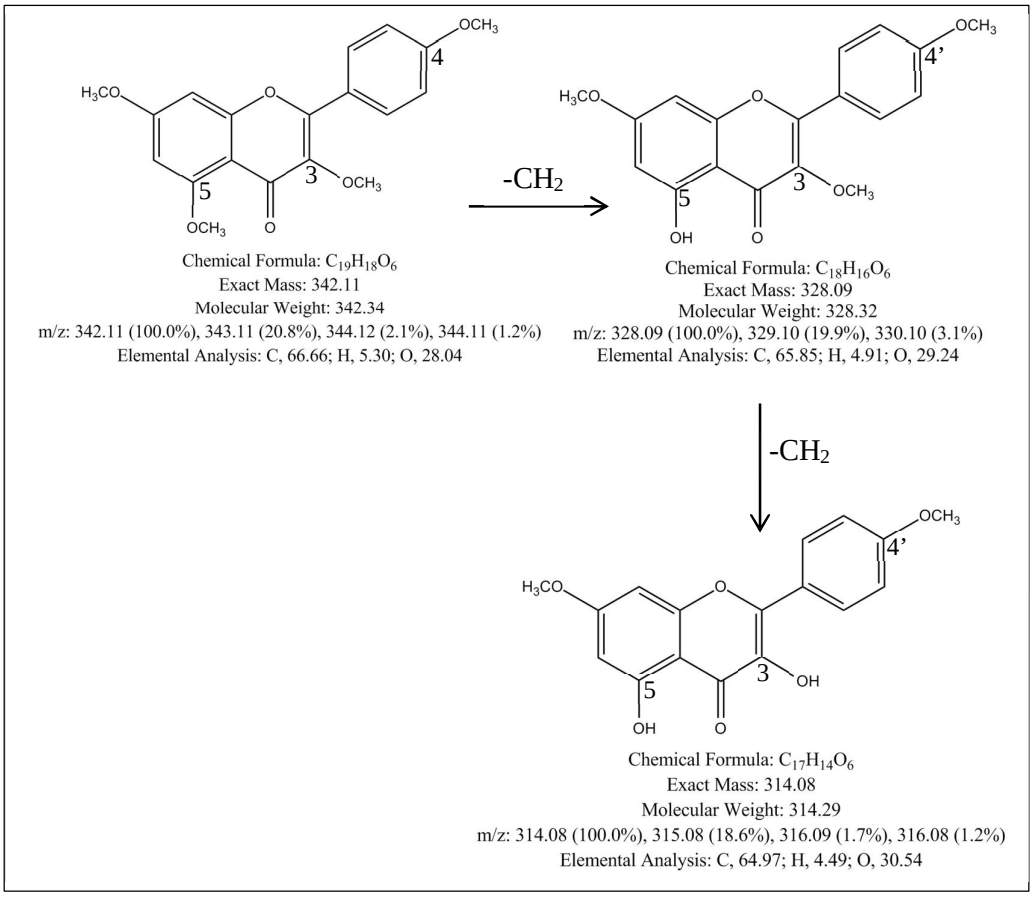

Figure 54 Proposed metabolic pathway of M3

4. $[M+H]^{+1}$ = 345 (M4)

The daughter ions at 329 m/z ratio resulted from the loss of oxygen (-16 amu.) and further fragmented into the ions at 299 m/z ratio (loss of $-OCH_3$), 285 m/z ratio (loss of $-CH_2$), and 255 m/z ratio (loss of $-OCH_3$) as shown in Figure 55B and 55C. From the parent ions mass at 345 amu, it was assumed that there was demethylation at C-3' and C-5 positions of PMF (Figure 56).

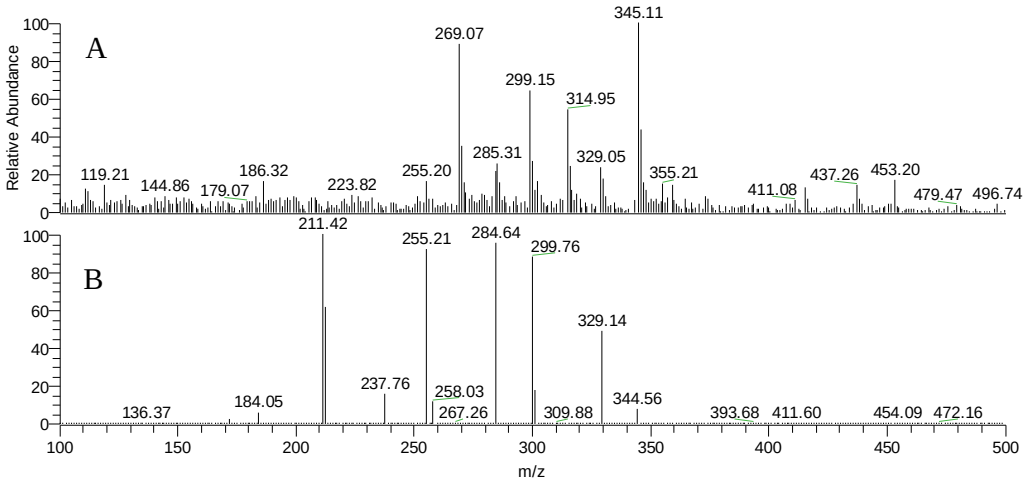

Figure 55 A: mass spectrum of metabolite in urine as full scan mode, B: product ions of the metabolite in MS/MS mode at m/z = 345 (M4), and C: fragmentation pathway of the metabolite in MS/MS mode

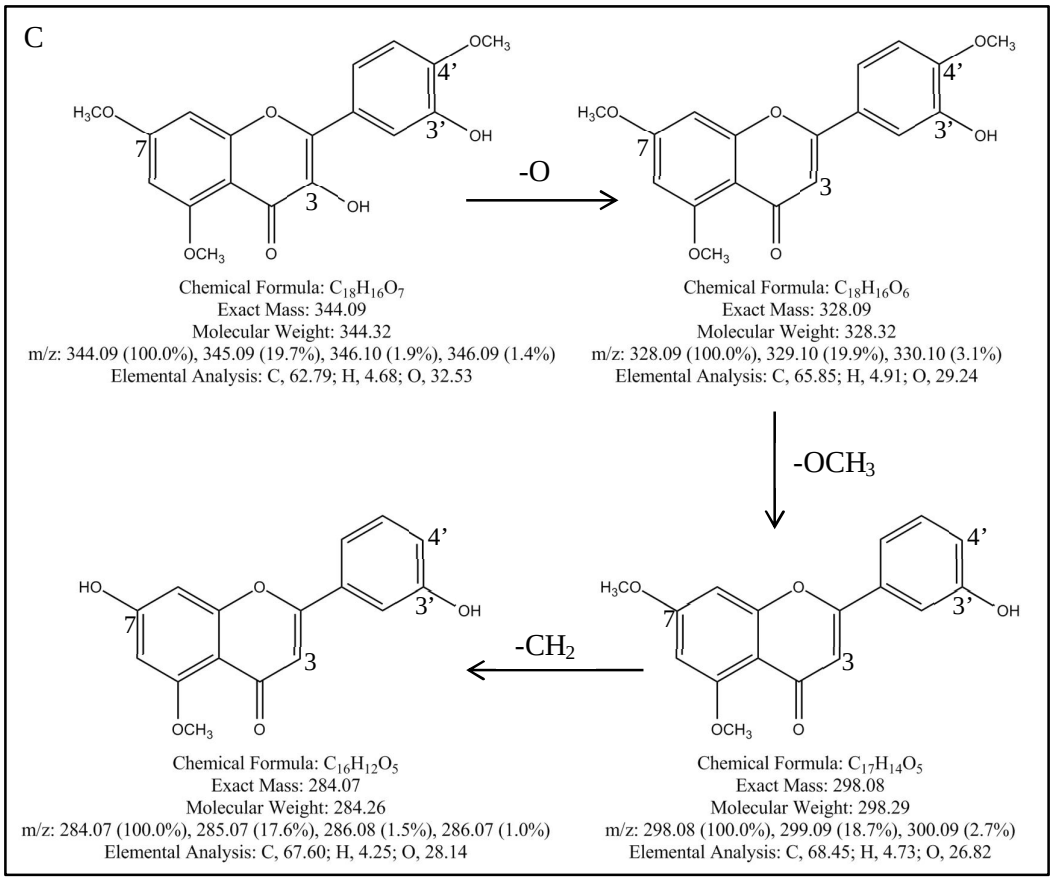

Figure 55 A: mass spectrum of metabolite in urine as full scan mode, B: product ions of the metabolite in MS/MS mode at m/z = 345 (M4), and C: fragmentation pathway of the metabolite in MS/MS mode (Cont.)

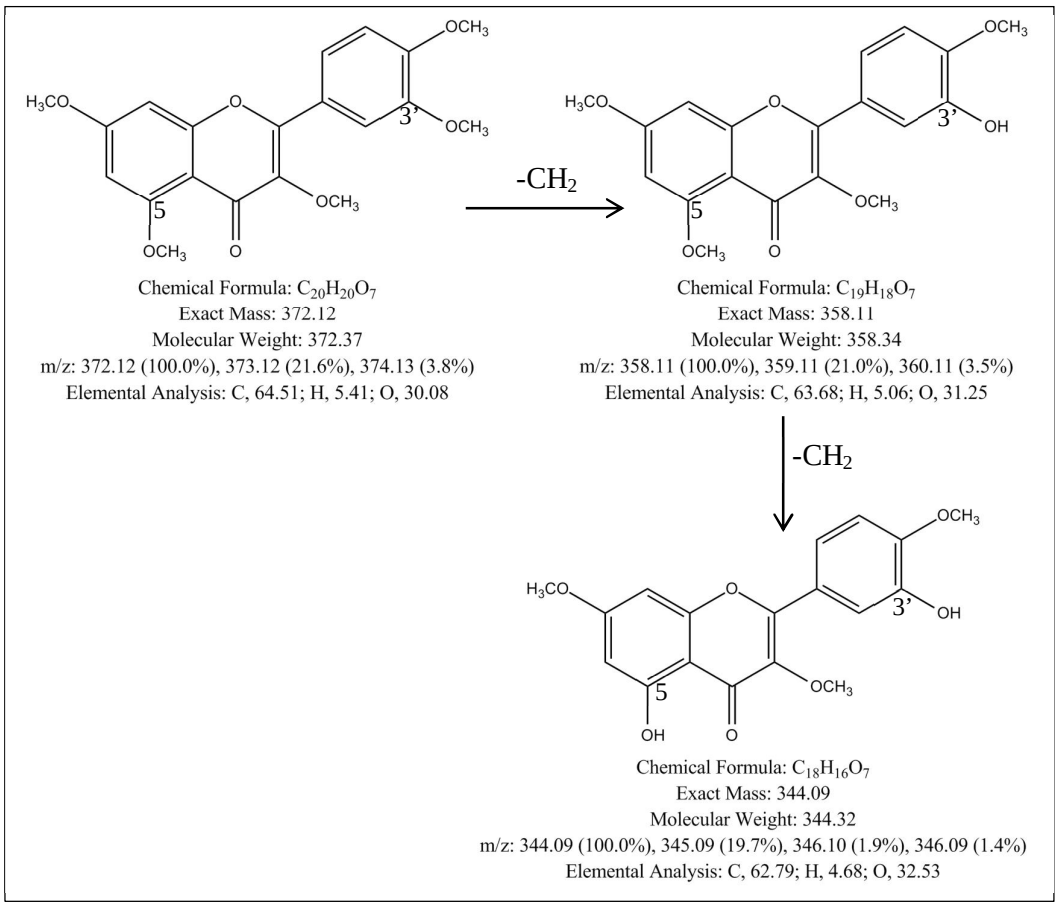

Figure 56 Proposed metabolic pathway of M4

5. $[M+H]^{+1}$ = 349 (M5)

M5 had $[M+H]^{+1}$ signal at 349 that showed the loss of 80 amu from the daughter ion (m/z ratio at 269) as shown in Figure 57B and 57C. This finding suggested that DMF ($[M+H]^{+1}$ signal at 283) was demethylation (-14 amu) at C-5 and then further sulfation reaction (Figure 58).

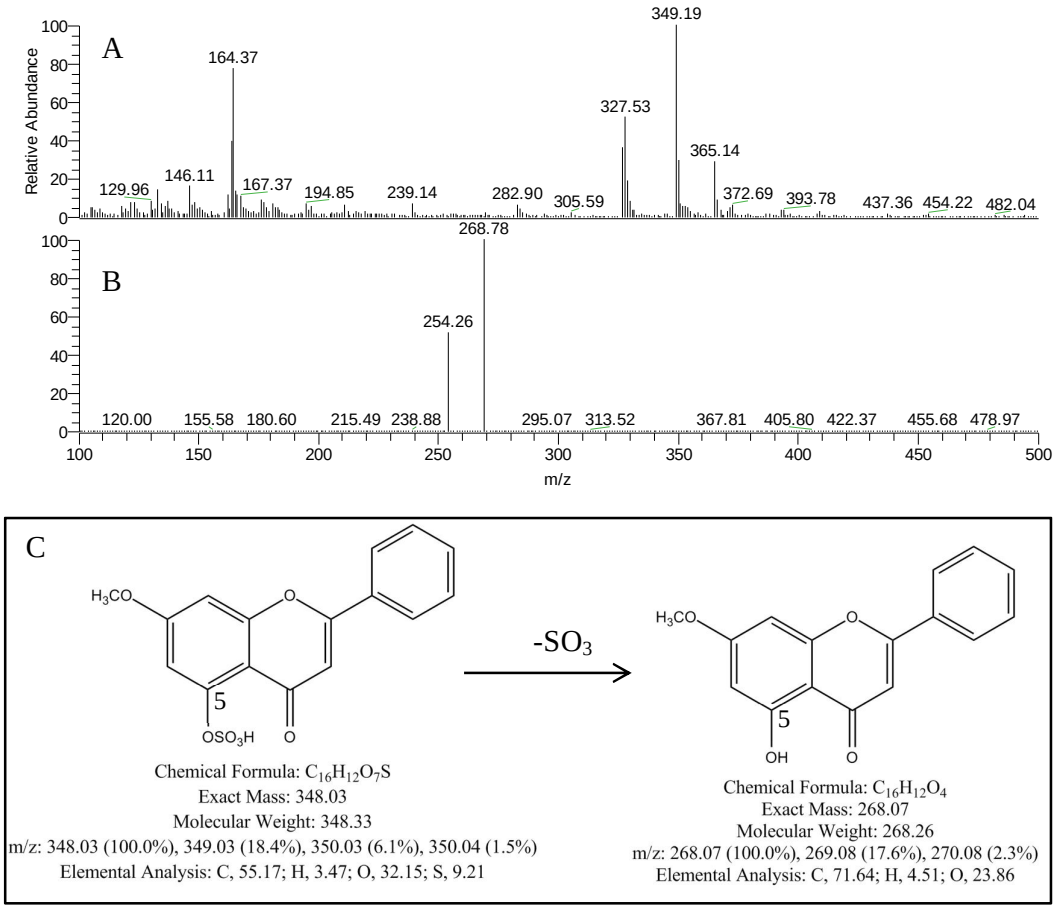

Figure 57 A: mass spectrum of metabolite in urine as full scan mode, B: product ions of the metabolite in MS/MS mode at m/z = 349 (M5), and C: fragmentation pathway of the metabolite in MS/MS mode

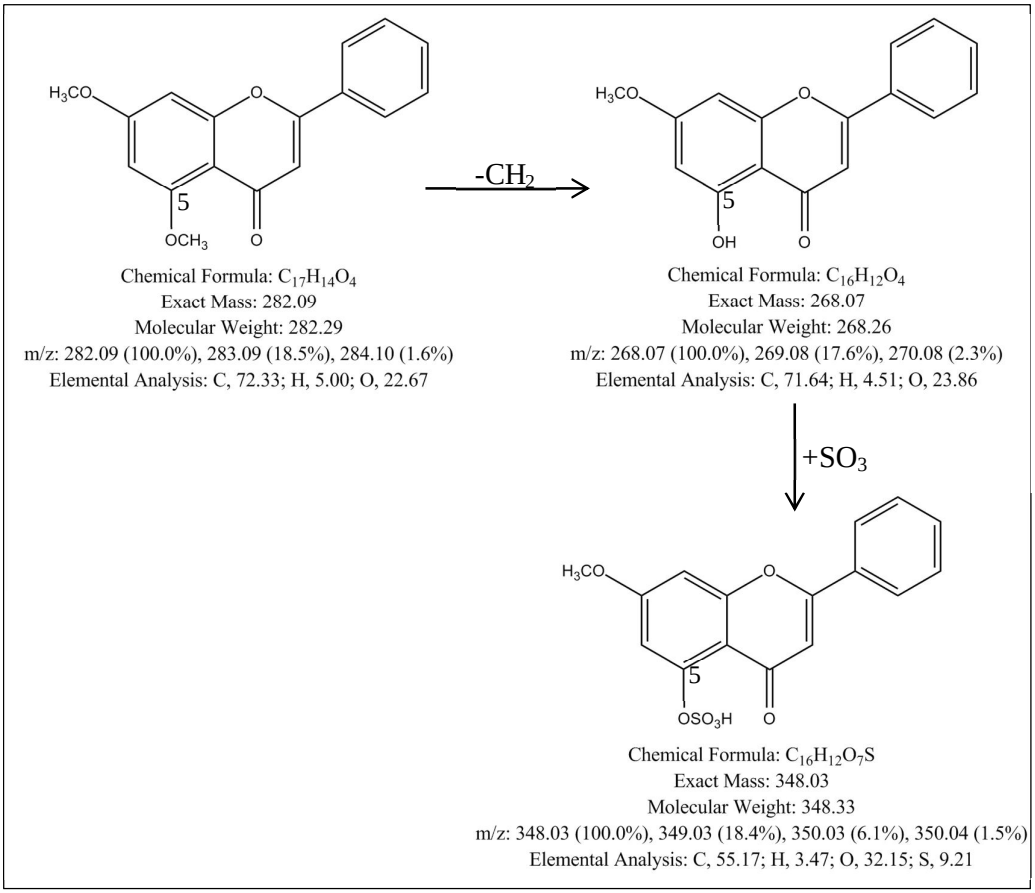

Figure 58 Proposed metabolic pathway of M5

6. $[M+H]^{+1}$ = 359 (M6)

The fragment ions at $[M+H]^{+1}$ signal at 342 formed by the loss of 16 amu (-O) from $[M+H]^{+1}$ signal at 359, from 342 amu to 328 amu resulting from the loss of $-CH_2$ molecule (-14), and from 328 amu to 298 amu resulting from the loss of $-OCH_3$ group (-30) as illustrated in Figure 59B and 59C. The molecular mass was 14 amu higher than that of PMF, indicating the demethylation of PMF at C-3' position (Figure 60).

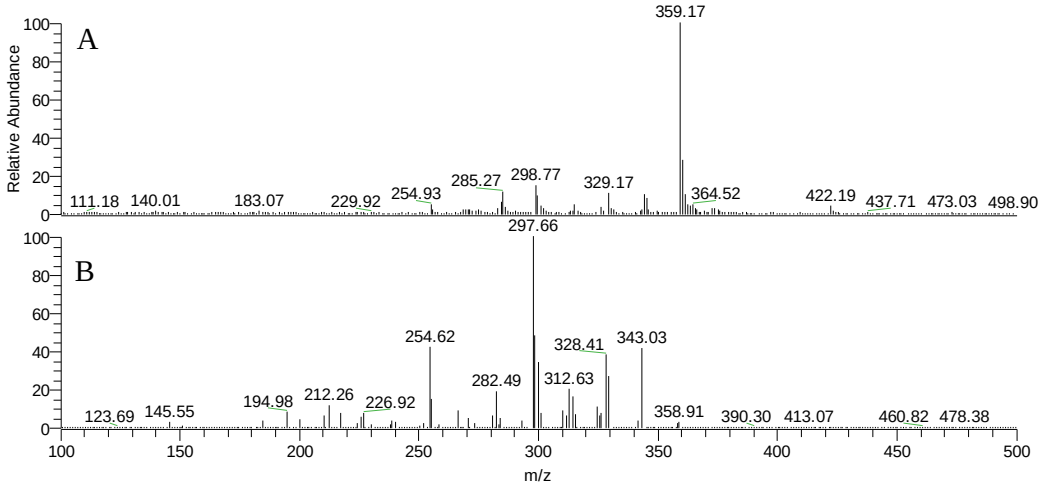

Figure 59 A: mass spectrum of metabolite in urine as full scan mode, B: product ions of the metabolite in MS/MS mode at m/z = 359 (M6), and C: fragmentation pathway of the metabolite in MS/MS mode

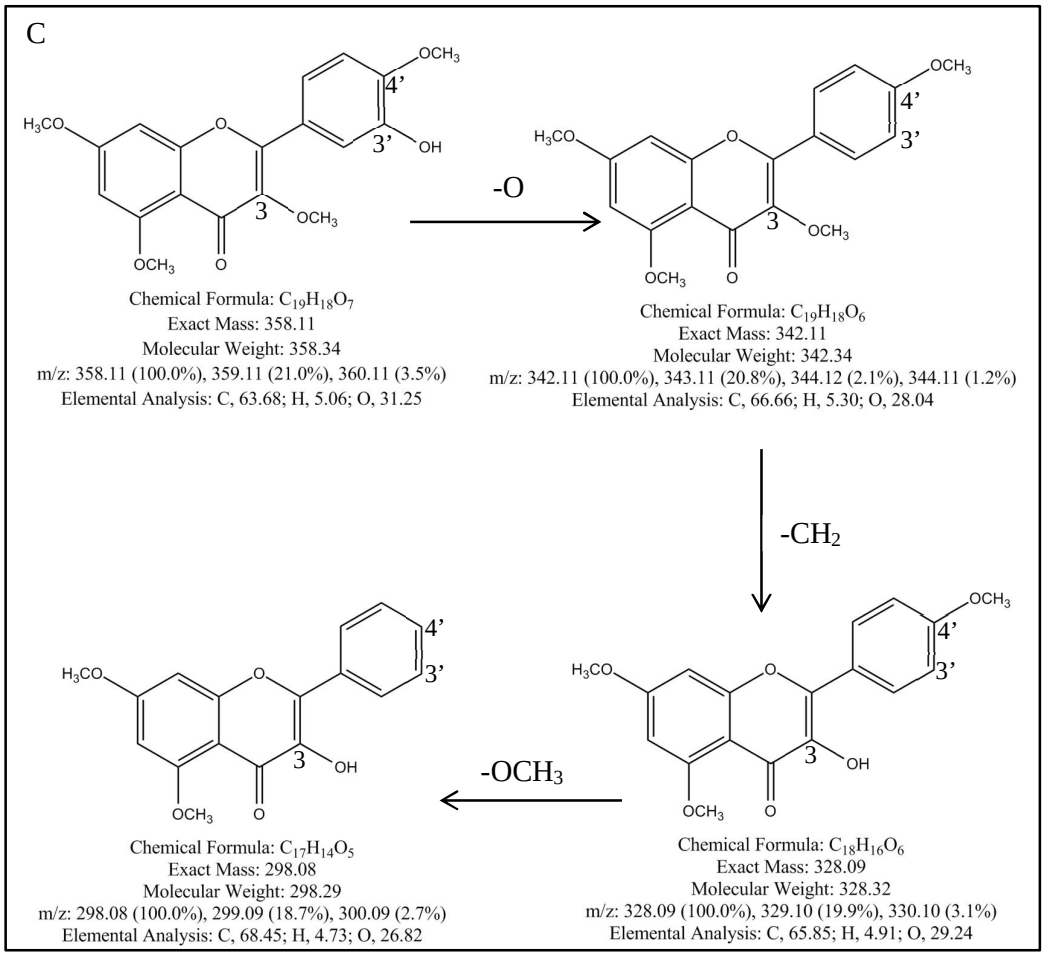

Figure 59 A: mass spectrum of metabolite in urine as full scan mode, B: product ions of the metabolite in MS/MS mode at m/z = 359 (M6), and C: fragmentation pathway of the metabolite in MS/MS mode (Cont.)

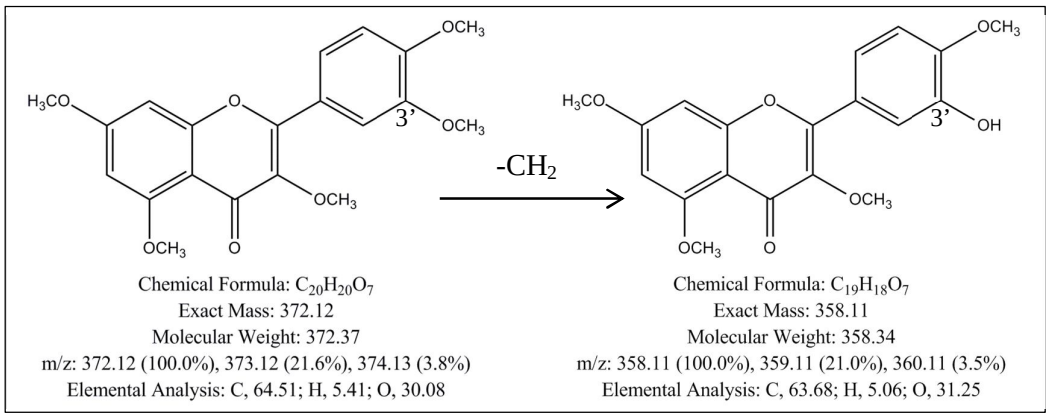

Figure 60 Proposed metabolic pathway of M6

7. $[M+H]^{+1}$ = 365 (M7)

The daughter ion spectrums obtained by MS/MS mode of parent ions at 365 m/z ratio contained fragment ions at $[M+H]^{+1}$ signals of 285, 269, and 255 amu (Figure 61B). These signals resulted from loss of $–SO_3$, -O, and $–CH_2$ for 285, 269, and 255 m/z ratios, respectively (Figure 61C). M7 was assumed that it was metabolized from TMF by demethylation reactions at C-5 and then further demethylation and sulfation reactions at C-7 of TMF molecule as shown in Figure 62.

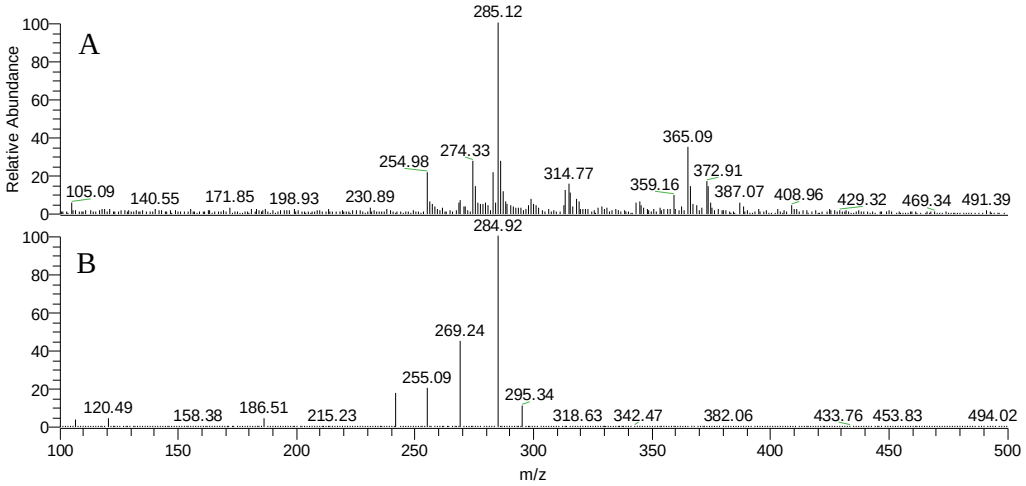

Figure 61 A: mass spectrum of metabolite in urine as full scan mode, B: product ions of the metabolite in MS/MS mode at m/z = 365 (M7), and C: fragmentation pathway of the metabolite in MS/MS mode

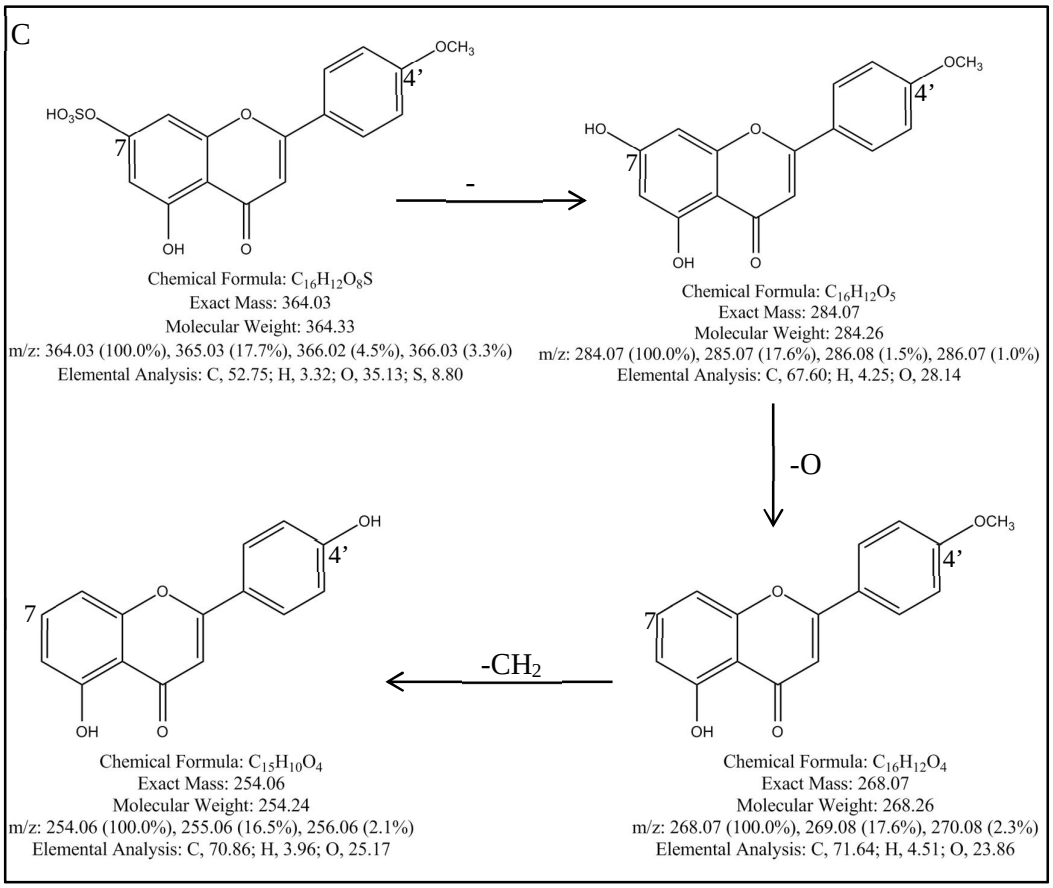

Figure 61 A: mass spectrum of metabolite in urine as full scan mode, B: product ions of the metabolite in MS/MS mode at m/z = 365 (M7), and C: fragmentation pathway of the metabolite in MS/MS mode (Cont.)

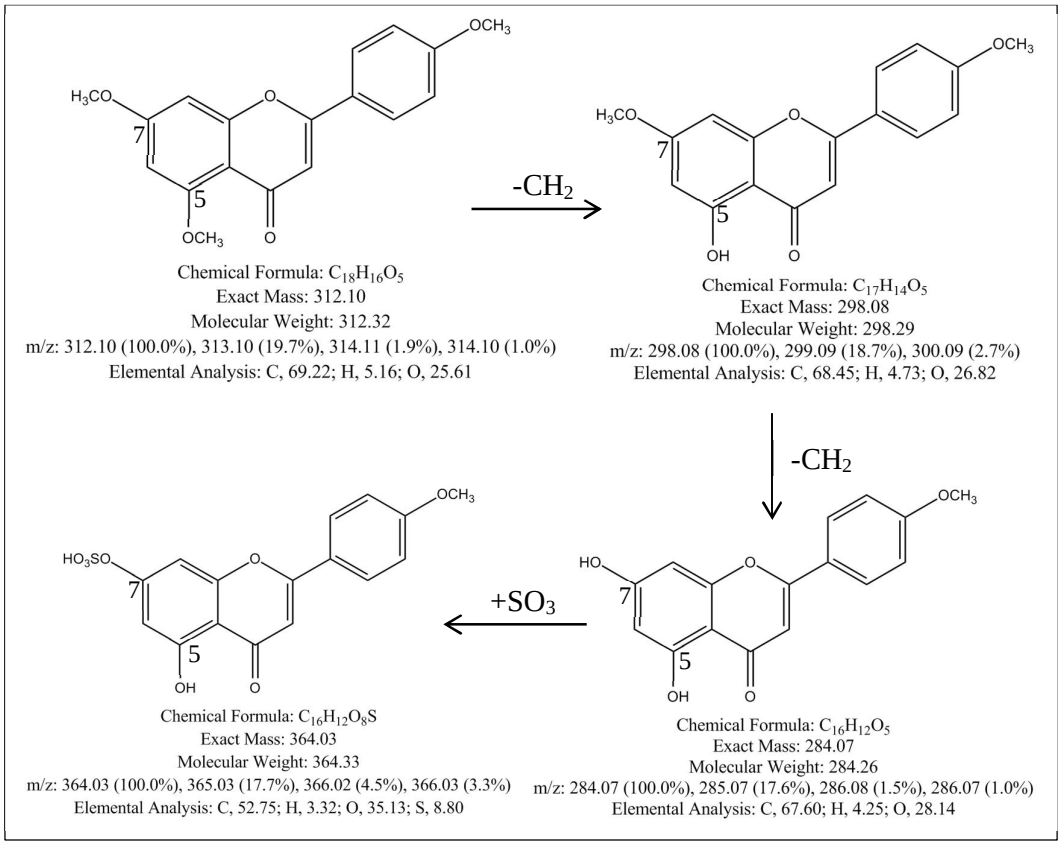

Figure 62 Proposed metabolic pathway of M7

8. $[M+H]^{+1}$ = 379 (M8)

The fragment ions at m/z 299, 285, and 255 came from loss of $–SO_3$ (-80 amu), $-CH_2$ (-14 amu), and $–OCH_3$ (-30 amu) groups, respectively (Figure 63B and 63C). M8 had a $[M+H]^{+1}$ signal at 379 that it was metabolized by demethylation and further sulfation reaction at C-5 position of TMF as presented in Figure 64.

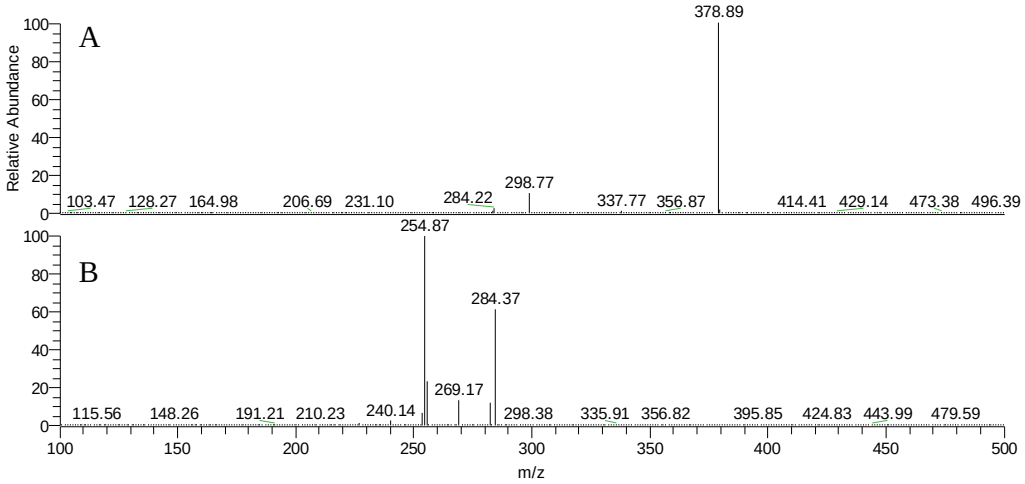

Figure 63 A: mass spectrum of metabolite in urine as full scan mode, B: product ions of the metabolite in MS/MS mode at m/z = 379 (M8), and C: fragmentation pathway of the metabolite in MS/MS mode

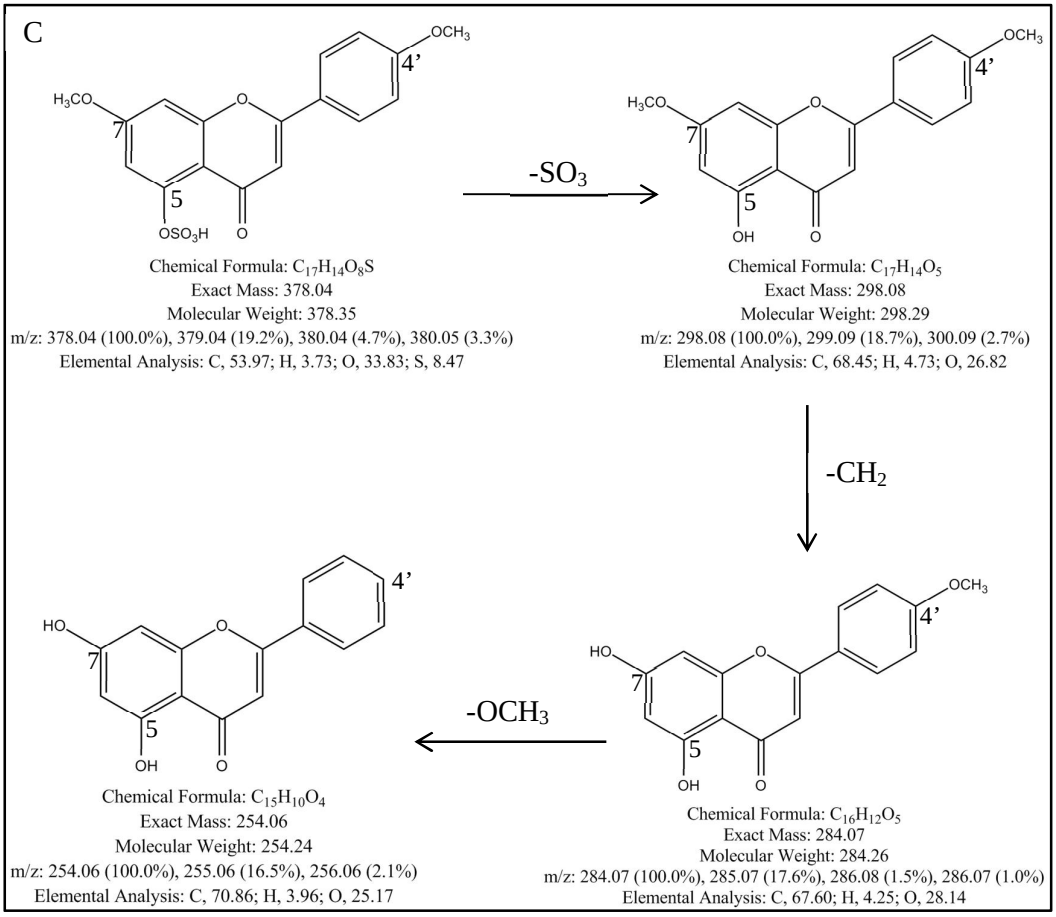

Figure 63 A: mass spectrum of metabolite in urine as full scan mode, B: product ions of the metabolite in MS/MS mode at m/z = 379 (M8), and C: fragmentation pathway of the metabolite in MS/MS mode (Cont.)

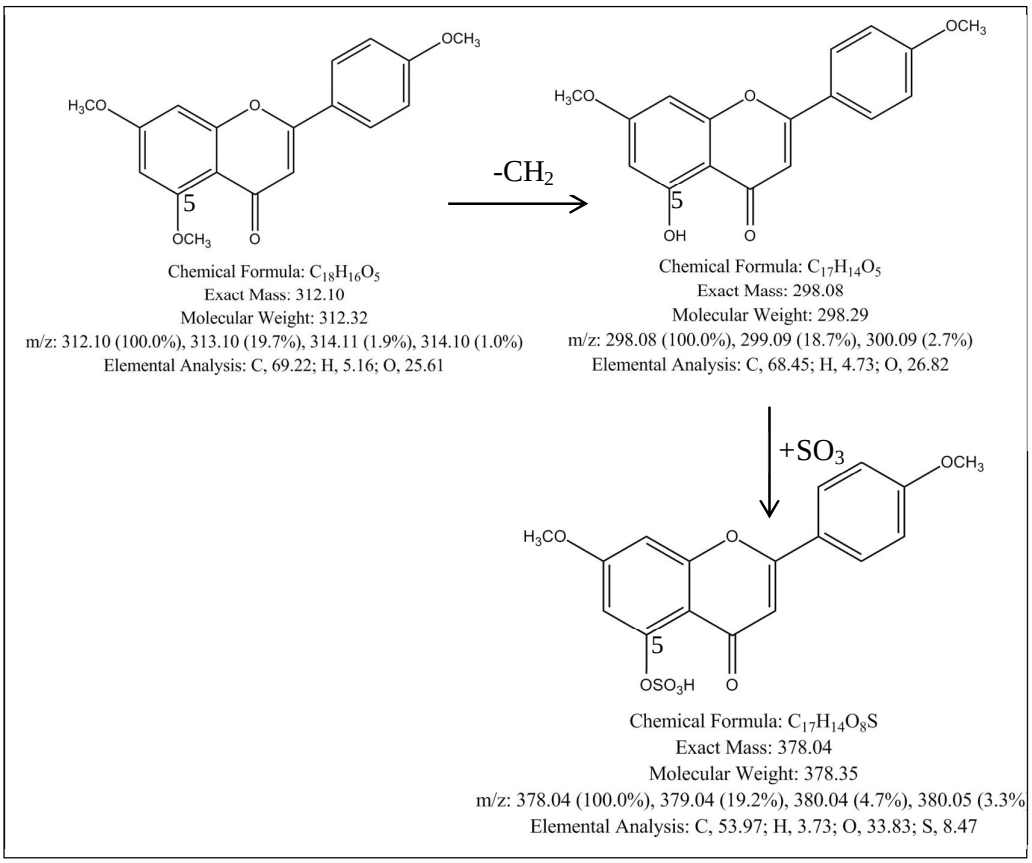

Figure 64 Proposed metabolic pathway of M8

9. $[M+H]^{+1}$ = 415 (M9)

The molecular mass was lost 176 amu (415 to 239 amu) as found in MS/MS mode (Figure 65B) indicating glucuronidation in the metabolism (Figure 65C). The demethylation at C-5 and C-7 positions of DMF occurred following oxidation at C-7 resulting in $[M+H]^{+1}$ signal at 239. Then, the compound at m/z 239 was metabolized by glucuronidation providing M9 as illustrated in Figure 66.

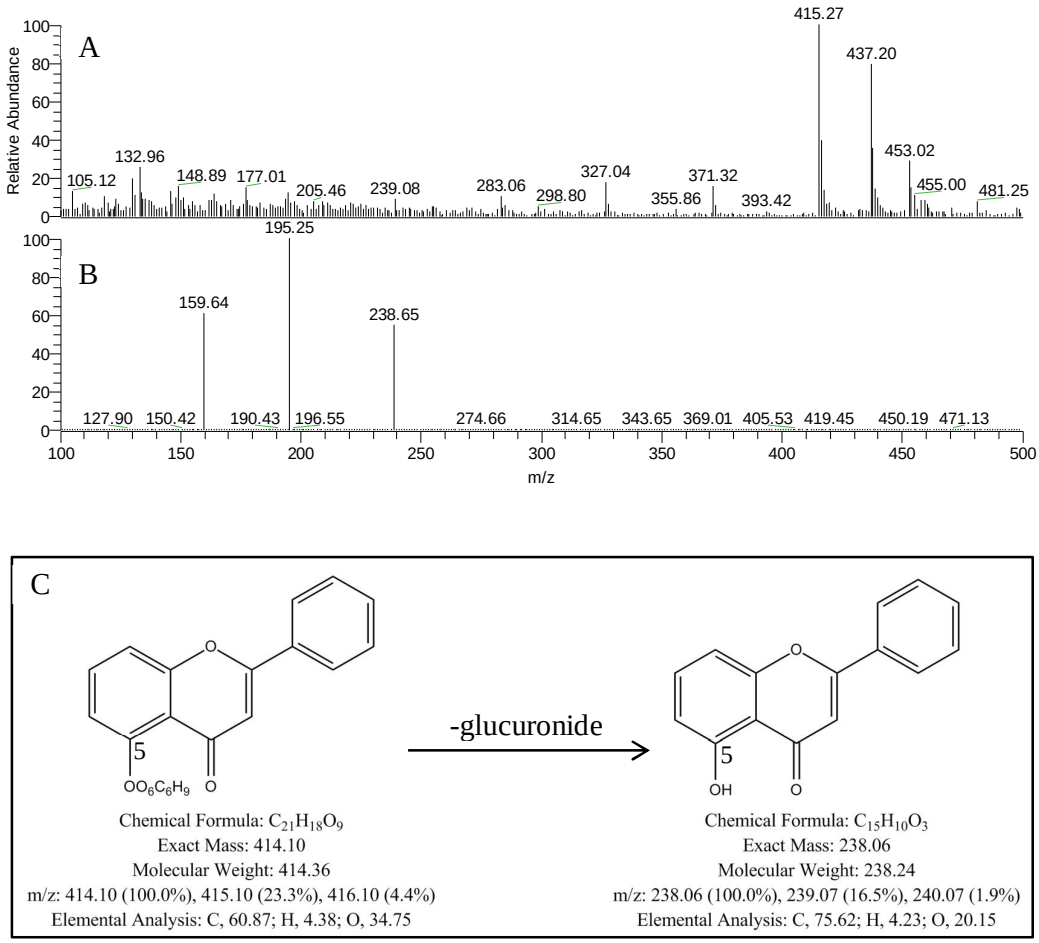

Figure 65 A: mass spectrum of metabolite in urine as full scan mode, B: product ions of the metabolite in MS/MS mode at m/z = 415 (M9), and C: fragmentation pathway of the metabolite in MS/MS mode

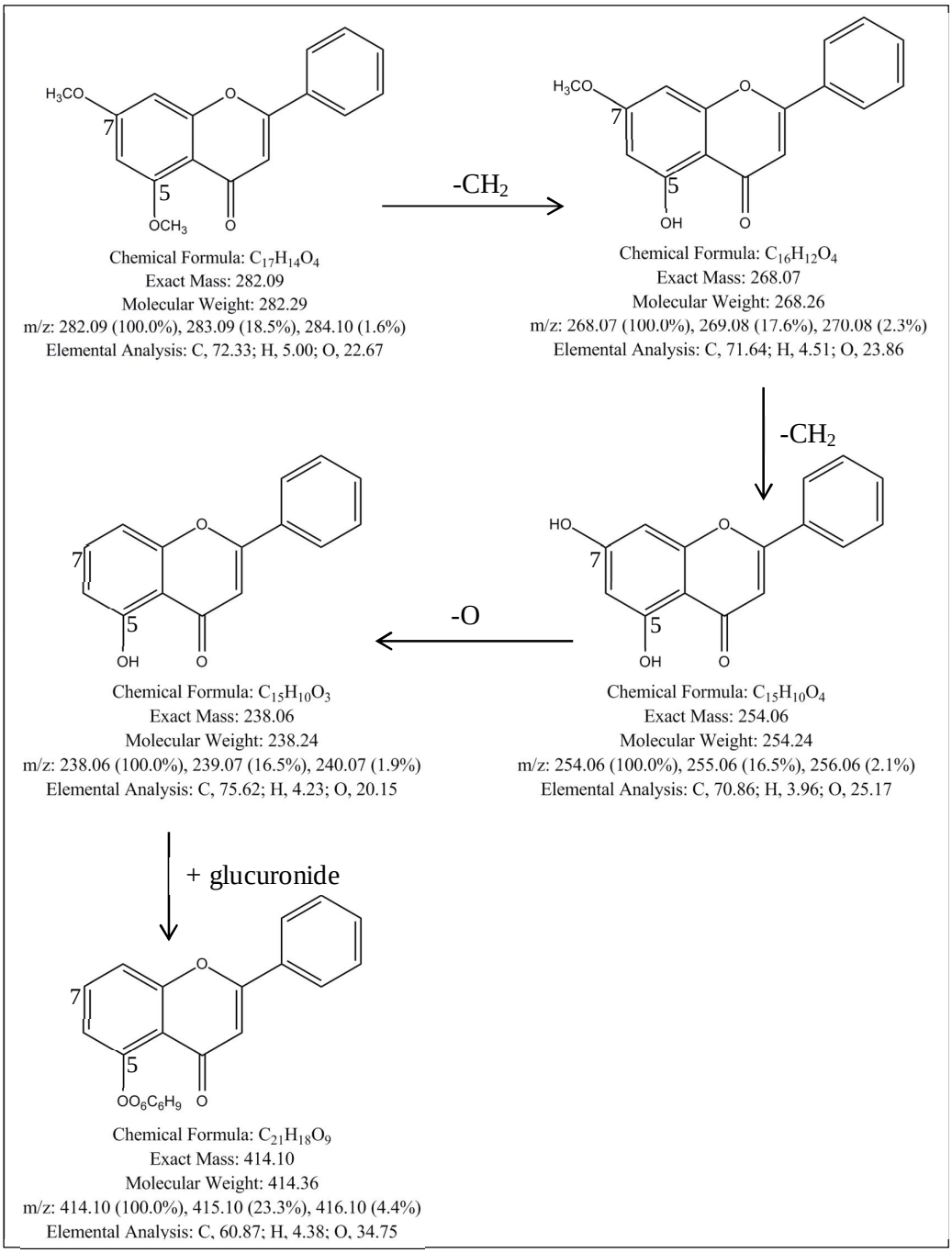

Figure 66 Proposed metabolic pathway of M9

Table 16 Proposed metabolic pathways of metabolites in rat urine receiving 750 mg/kg of KP solution

No.	$[M+H]^{+1}$	Reactions	Possible substrate of the metabolite
M1	255	demethylation	DMF
M2	285	demethylation	TMF
M3	315	demethylation	3,5,7,4'-tetramethoxyflavone
M4	345	demethylation	PMF
M5	349	demethylation, sulfation	DMF
M6	359	demethylation	PMF
M7	365	demethylation, sulfation	TMF
M8	379	demethylation, sulfation	TMF
M9	415	Glucuronidation	DMF

5.5.2.2 Metabolites in Feces of rat received KP solution

1. $[M+H]^{+1}$ = 255 (M10)

From the fragment pathway (Figure 67C), the fragment ion at m/z 239 resulted from loss of oxygen (-16 amu.) of parent ion (m/z 255) as shown in Figure 67B. M10 had a $M+H]^{+1}$ signal at m/z 255, that was 28 amu lower than DMF molecule ($M+H]^{+1}$ = 283). This finding suggested the loss of two molecules of $-CH_2$ at C-5 and C-7 position of DMF (Figure 68).

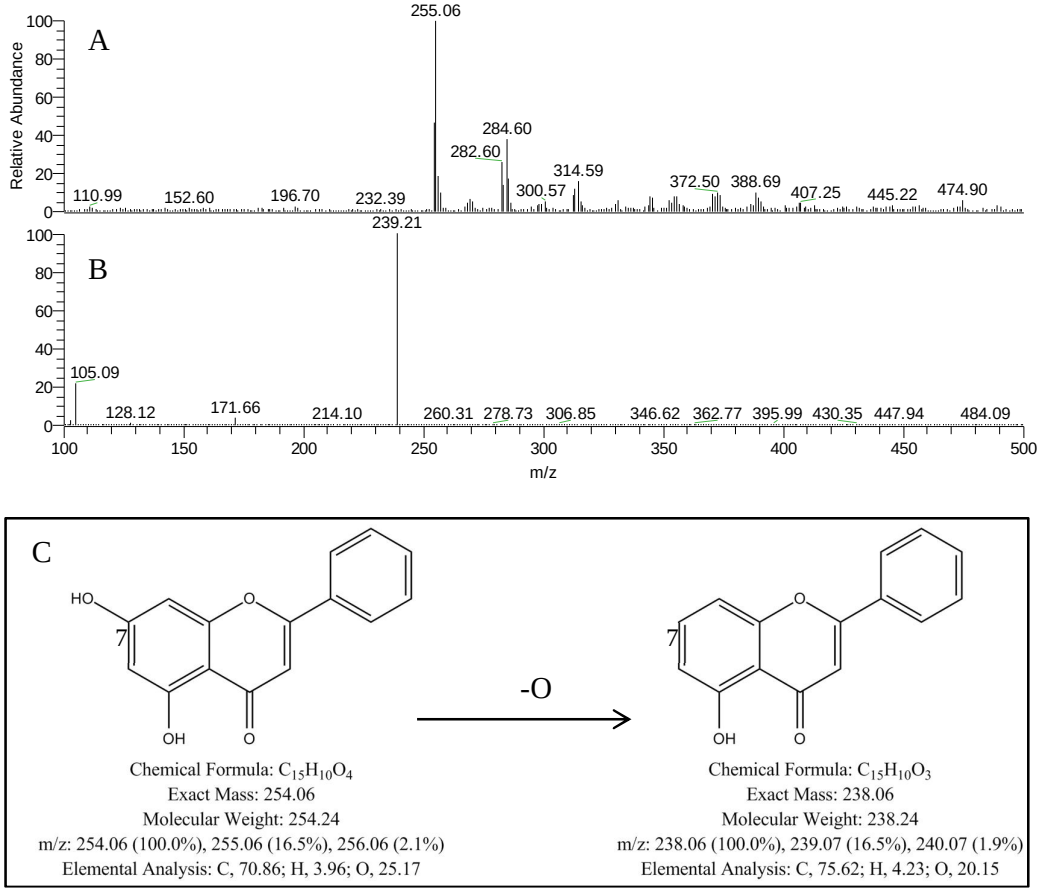

Figure 67 A: mass spectrum of metabolite in feces as full scan mode, B: product ions of the metabolite in MS/MS mode at m/z = 255 (M10), and C: fragmentation pathway of the metabolite in MS/MS mode

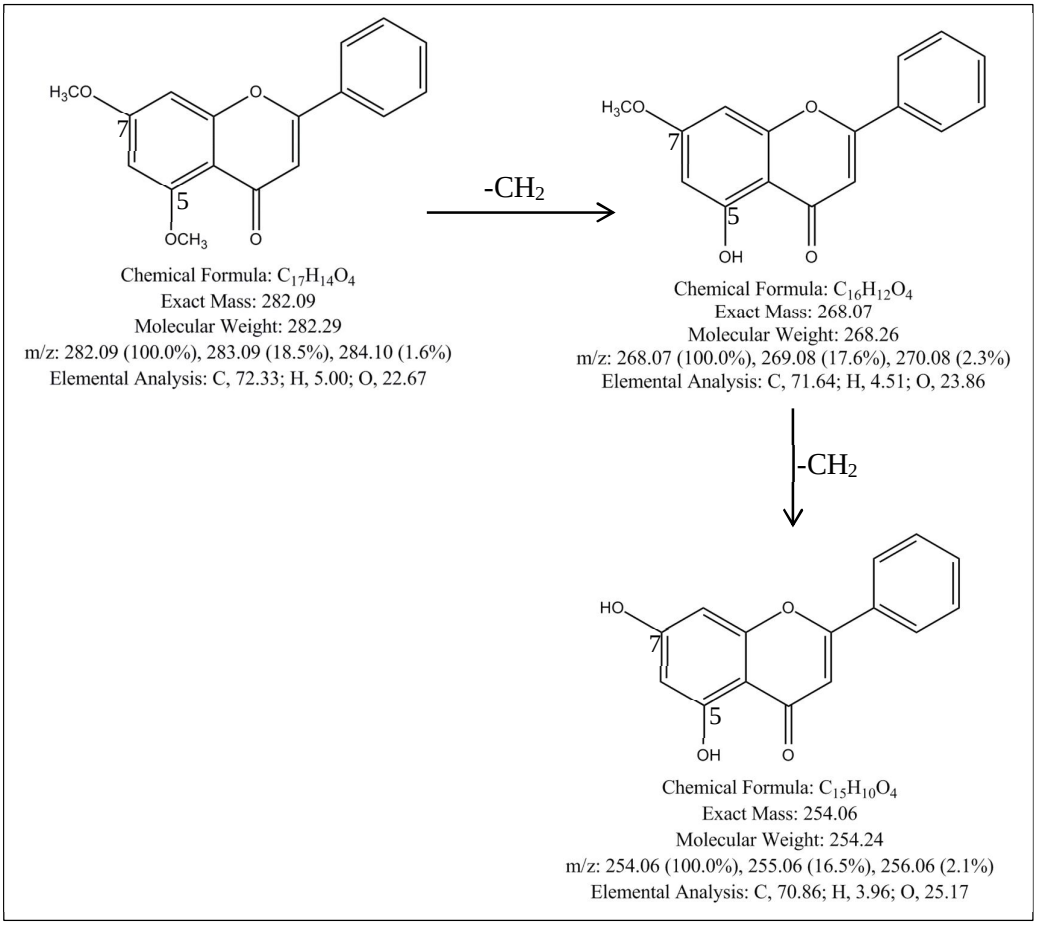

Figure 68 Proposed metabolic pathway of M10

2. $[M+H]^{+1}$ = 285 (M11)

The daughter ion that obtained from MS/MS mode of parent ion at m/z 285 was 269 amu suggesting the loss of oxygen atom (-16 amu) from parent ion as illustrated in Figure 69B and 69C. $[M+H]^{+1}$ signal at m/z 285 was assumed that it was metabolized from TMF by demethylation reaction at C-5 and C-4' of TMF molecule (Figure 70).

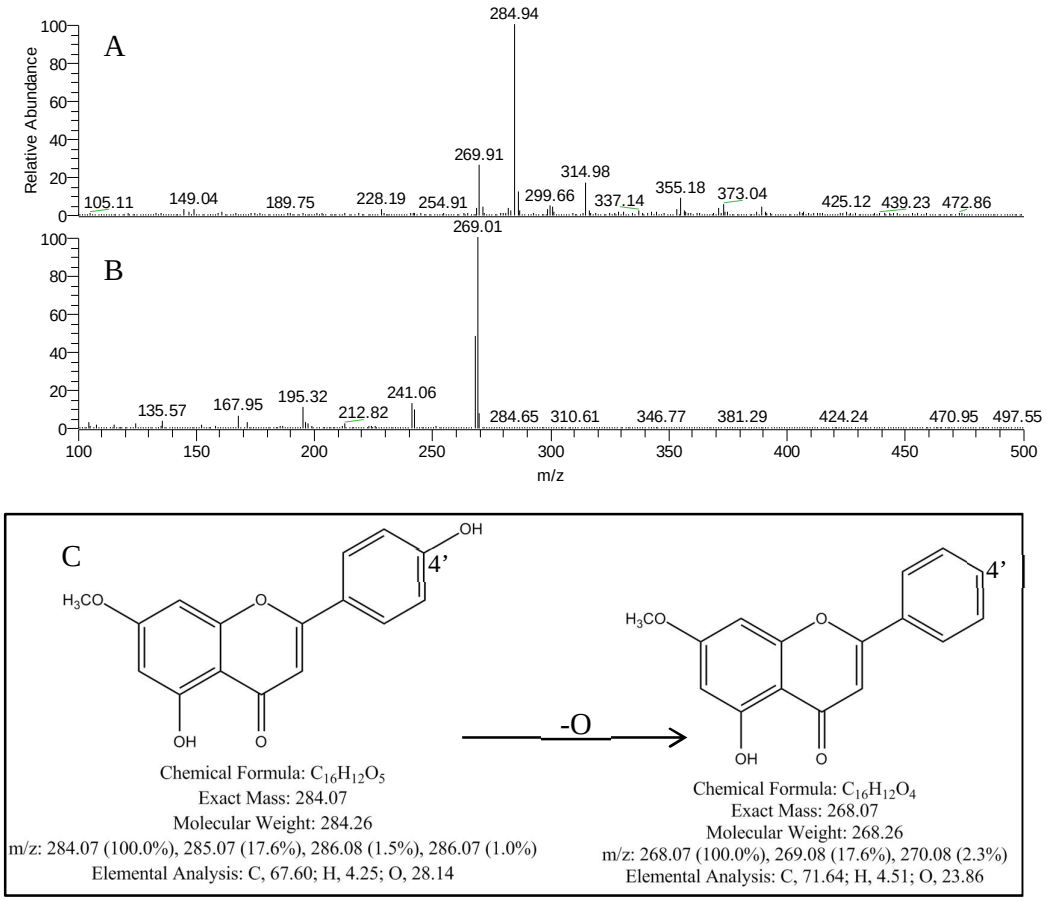

Figure 69 A: mass spectrum of metabolite in feces as full scan mode, B: product ions of the metabolite in MS/MS mode at m/z = 285 (M11), and C: fragmentation pathway of the metabolite in MS/MS mode

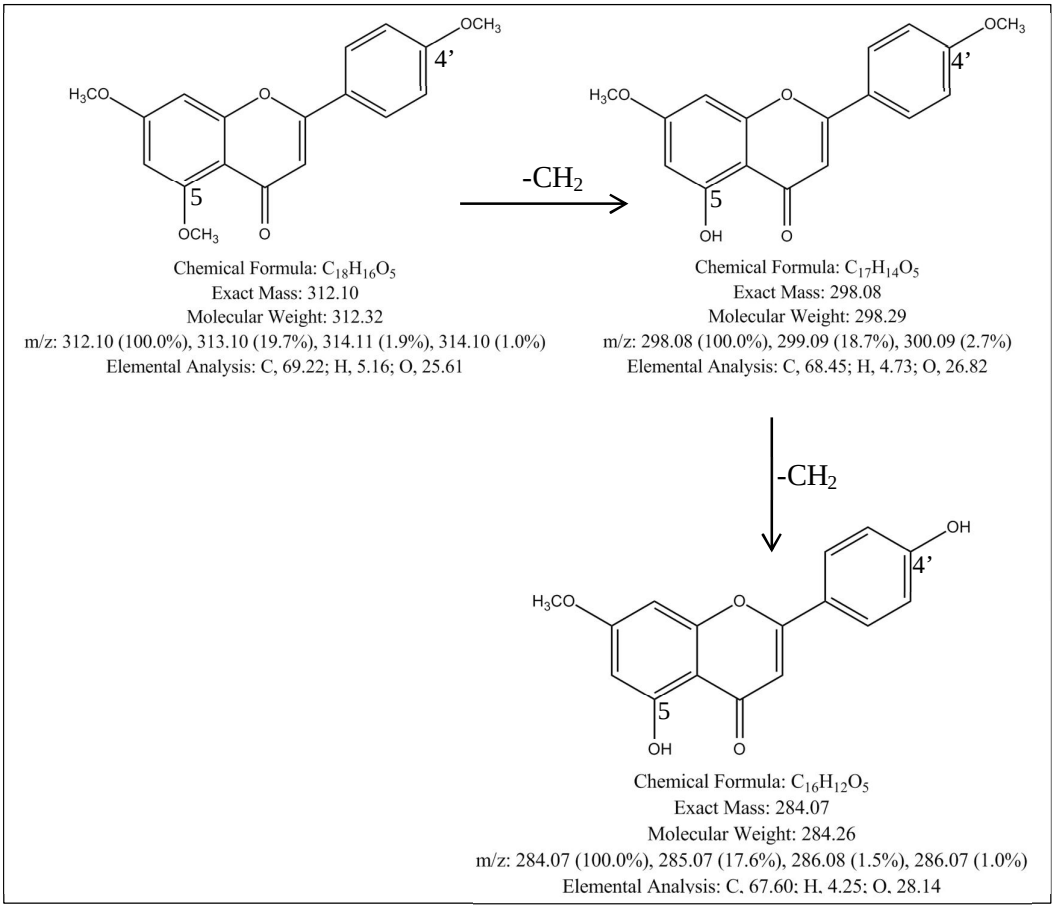

Figure 70 Proposed metabolic pathway of M11

3. $[M+H]^{+1}$ = 301 (M12)

The daughter ion at m/z 285 was produced by loss of 16 amu (-O) from the $[M+H]^{+1}$ signal at m/z 301, from m/z 285 to m/z 269 by loss –O, from m/z 269 to m/z 255 by loss $–CH_2$ as presented in Figure 71B and 71C. 3,5,7,4'-tetramethoxyflavone was metabolized at C-5, C-3, and C-4' positions by demethylation reactions providing M12 (Figure 72).

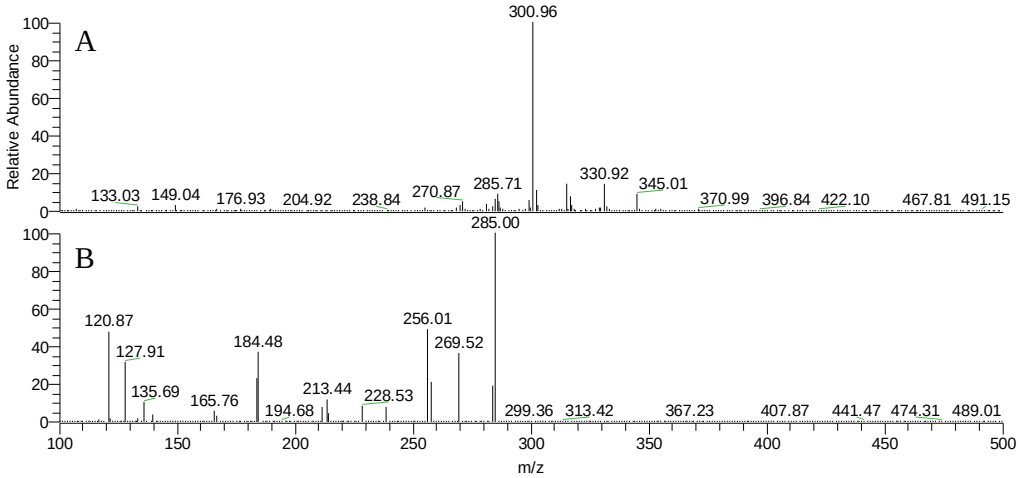

Figure 71 A: mass spectrum of metabolite in feces as full scan mode, B: product ions of the metabolite in MS/MS mode at m/z = 301 (M12), and C: fragmentation pathway of the metabolite in MS/MS mode

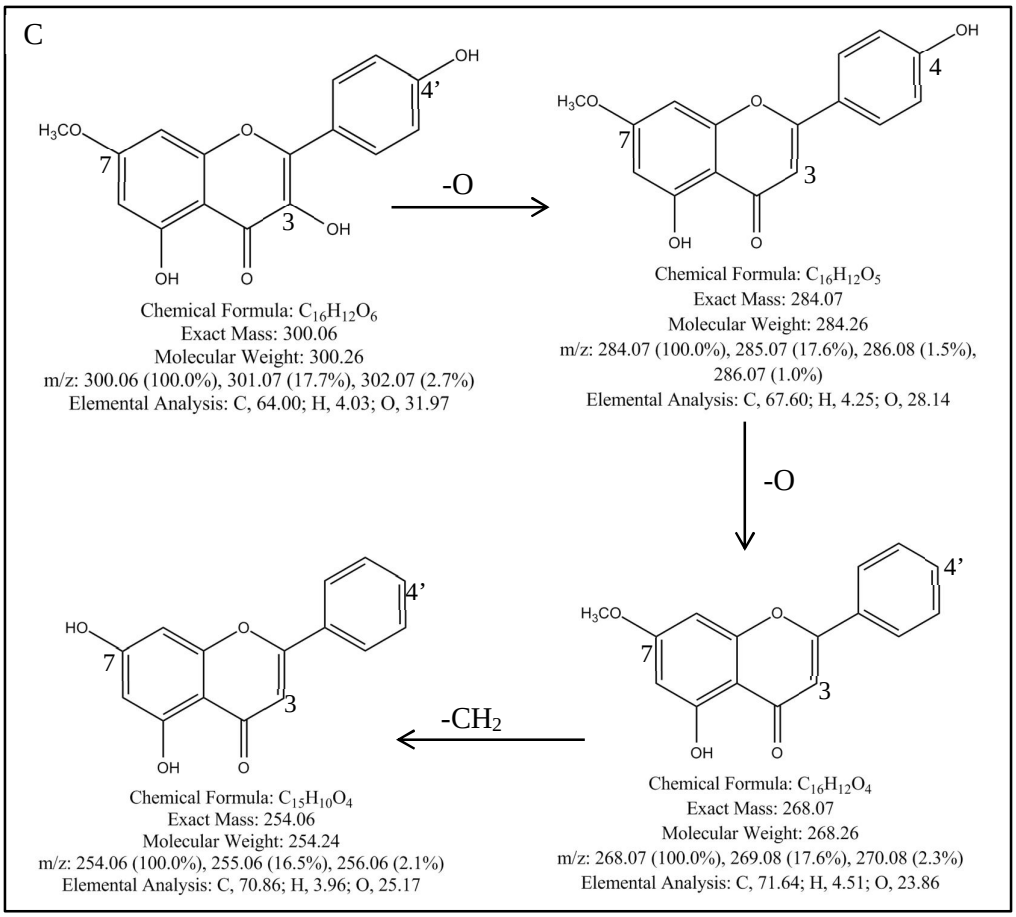

Figure 71 A: mass spectrum of metabolite in feces as full scan mode, B: product ions of the metabolite in MS/MS mode at m/z = 301 (M12), and C: fragmentation pathway of the metabolite in MS/MS mode (Cont.)

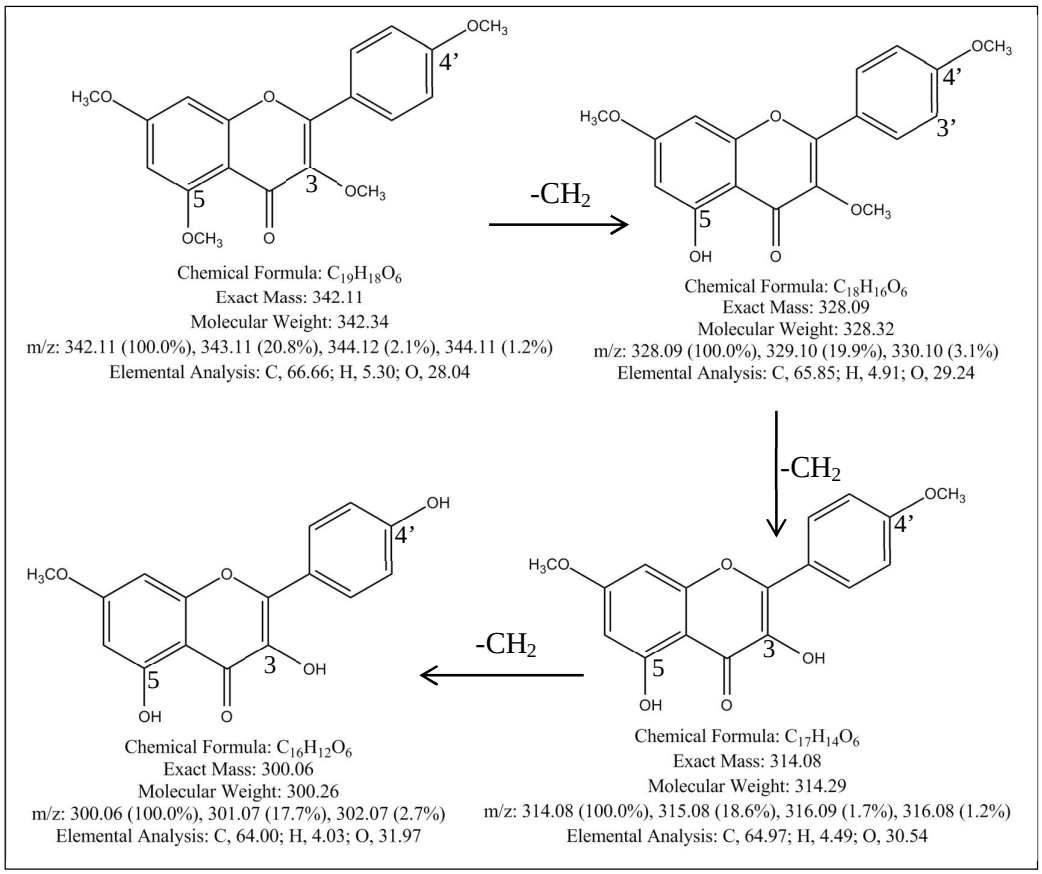

Figure 72 Proposed metabolic pathway of M12

4. $[M+H]^{+1}$ = 315 (M13)

M/z ratios at 299, 285, and 271 were the fragment ions from $[M+H]^{+1}$ signal m/z at 315 suggesting loss of –O, $–CH_2$, and $–CH_2$ molecules from the parent ion, respectively as shown (Figure 73B and 73C). M13 was the metabolite of 3,5,7,4'-tetramethoxyflavone by demethylation at C-5 and C-3 positions (Figure 74).

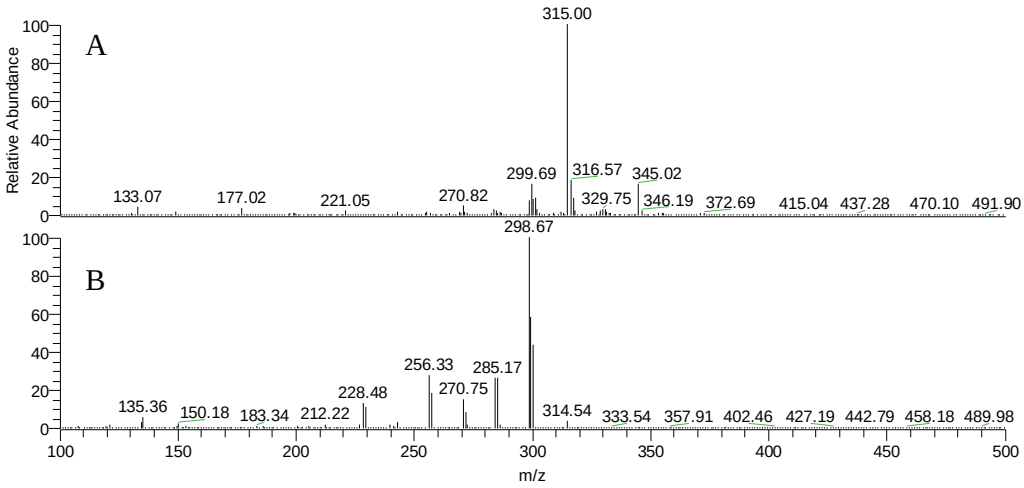

Figure 73 A: mass spectrum of metabolite in feces as full scan mode, B: product ions of the metabolite in MS/MS mode at m/z = 315 (M13), and C: fragmentation pathway of the metabolite in MS/MS mode

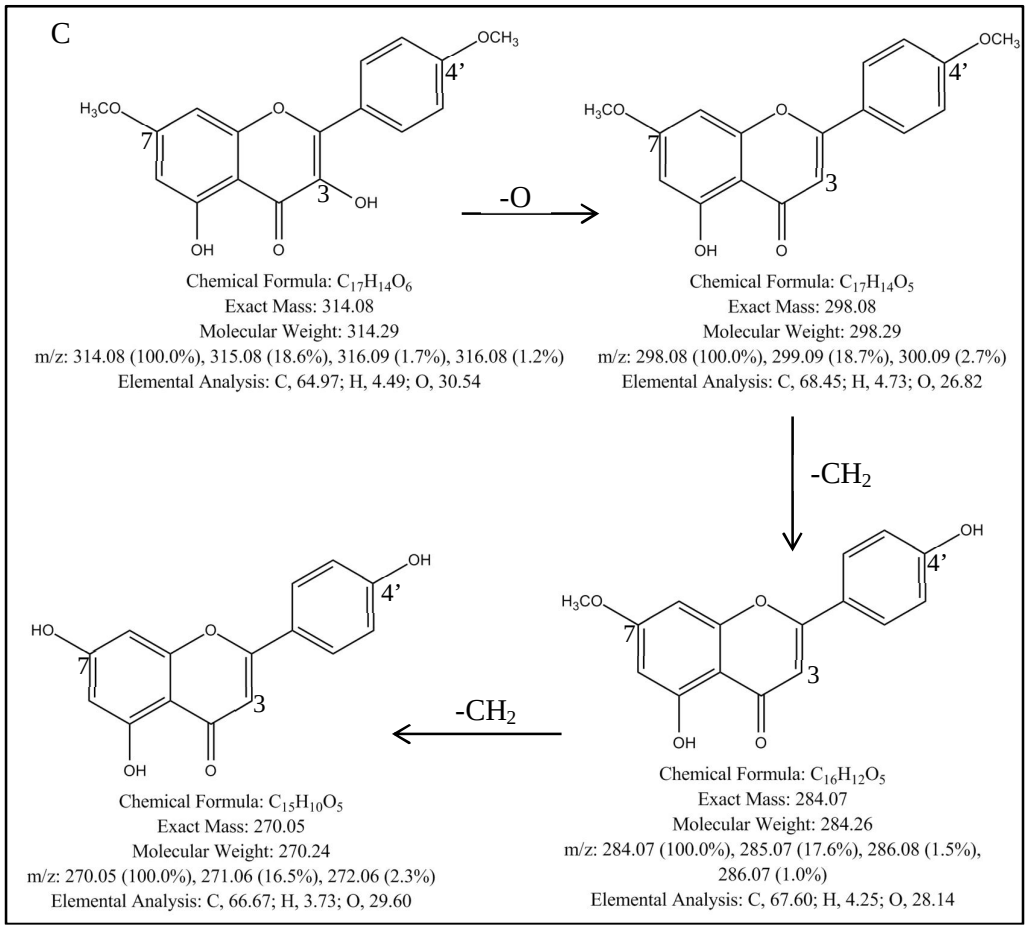

Figure 73 A: mass spectrum of metabolite in feces as full scan mode, B: product ions of the metabolite in MS/MS mode at m/z = 315 (M13), and C: fragmentation pathway of the metabolite in MS/MS mode (Cont.)

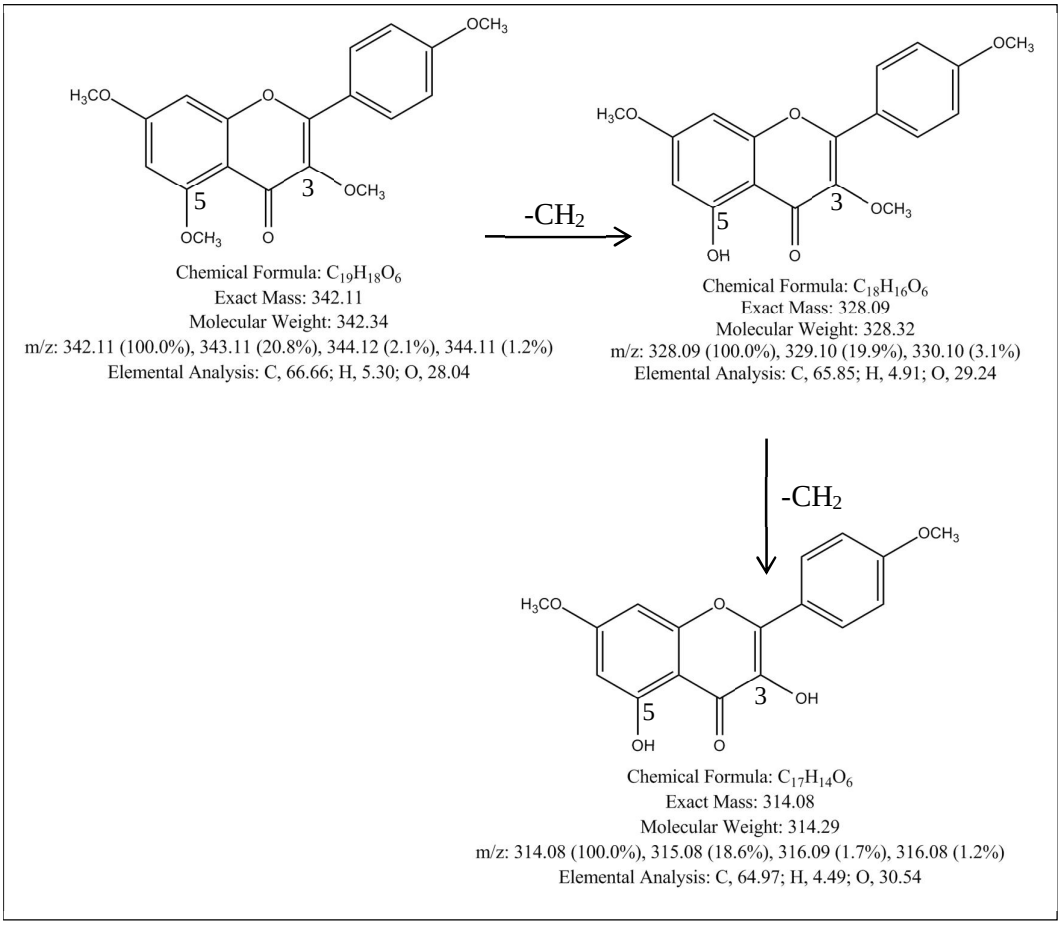

Figure 74 Proposed metabolic pathway of M13

5. $[M+H]^{+1}$ = 331 (M14)

$[M+H]^{+1}$ signal m/z at 331 was fragmented in MS/MS mode providing the fragment ions at 315, 299, 285, 269, and 255 amu (Figure 75B). As shown in Figure 73C, the daughter ion at 315 was loss –O from m/z 331, m/z 299 was loss –O from m/z 315, m/z 285 was loss $–CH_2$ from m/z 299, m/z 269 was loss – CH_2 from m/z 285, and m/z 255 was loss – CH_2 from m/z 269. M14 was assumed that it was demethylated at C-3', C-5, and C-3 positions of PMF molecule (Figure 76).

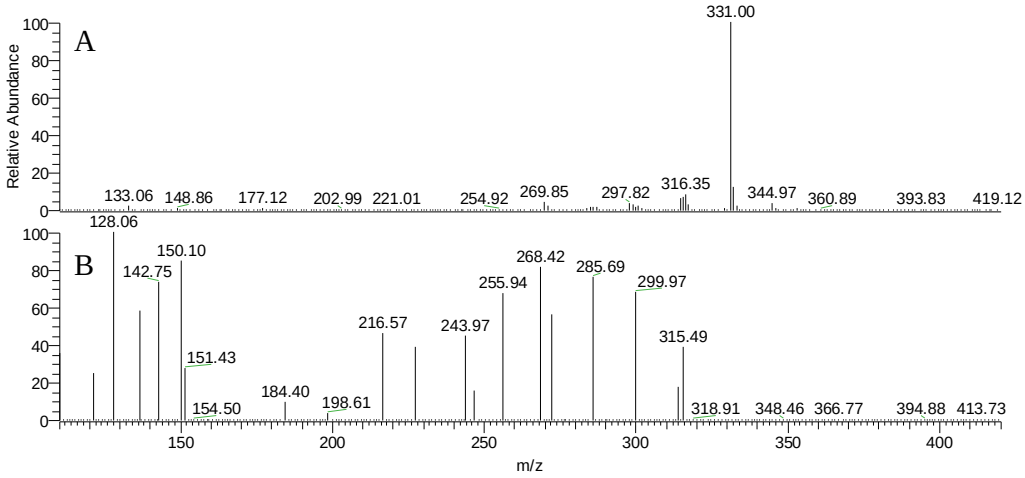

Figure 75 A: mass spectrum of metabolite in feces as full scan mode, B: product ions of the metabolite in MS/MS mode at m/z = 331 (M14), and C: fragmentation pathway of the metabolite in MS/MS mode

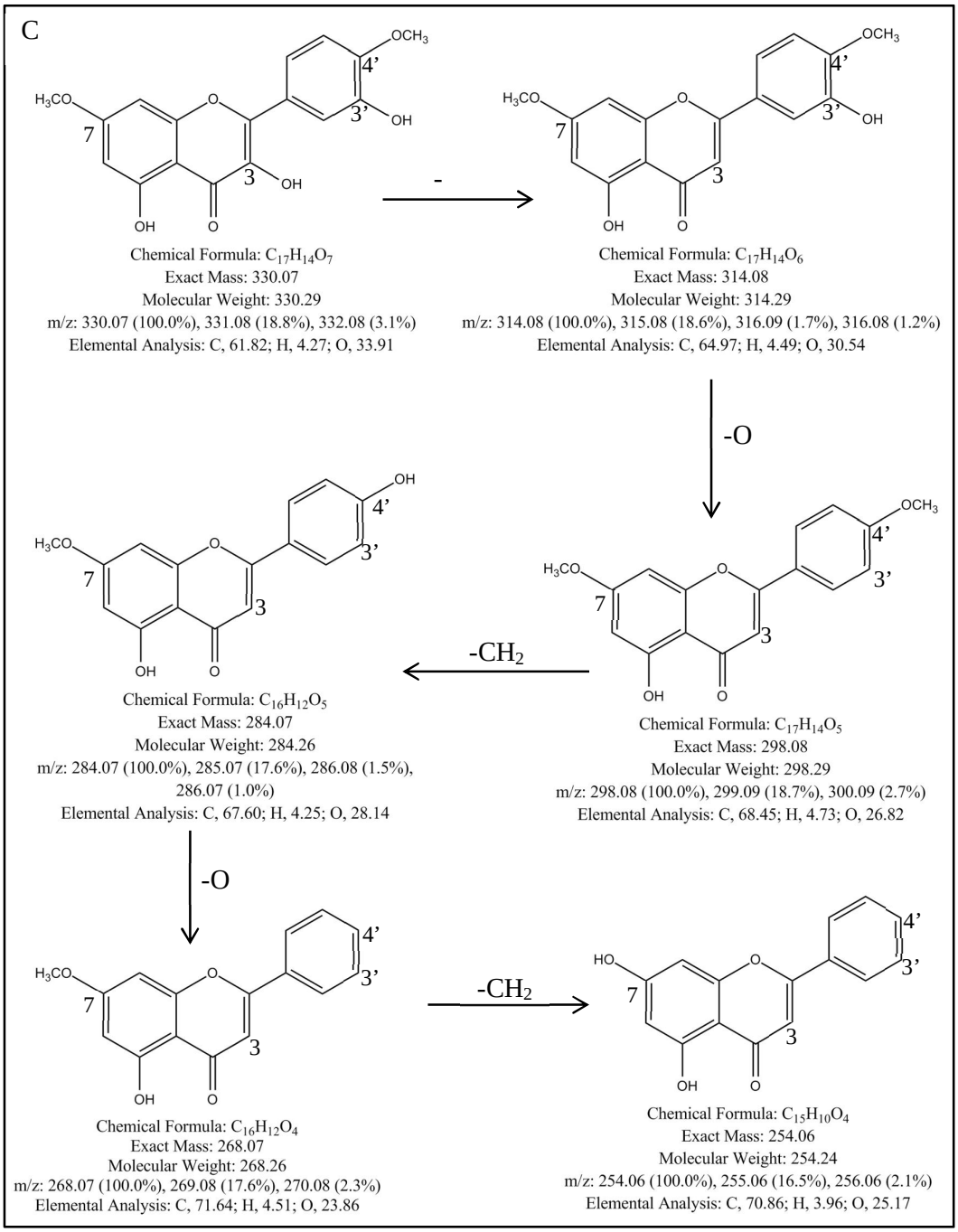

Figure 75 A: mass spectrum of metabolite in feces as full scan mode, B: product ions of the metabolite in MS/MS mode at m/z = 331 (M14), and C: fragmentation pathway of the metabolite in MS/MS mode (Cont.)

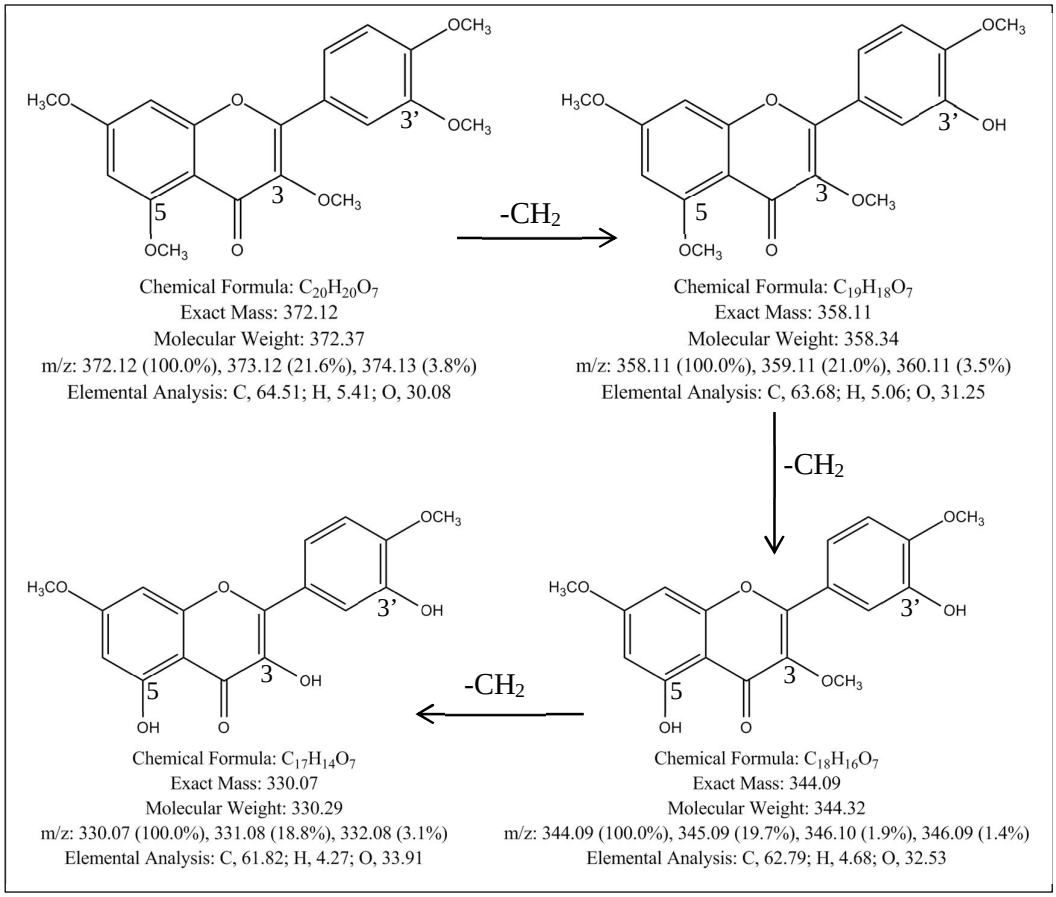

Figure 76 Proposed metabolic pathway of M14

6. $[M+H]^{+1}$ = 345 (M15)

From Figure 77B, m/z 329, 299, and 285 were the daughter ions in MS/MS mode of the parent ion at $[M+H]^{+1}$ 345. The proposed fragment pathway was illustrated in Figure 77C including the loss of -O, -OCH_2, and –CH_2. Demethylation at C-3' and C-5 position of PMF molecules were the reaction providing M15 (Figure 78).

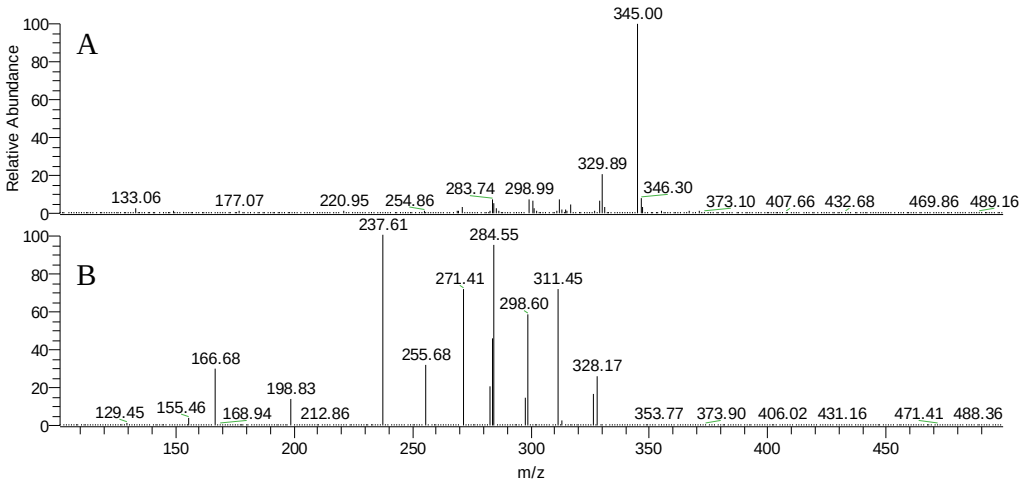

Figure 77 A: mass spectrum of metabolite in feces as full scan mode, B: product ions of the metabolite in MS/MS mode at m/z = 345 (M15), and C: fragmentation pathway of the metabolite in MS/MS mode

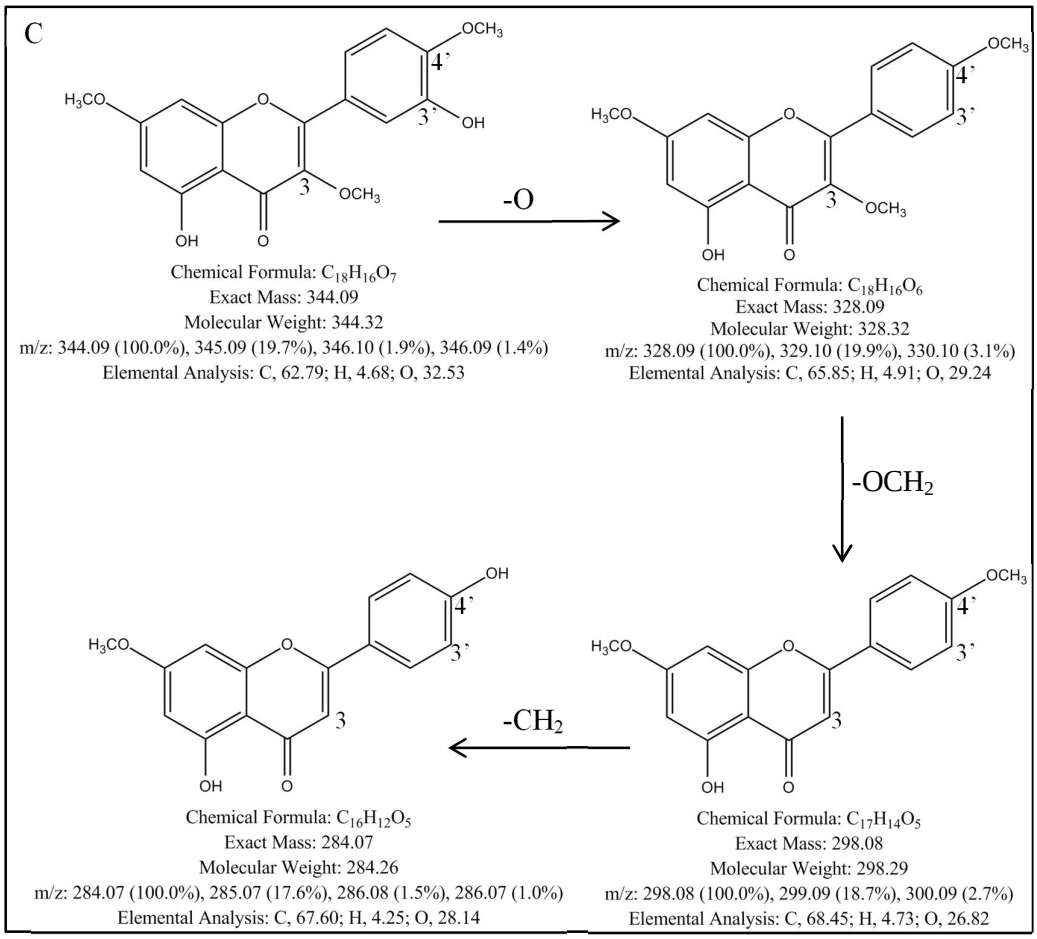

Figure 77 A: mass spectrum of metabolite in feces as full scan mode, B: product ions of the metabolite in MS/MS mode at m/z = 345 (M15), and C: fragmentation pathway of the metabolite in MS/MS mode (Cont.)

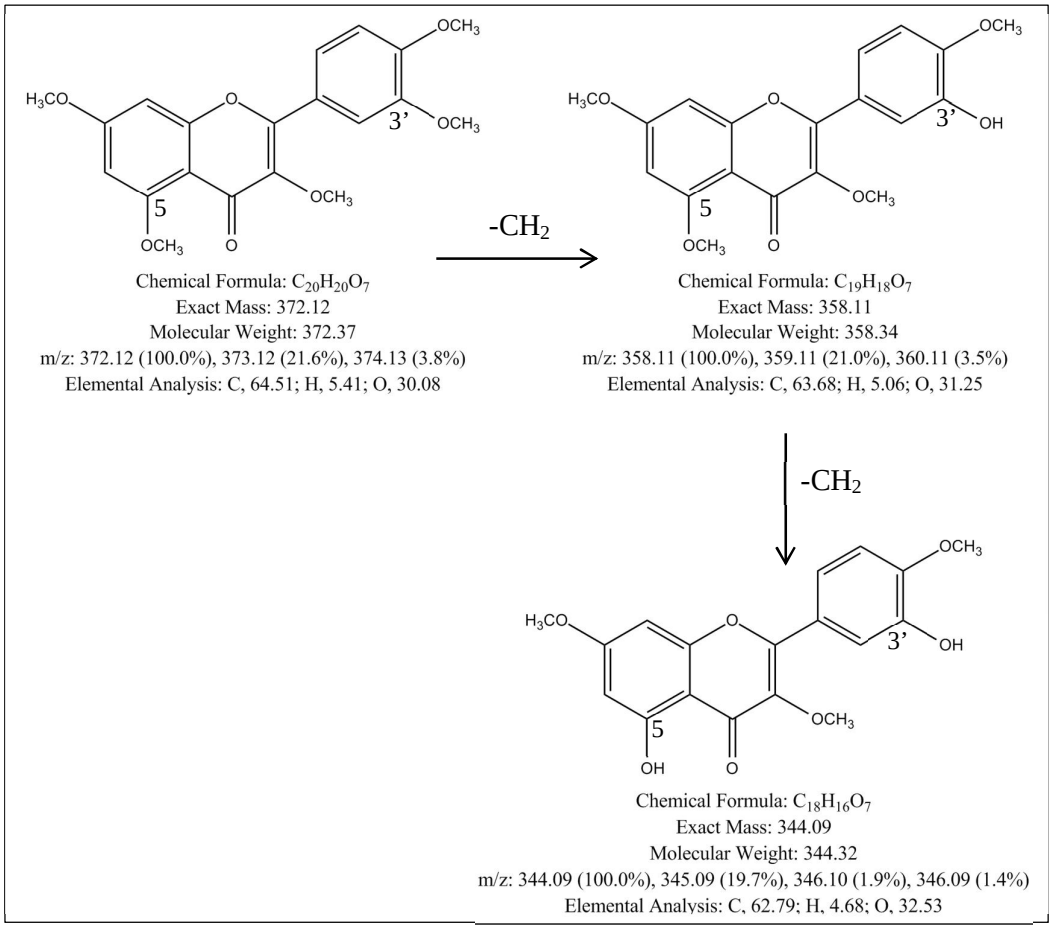

Figure 78 Proposed metabolic pathway of M15

Table 17 Proposed metabolic pathways of metabolites in rat feces receiving 750 mg/kg of KP solution

No.	$[M+H]^{+1}$	Reactions	Possible substrate of the metabolite
M10	255	demethylation	DMF
M11	285	demethylation	TMF
M12	301	demethylation	3,5,7,4'-tetramethoxyflavone
M13	315	demethylation	3,5,7,4'-tetramethoxyflavone
M14	331	demethylation	PMF
M15	345	demethylation	PMF

6. Products development for oral bioavailability enhancement of KP crude extract

6.1 HPLC system

HPLC system that was developed by using Shimadzu®-UFLC DAD detector was successfully analyzed the methoxyflavones in KP crude extract. The HPLC chromatograms of KP crude extract and the mixture of PMF, TMF and DMF were shown in Figure 79 and 80, respectively.

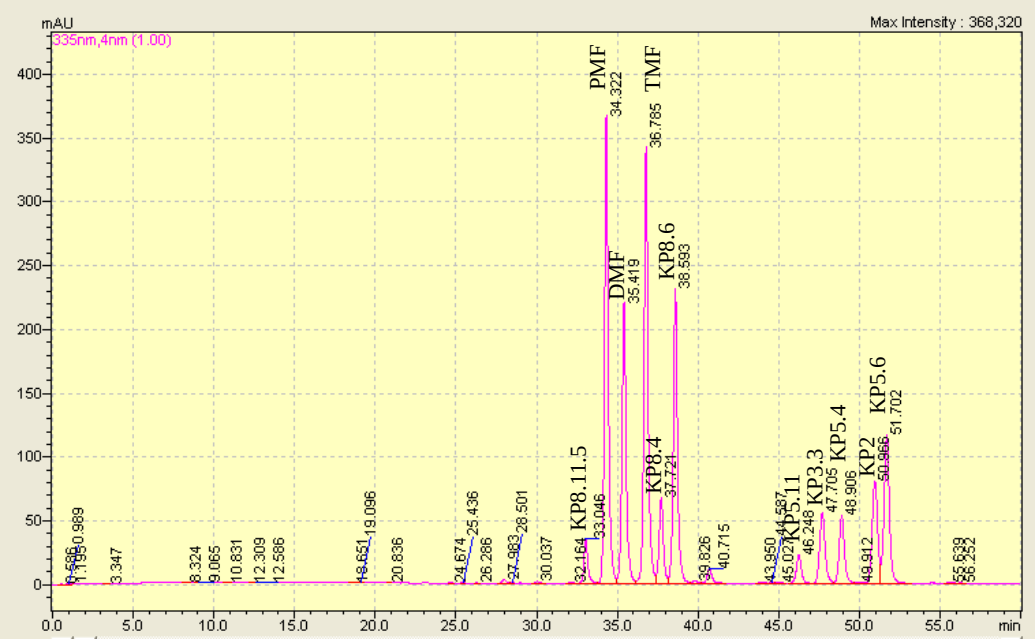

Figure 79 HPLC chromatogram of KP crude extract (0.400 mg/ml, KP8.11.5: 5,7,3',4'-tetramethoxyflavone, KP8.4: 3,5,7-trimethoxyflavone, KP8.6: 3,5,7,4'-tetramethoxyflavone, KP5.11: 5-OH-3,7,3',4'-tetramethoxyflavone, KP3.3: 5-OH-7-methoxyflavone, KP5.4: 5-OH-7,4'-dimethoxyflavone, KP2: 5-OH-3,7-dimethoxyflavone KP5.6: 5-OH-3,7,4'-trimethoxyflavone)

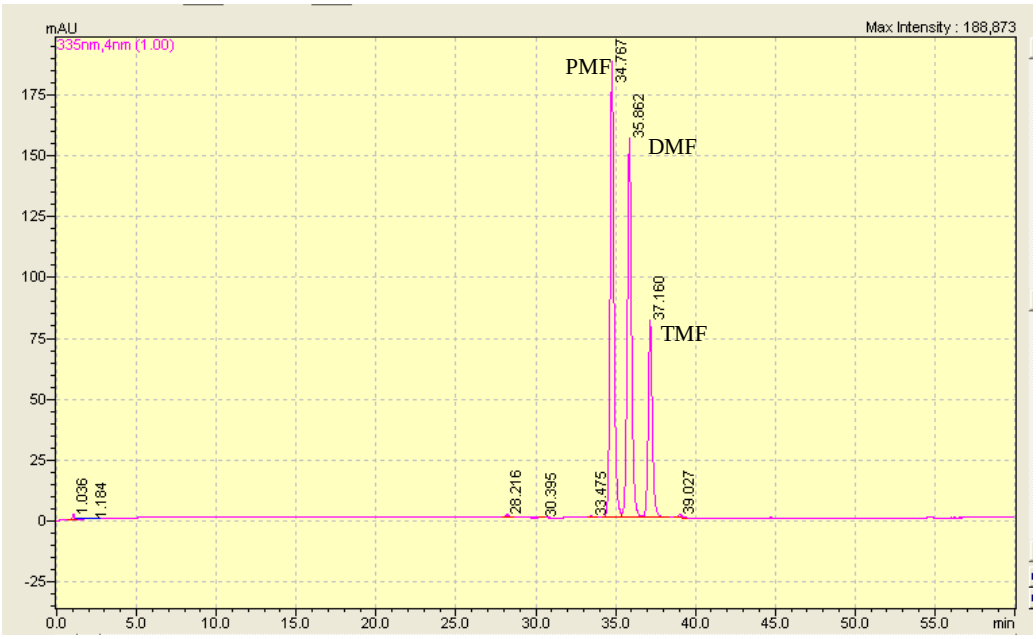

Figure 80 HPLC chromatogram of the mixture of PMF (2.60 µg/ml), TMF (3.33 µg/ml), and DMF (1.77 µg/ml)

Method validation of HPLC system for analyzing of methoxyflavones in KP in product development was presented in Table 18. Precision was evaluated at four concentration levels of three replicates on three validation days. Intra-day precision of PMF, TMF, and DMF ranged from 0.11 to 2.46 %RSD and Inter-day precision ranged from 1.94 to 6.92 %RSD. LOD of PMF, TMF, and DMF were 0.260, 0.333, and 0.177 µg/ml, respectively. LOQ was 0.833, 1.067, and 0.567 µg/ml for PMF, TMF, and DMF, respectively. At concentrations ranging of 5.21-41.67 µg/ml for PMF, 6.67-53.33 µg/ml for TMF, and 3.54-56.67 µg/ml for DMF, the linearity with the correlation coefficients (R^2) better than 0.999 were obtained. The %error of accuracy as assayed at two concentration levels (1 and 50 µg/ml) were 3.08 or below.

Table 18 Method validation of HPLC method

Flavo-noids	**Precision (%RSD)**			**LOD** (µg/ml)	**LOQ** (µg/ml)	**Linearity** (R^2)	**Accuracy** (% error)	
	Conc. (µg/ml)	Intra -day	Inter -day				1 µg/ml	50 µg/ml
DMF	3.54	1.032	2.413	0.177	0.567	y = 262011x - 352602 (R^2 = 0.9999)	3.076	1.087
	14.17	0.453	1.935					
	28.33	2.462	4.643					
	56.67	0.143	3.755					
TMF	6.67	1.935	2.632	0.333	1.067	y = 267789x - 321519 (R^2 = 0.9997)	1.793	2.069
	13.33	1.052	4.153					
	26.67	0.111	4.501					
	53.33	0.106	5.235					
PMF	5.21	0.153	5.973	0.260	0.833	y = 347091x – 369227 (R^2 = 0.9999)	0.986	2.354
	10.42	1.012	4.267					
	21.83	0.825	3.578					
	41.67	2.342	6.924					

6.2 Pre-formulation study

The solubility of KP crude extract in various solvents as shown in Table 19 indicated that PMF and TMF were highly soluble in ethanol and propylene glycol but sparingly soluble in 0.01 M HCl, 0.1 M NaOH, water, NSS, and 0.2 M PBS pH 7.4.

Log P of PMF and TMF in KP crude extract were 1.763 ± 0.282 and 1.921 ± 0.317, respectively.

Table 19 Solubility of methoxyflavones in various vehicles

Solvents	Solubility of methoxyflavones in crude (mg/ml)	
	PMF	TMF
0.01 M HCl	0.193 ± 0.044	0.124 ± 0.005
0.1 M NaOH	0.3661 ± 0.056	0.264 ± 0.008
Ethanol	6.260 ± 0.345	5.371 ± 0.793
Water	0.199 ± 0.033	0.145 ± 0.007
NSS	0.264 ± 0.034	0.177 ± 0.002
Propylene glycol	3.037 ± 0.643	4.732 ± 0.563
0.2 M PBS pH7.4	0.209 ± 0.012	0.130 ± 0.004

6.3 Oral bioavailability enhancement of KP crude extract by SMEDDS

6.3.1 Determination of KP solubility in oils, surfactants, and co-surfactants

Solubility of methoxyflavones in KP crude extract in various oils, surfactants, and co-surfactants were shown in Figure 81. Among oils, triglyceride of coconut oil, and Miglyol 810N were suitable for KP-SMEDDS formulation. In the case of surfactants, several surfactants including Tween 20, Tween 80, Cremophor® EL, and DGME can dissolve the methoxyflavones. Among co-surfactants, ethanol, and propylene glycol had the best solubility for methoxyflavones, followed by PEG 200 and PEG 400.

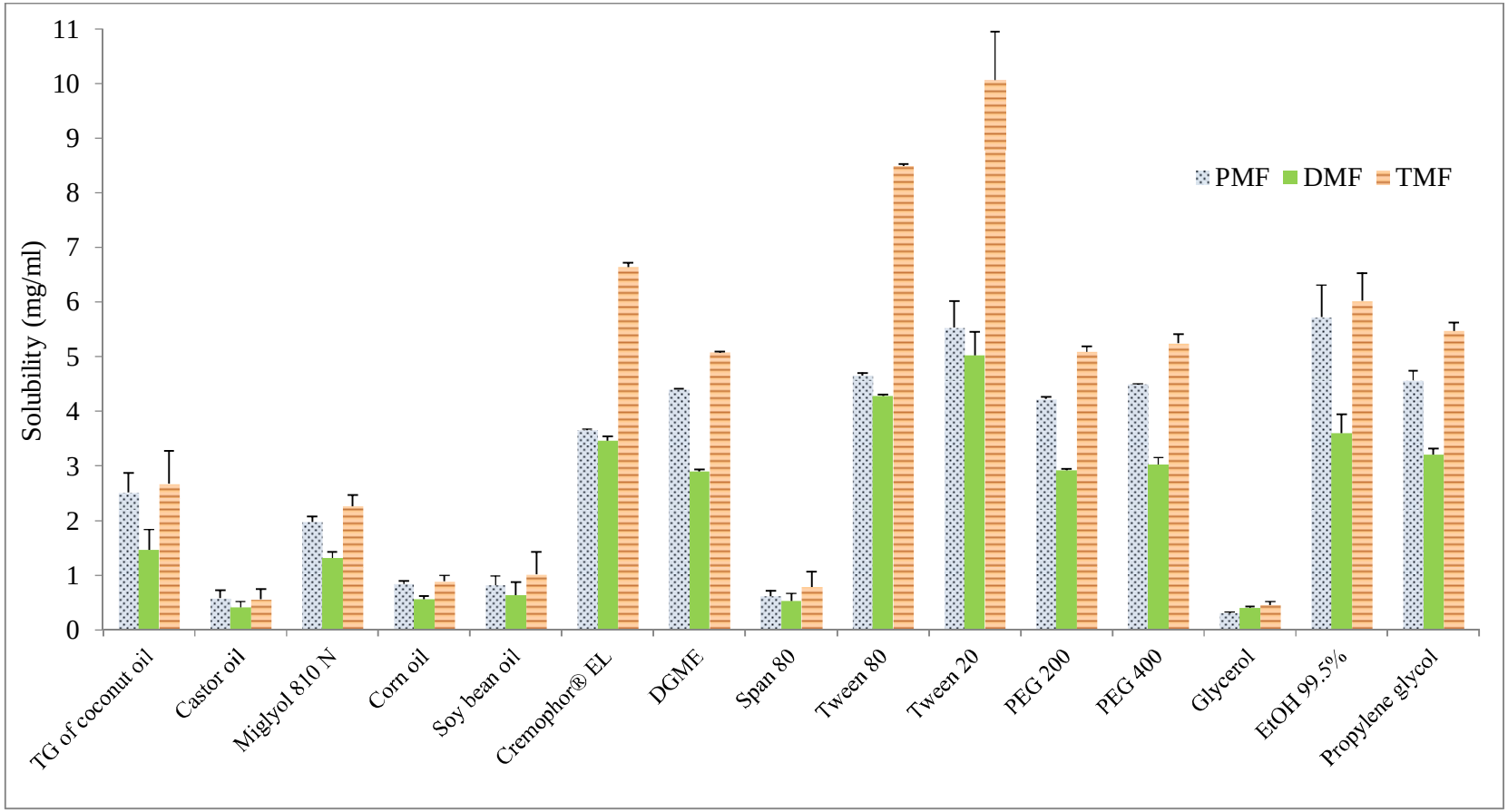

Figure 81 KP solubility in various oils, surfactants, and co-surfactant

6.3.2 Compatibility tests

In order to determine surfactants and the mixture of surfactant and co-surfactant with the best compatibility with oil, various surfactants and the mixture of surfactants and co-surfactants in 1:1 and 2:1 ratios were carried out and the results were showed in Table 20. Cremophor® EL, DGME, and Tween 80 were compatible with triglyceride of coconut oil and Miglyol 810N. When the ratio of surfactant and co-surfactant at 1:1, Cremophor® EL:ethanol, DGME:PEG200, DGME:PEG400, DGME:ethanol, Tween80:ethanol, and Tween80:propylene glycol gave the homogenous mixtures with triglyceride of coconut oil and Miglyol 810N. For the ratio of 2:1, Cremophor® EL:ethanol, Cremophor® EL:propylene glycol, DGME:PEG200, DGME:PEG400, DGME:ethanol, Tween80:ethanol, and Tween80:propylene glycol were the good compositions with triglyceride of coconut oil and Miglyol 810N. Therefore, the compositions at both of 1:1 and 2:1 ratios were further used to construct the pseudo-ternary phase diagram.

Table 20 Compatibility between surfactants, co-surfactants and oils

Surfactants/ co-surfactants (1 ml)	**Volume of Oil (ml)**	
	Triglyceride coconut oil	Miglyol 810N
Cremophor® EL	1.000	1.000
DGME	1.000	1.000
Tween 80	1.000	1.000
Tween 20	0.400	0.500
Cremophor® EL: PEG200 (1:1)	0.400	0.500
Cremophor® EL: PEG400 (1:1)	0.300	0.300
Cremophor® EL: ethanol (1:1)	>1.000	>1.000
Cremophor® EL: propylene glycol (1:1)	0.500	0.500
DGME : PEG200 (1:1)	>1.000	>1.000
DGME : PEG400 (1:1)	0.900	0.900
DGME : ethanol (1:1)	>1.000	>1.000
DGME : propylene glycol (1:1)	0.100	0.100
Tween 80 : PEG200 (1:1)	0.400	0.400
Tween 80 : PEG400 (1:1)	0.300	0.300
Tween 80 : ethanol (1:1)	>1.000	>1.000
Tween 80 : propylene glycol (1:1)	1.000	1.000
Cremophor® EL: PEG200 (2:1)	0.500	0.500
Cremophor® EL: PEG400 (2:1)	0.500	0.500
Cremophor® EL: ethanol (2:1)	>1.000	>1.000
Cremophor® EL: propylene glycol (2:1)	>1.000	>1.000
DGME : PEG200 (2:1)	>1.000	>1.000
DGME : PEG400 (2:1)	1.000	1.000
DGME : ethanol (2:1)	>1.000	>1.000
DGME : propylene glycol (2:1)	0.200	0.200
Tween 80 : PEG200 (2:1)	0.500	0.500
Tween 80 : PEG400 (2:1)	0.500	0.500
Tween 80 : ethanol (2:1)	>1.000	>1.000
Tween 80 : propylene glycol (2:1)	>1.000	>1.000

6.3.3 Pseudo-ternary phase diagram study

Pseudo-ternary phase diagrams of various oils, surfactants and co-surfactants were constructed. S-3 formulations at both of 1:1 and 2:1 ratios of surfactant and co-surfactant showed the broad area of oil-in-water microemulsion, as shown in Figure 82 and Figure 83, respectively. However, it was found that S-3 at the ratio of 2:1 was the broadest area. Consequently, the compositions were used to develop the SMEDDS formulation.

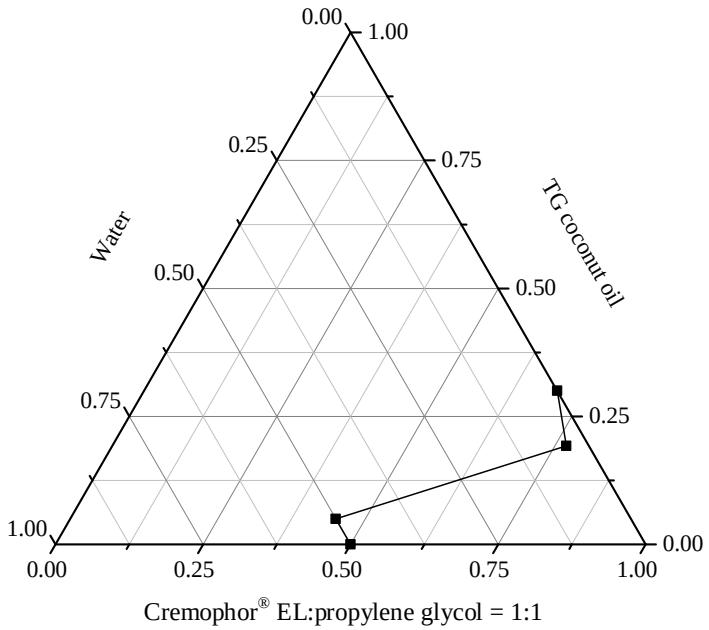

Figure 82 Pseudo-ternary phase diagram composed of S-3 (1:1 ratio of Cremophor® EL and propylene glycol)

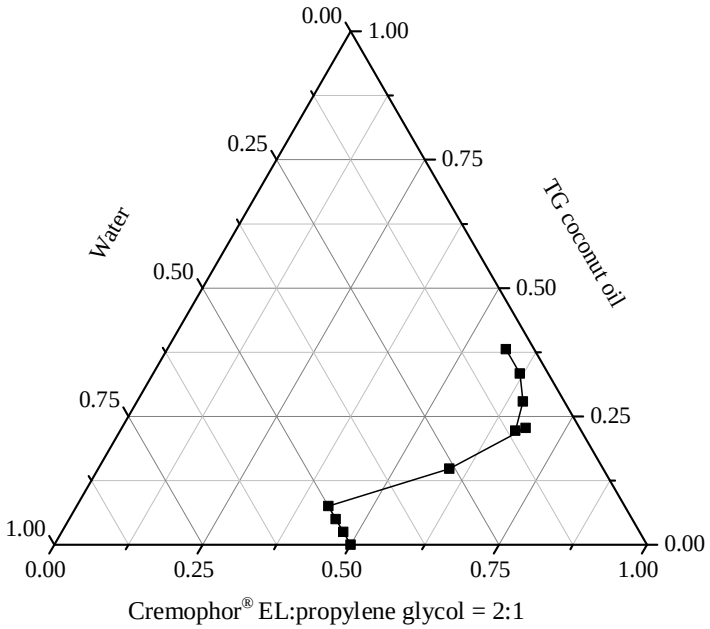

Figure 83 Pseudo-ternary phase diagram composed of S-3 (2:1 ratio of Cremophor® EL and propylene glycol)

6.3.4 Development and characterization of KP-SMEDDS formulations

As varied the percent of Cremophor® EL with propylene glycol (2:1) and triglyceride of coconut oil (S-3), the particle size, speed of formation of microemulsion, and drug precipitation at 0 min and 24 h were shown in Table 21. The optimal compositions were 80 and 85% of mixture of surfactant and co-surfactant (S-3-80 and S-3-85, respectively) because these systems had the particle size less than 22 nm, quickly formed microemulsion when added water, and stable for 24 h. In addition, it was found that the presence of KP in S-3-80 and S-3-85 did not affect on the particle size. Therefore, S-3-80 and S-3-85 were selected for evaluation of physicochemical properties and drug absorption both of *in vitro* and *in vivo*. S-3-80 and S-3-85 with clear brown liquid formulations were shown in Figure 84.

Table 21 Physicochemical properties of KP-SMEDDS

Parameters	Cremophor® EL and PG (2:1) : TG of coconut oil	KP-SMEDDS	Blank-SMEDDS
Size (nm)	70:30 (S-3-70)	127.533 ± 12.886	118.687 ± 18.550
	75:25 (S-3-75)	33.333 ± 2.373	15.670 ± 4.200
	80:20 (S-3-80)	21.947 ± 1.408	25.027 ± 1.001
	85:15 (S-3-85)	17.287 ± 0.140	20.460 ± 0.346
PdI	S-3-70	0.304 ± 0.018	0.296 ± 0.009
	S-3-75	0.200 ± 0.034	0.104 ± 0.115
	S-3-80	0.163 ± 0.064	0.061 ± 0.016
	S-3-85	0.0557 ± 0.012	0.047 ± 0.007
Speed of formation of emulsification	S-3-70	slowly	slowly
	S-3-75	fairy quickly	very quickly
	S-3-80	quickly	quickly
	S-3-85	very quickly	fairy quickly
Precipitation @ 0 h	S-3-70	turbid	turbid
	S-3-75	turbid	clear
	S-3-80	clear	clear
	S-3-85	clear	clear
Precipitation @ 24 h	S-3-70	turbid	turbid
	S-3-75	turbid	clear
	S-3-80	clear	clear
	S-3-85	clear	clear

N = 3

Figure 84 KP-SMEDDS formulations

6.4 Preparation of KP-CD complex

6.4.1 Phase solubility study

As shown in Figure 85 and Figure 86, phase solubility diagram of β-CD and KP crude extract was a non-linear regression, whereas the diagram of HP-β-CD was a linear relation between the concentration of methoxyflavones and HP-β-CD. The water solubility of methoxyflavones in β-CD (30 mM) were 0.373 ± 0.004, 0.478 ± 0.001, and 0.811 ± 0.018 mM for PMF, TMF and DMF, respectively. Whereas, the solubility of PMF, TMF and DMF in HP-β-CD (60 mM) were 3.816 ± 0.264, 7.496 ± 0.673, and 6.340 ± 0.424 mM, respectively at room temperature. KP crude extract can be soluble in HP-β-CD more than in β-CD. According to Higuchi and Conners (1965), the diagram of HP-β-CD and methoxyflavones in KP crude extract may be attributed to the formation of 1:1 ratio of methoxyflavones and HP-β-CD complex with the apparent binding constants of 0.332 ± 0.028, 0.9002 ± 0.035, 0.837 ± 0.051 L/mmol for PMF, TMF and DMF, respectively. Moreover, the slope of this diagram was always lower than 1.0, indicating that the inclusion complex in 1:1 molar ratio of methoxyflavones and HP-β-CD molecules.

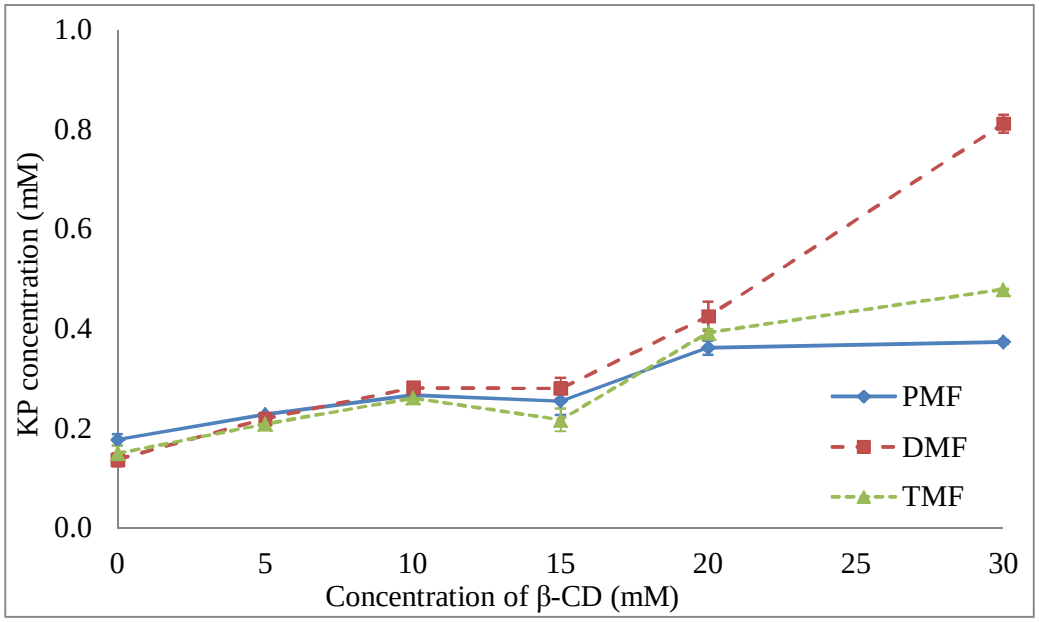

Figure 85 Phase solubility profile of KP crude extract and β-CD

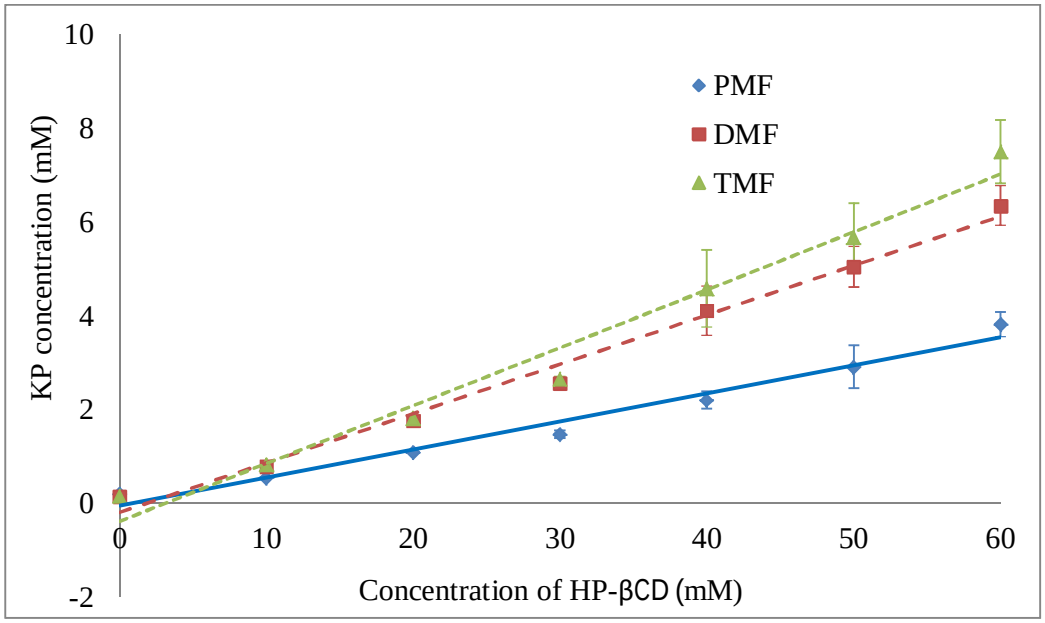

Figure 86 Phase solubility profile of KP crude extract and HP-β-CD

Then, KP crude extract and HP-β-CD was prepared by using freeze-drying technique at 1:1 molar ratio of methoxyflavones and HP-β-CD, the formulation as shown in Figure 87. The complex as fine white-purple powder was obtained.

Figure 87 KP-HP-β-CD complex

6.4.2 Differential scanning calorimetry (DSC) measurement

The DSC curves of KP crude extract, physical mixture, KP-HP-β-CD complex, and HP-β-CD were shown in Figure 88. KP crude extract and the physical mixture showed the same melting endotherm at 120^{o}C. HP-β-CD showed the endothermal peak at about 110^{o}C. While, there was no thermal curve of KP-HP-β-CD complex.

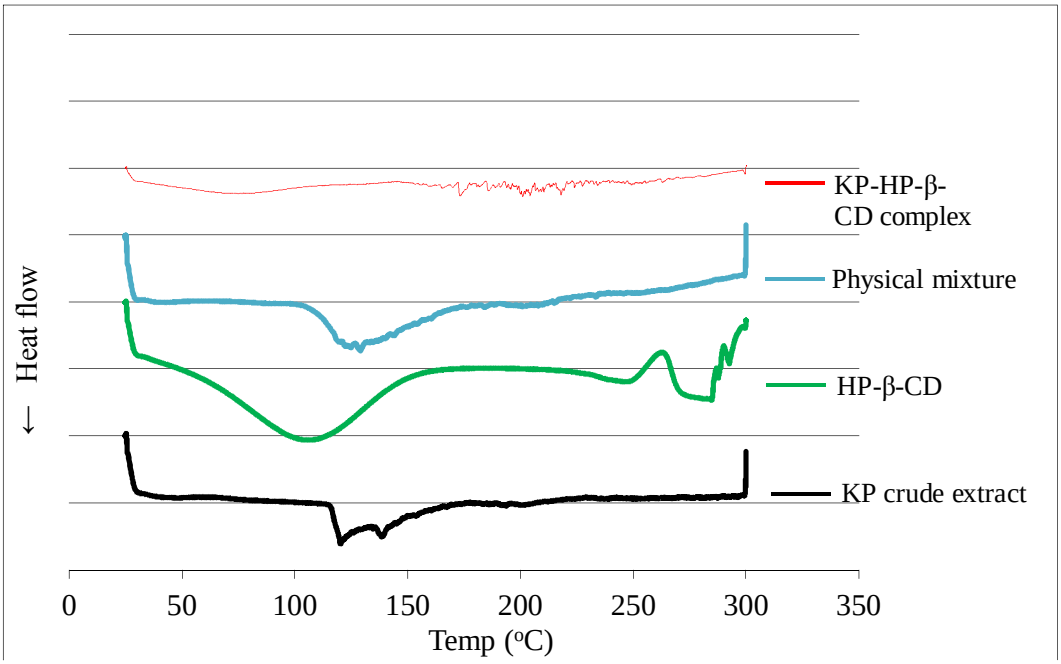

Figure 88 DSC curves of KP crude extract, physical mixture, KP-HP-β-CD complex, and HP-β-CD

6.5 Evaluation of physicochemical properties and drug absorption

6.5.1 *In vitro* dissolution study

The releases of methoxyflavones from developed formulations were measured using *in vitro* dissolution test. The dissolution profiles of formulations in both media were shown in Figure 89-96. The methoxyflavones released from the S-3-80, S-3-85, and KP-HP-β-CD complex in 0.1 N HCl (the pH range of gastric fluids) and 0.2 M PBS pH 6.8 (the pH range of intestinal fluids) were greater than that of KP crude extract. The dissolution of S-3-80 and S-3-85 reached 100% drug release within 20 min in 0.1 N HCl and 0.2 M PBS pH 6.8. KP-HP-β-CD complex released from the formulation within 10 min in both media. Whereas, the methoxyflavones release from KP crude extract were less than 100% release both in 0.1 N HCl and 0.2 M PBS pH 6.8.

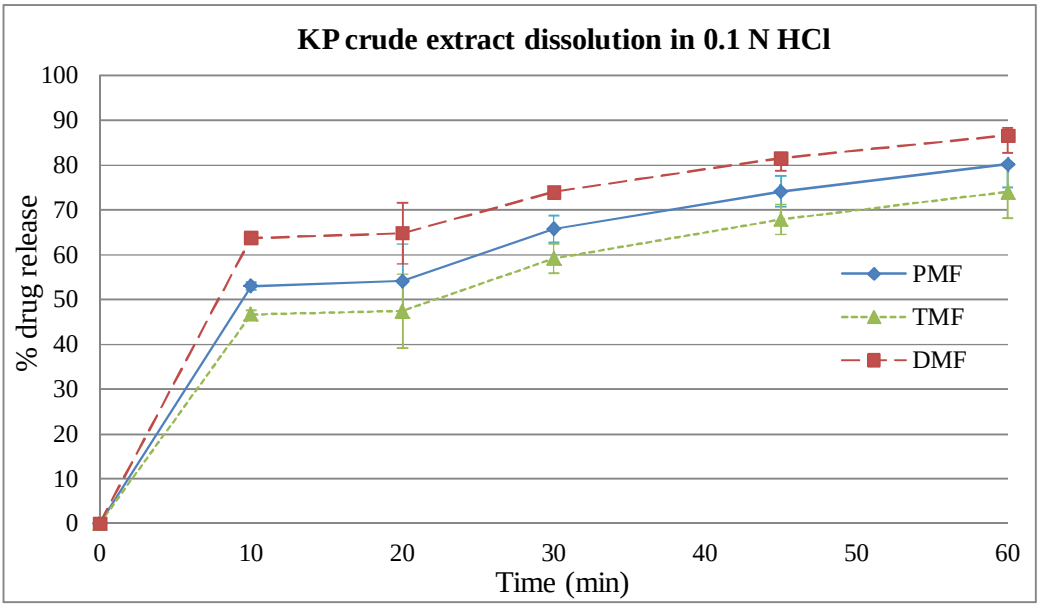

Figure 89 Dissolution profile of KP crude extract in 0.1 N HCl

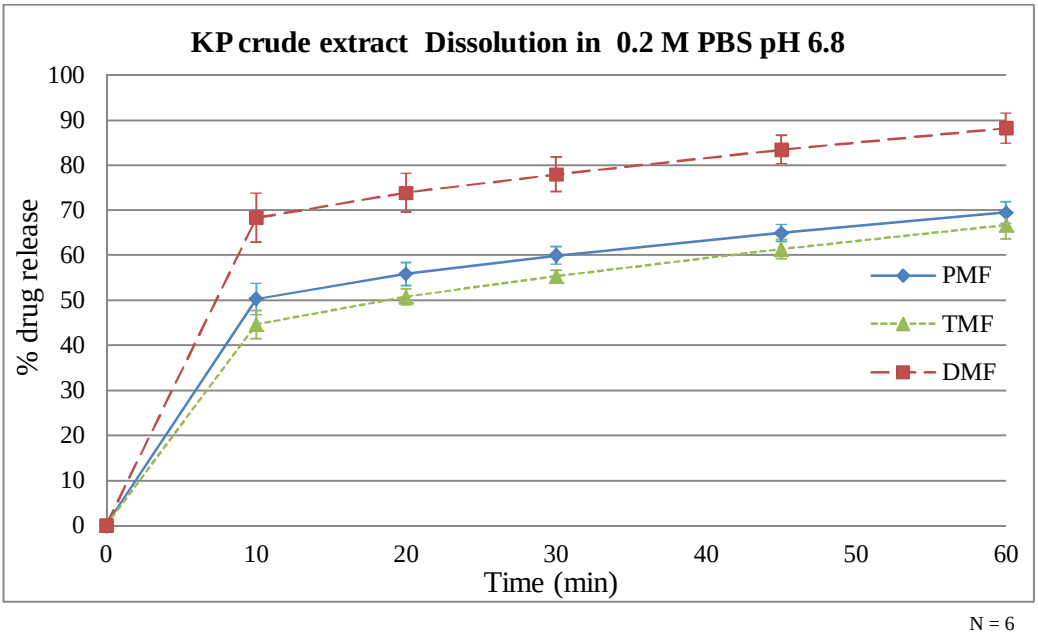

Figure 90 Dissolution profile of KP crude extract in 0.2 M PBS pH 6.8

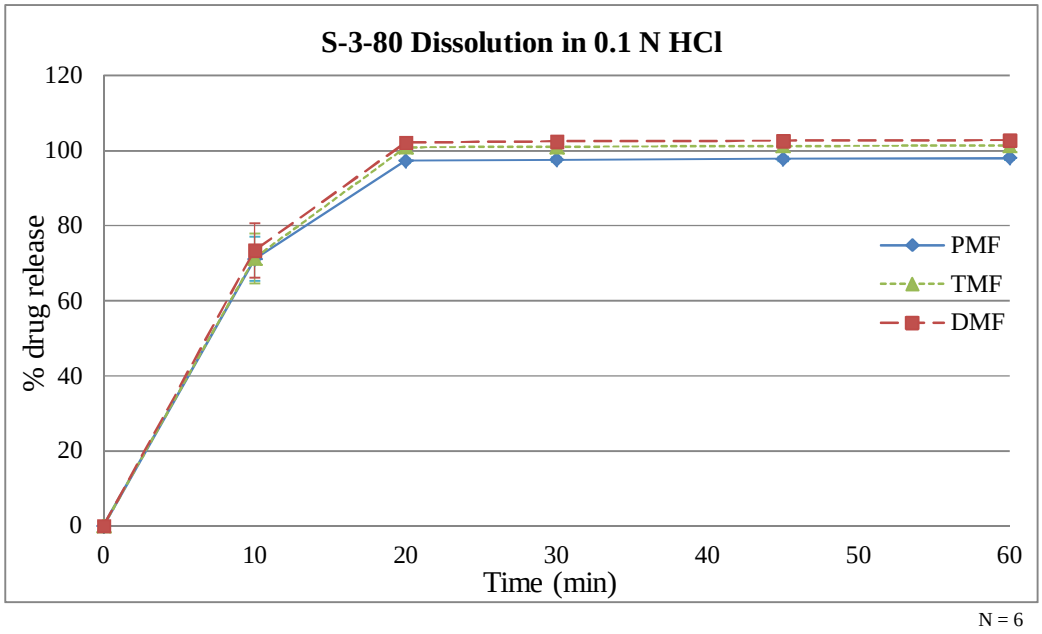

Figure 91 Dissolution profile of S-3-80 in 0.1 N HCl

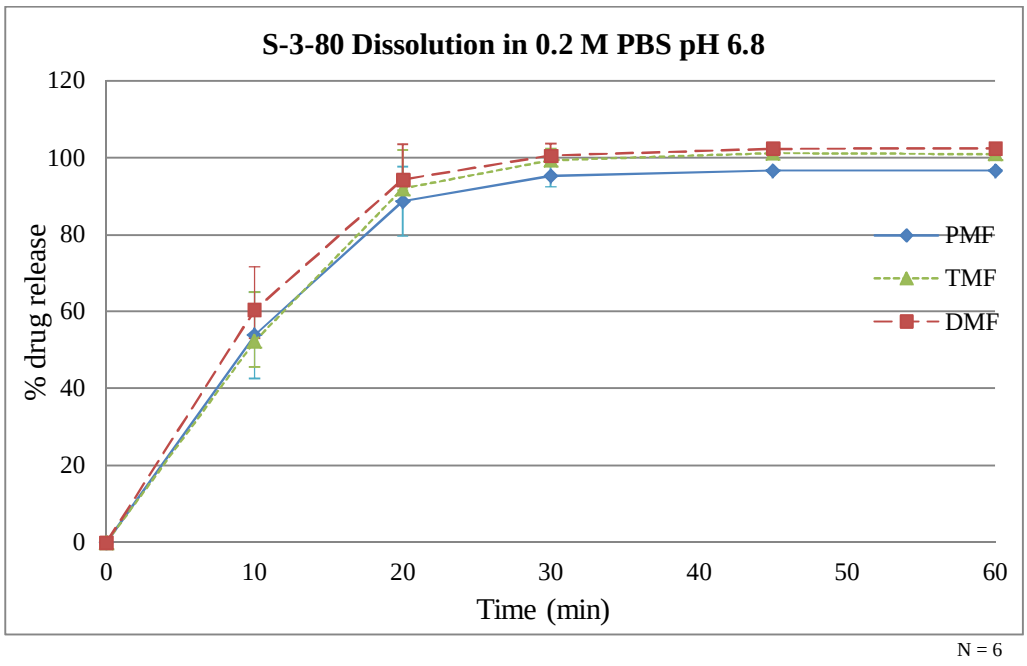

Figure 92 Dissolution profile of S-3-80 in 0.2 M PBS pH 6.8

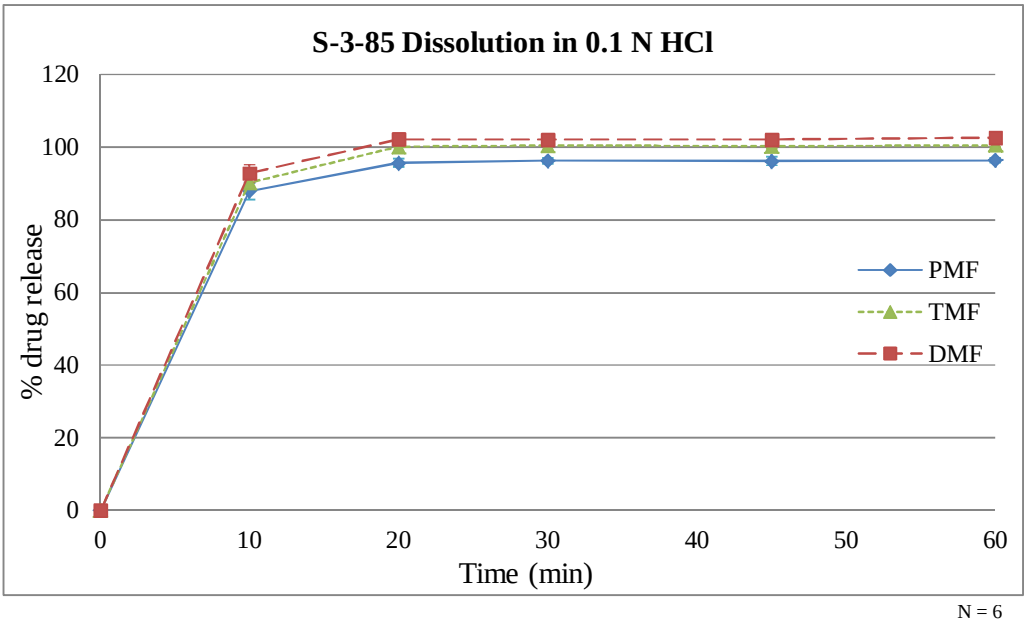

Figure 93 Dissolution profile of S-3-85 in 0.1 N HCl

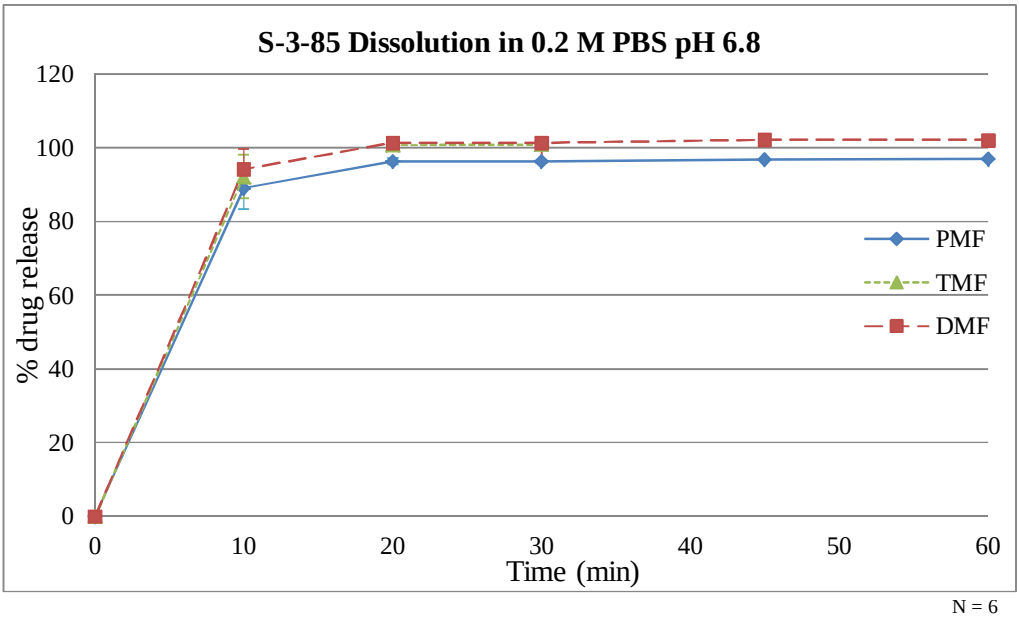

Figure 94 Dissolution profile of S-3-85 in 0.2 M PBS pH 6.8

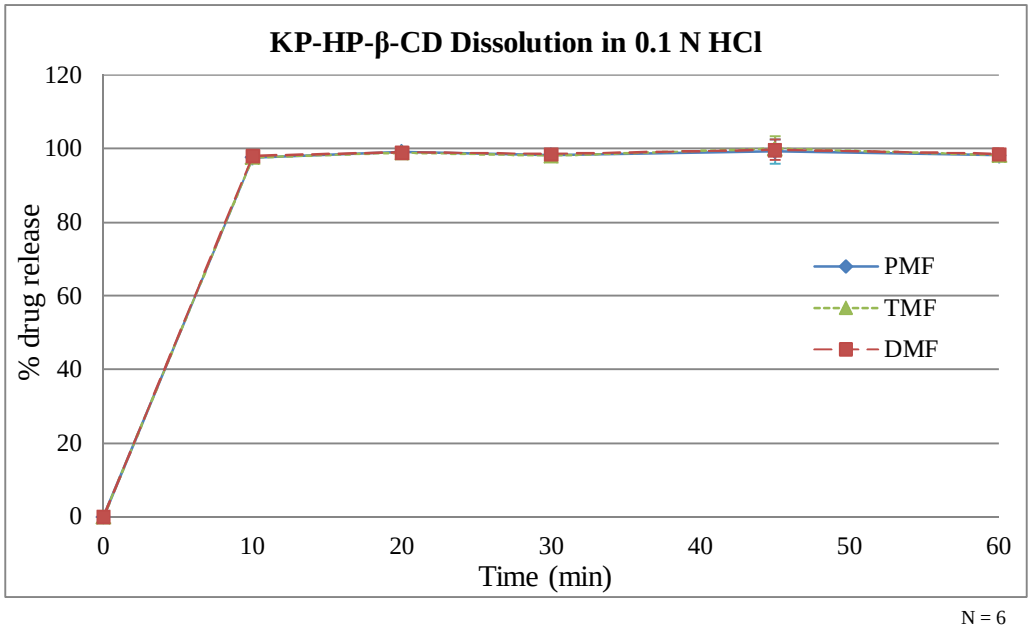

Figure 95 Dissolution profile of KP-HP-β-CD in 0.1 N HCl

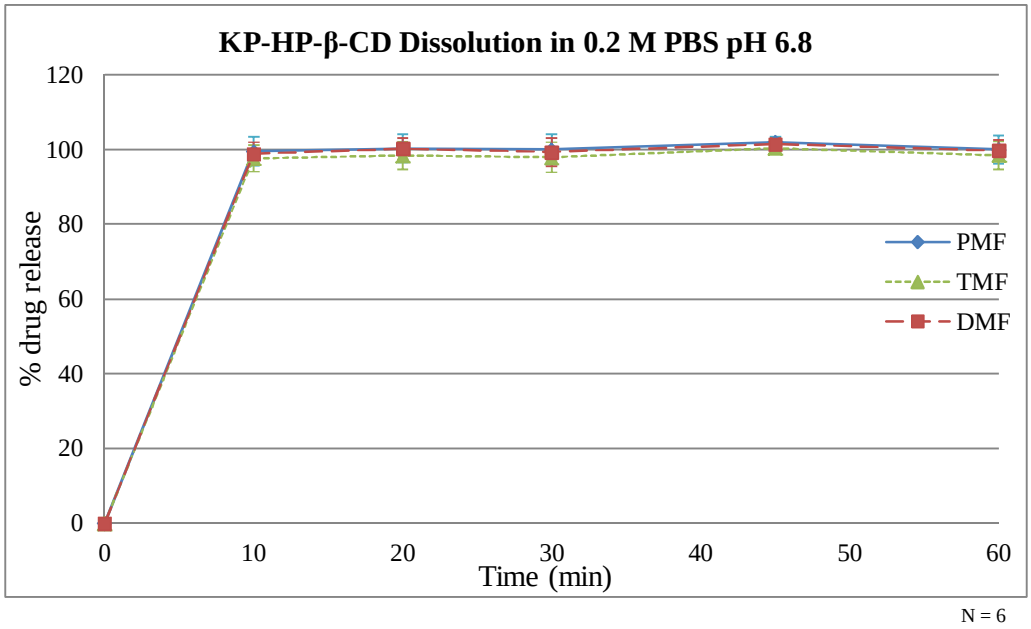

Figure 96 Dissolution profile of KP-HP-β-CD in 0.2 M PBS pH 6.8

6.5.2 Stability study

The developed formulation including S-3-80, S-3-85 and KP-HP-β-CD formulations were investigated for their stability at 4, 25, and 40°C for 3 months. There were no changes in the appearance such as color of these three formulations after storage for 3 months. As shown in Figure 97-99, the % retaining contents of methoxyflavones in S-3-80 and S-3-85 formulations were stable at all conditions until 3 months. Their methoxyflavones concentrations were not significantly lower than that of initial time. The particle sizes of the S-3-80 and S-3-85 formulations did not change (Figure 100-101). Nevertheless, methoxyflavones concentrations of KP-HP-β-CD keeping at 40°C for 2 and 3 months significantly decreased when compared with initial time.

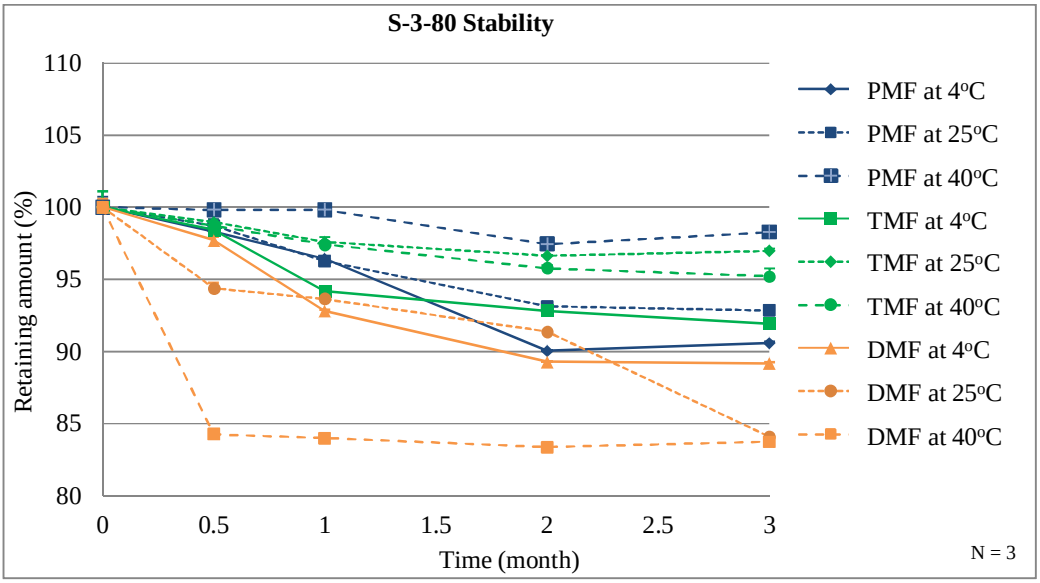

Figure 97 Time courses of degradation of methoxyflavones in S-3-80 in various conditions

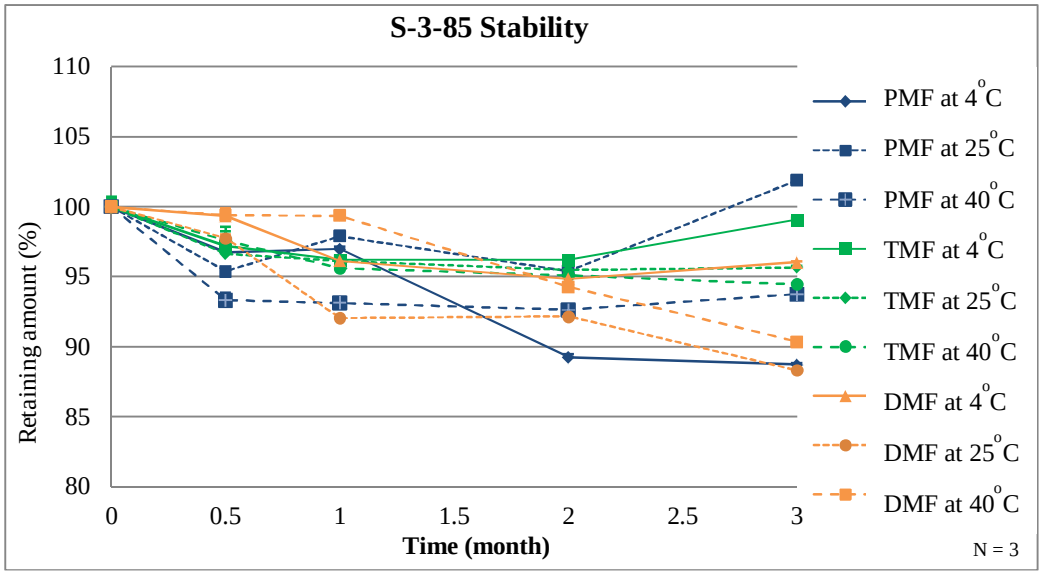

Figure 98 Time courses of degradation of methoxyflavones in S-3-85 in various conditions

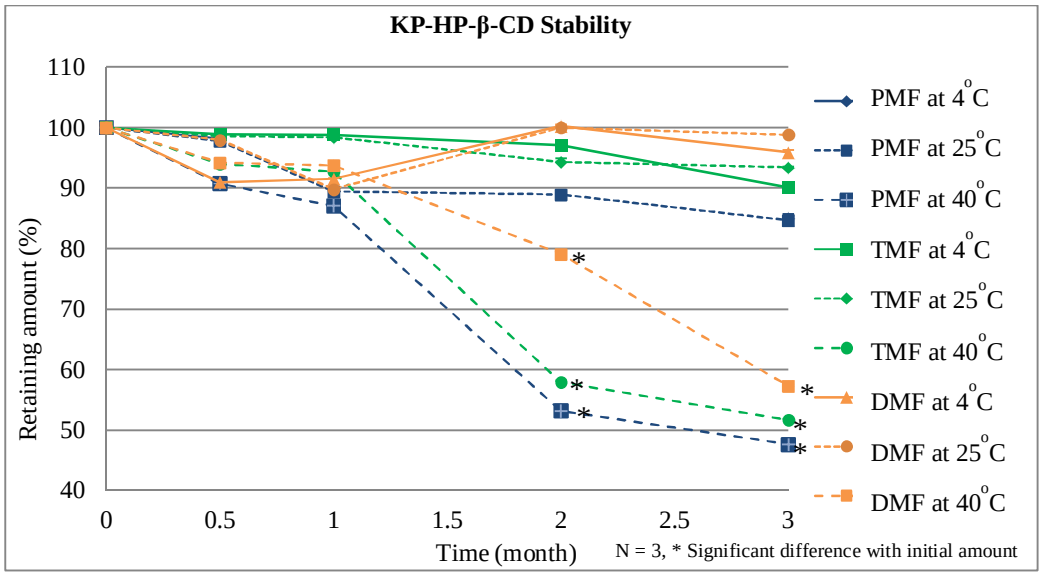

Figure 99 Time courses of degradation of methoxyflavones in KP-HP-β-CD in various conditions

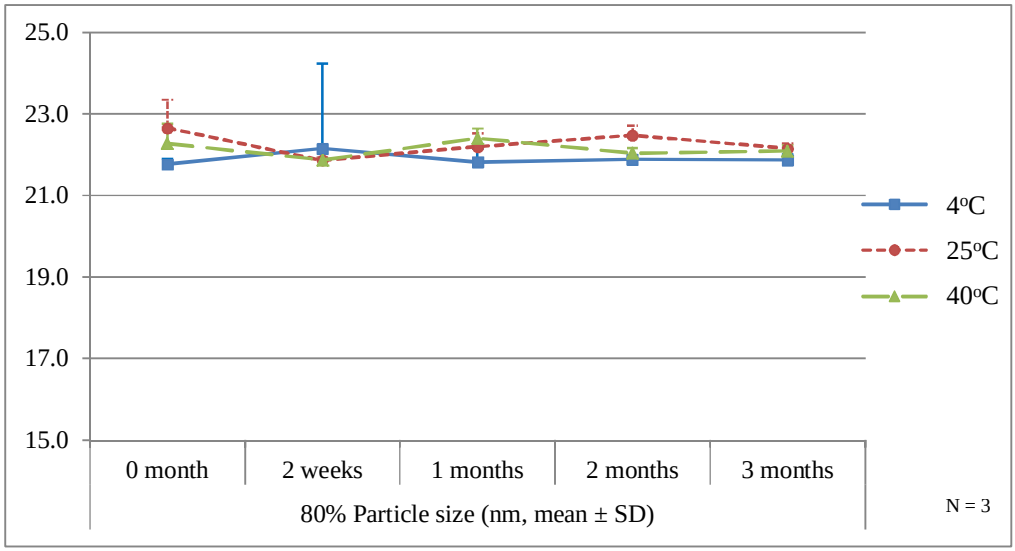

Figure 100 Particle size of S-3-80 in various conditions

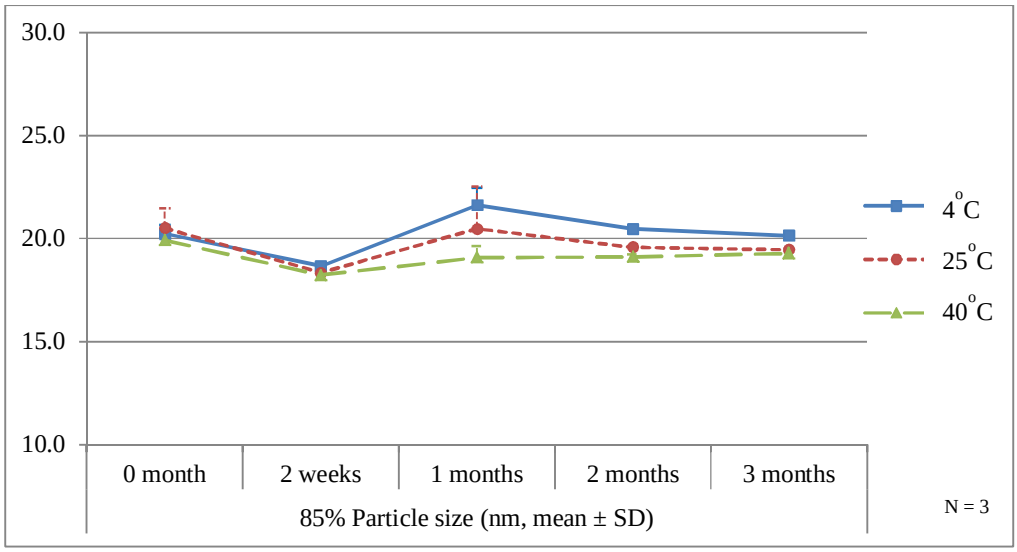

Figure 101 Particle size of S-3-85 in various conditions

6.5.3 *In vitro* KP absorption study by using Caco-2 cells

The permeability of methoxyflavones in Caco-2 cells of the formulations in was shown in Table 22. ^{14}C-Mannitol and antipyrine which are low and high permeability controls had the apparent permeability of 0.013 ± 0.004, and

0.469 ± 0.047 μm/sec, respectively. The apparent permeability of both of S-3-80 and S-3-85 were not significant difference (P-value = 0.05). In addition, both KP-SMEDDS formulations had the apparent permeability significantly greater than those of KP crude extract at 9.94, 6.66, and 9.31–fold for PMF, TMF and DMF, respectively. Apparent permeability of methoxyflavones in KP-HP-β-CD complex were 3.77, 5.01, and 5.12-fold higher than those of KP crude extract for PMF, TMF and DMF, respectively at P-value < 0.05.

Table 22 Appearance permeability of formulations in Caco-2 cells

Samples	Papp (μm/sec)		
	PMF	TMF	DMF
S-3-80	29.648 ± 0.328*	19.148 ± 0.192*	39.238 ± 0.147*
S-3-85	29.668 ± 0.106*	19.246 ± 0.228*	39.427 ± 0.399*
KP -HP-β-CD	11.243 ± 0.237*	12.537 ± 0.211*	21.581 ± 0.372*
KP crude extract	2.982 ± 0.062	2.500 ± 0.055	4.213 ± 0.080
^{14}C-Mannitol		0.013 ± 0.004	
Antipyrine		0.469 ± 0.047	

*: significant difference from KP crude extract, mannitol, and antipyrine at P < 0.05

6.5.4 *In vivo* oral bioavailability study in rats

KP-HP-β-CD complex and S-3-80 having excellent appearance, physicochemical properties, dissolution rate, and appearance permeability in Caco-2 cells, were further evaluated for their oral bioavailabilites. Blood concentration-time profiles of these methoxyflavones (PMF, TMF, and DMF) in rats after intravenous or oral receiving of KP crude extract, KP-HP-β-CD complex, and S-3-80 were shown in Figure 102-104. Their pharmacokinetic parameters of the methoxyflavones were presented in Table 23-28. The AUC of PMF and TMF in KP-HP-β-CD complex in IV route were significantly higher than that of KP crude extract at P-value < 0.05. S-3-80 gave higher AUC of DMF in IV route than that of KP crude

extract at P-value < 0.05. Moreover, $t_{1/2}$ values of PMF, TMF and DMF in the developed formulations when administered via IV route were similar to that of KP crude extract. In term of Cl, Vd, and Ke of PMF, TMF, and DMF, there were no significant differences of KP-HP-β-CD complex, and S-3-80 when compared to KP crude extract.

After oral administration, AUC and Cmax of PMF, TMF and DMF in KP-HP-β-CD complex, and S-3-80 formulations were greater than that of KP crude extract at P-value < 0.05. The developed formulations, KP-HP-β-CD complex, and S-3-80, greatly enhanced the oral bioavailability of PMF, TMF and DMF. The oral bioavailability values of KP crude extract, KP-HP-β-CD complex, and S-3-80 were 2.97, 64.25, and 75.38% for PMF, 1.84, 62.92, 77.28% for TMF, and 2.79, 63.88, and 72.56% for DMF, respectively. There was no significant difference of clearance value among three formulations. Vd values of PMF in KP-HP-β-CD complex, and S-3-80 were lower than that of KP crude extract but the values of TMF and DMF in developed formulations were similar to KP crude extract. Moreover, S-3-80 had the Ke of PMF, Tmax value of TMF higher than those of KP crude extract. While, Tmax of PMF and DMF in KP-HP-β-CD complex, and S-3-80 were similar to those of KP crude extract. The $t_{1/2}$ of TMF and DMF in S-3-80 were lower than those of KP crude extract whereas the value of PMF was not different.

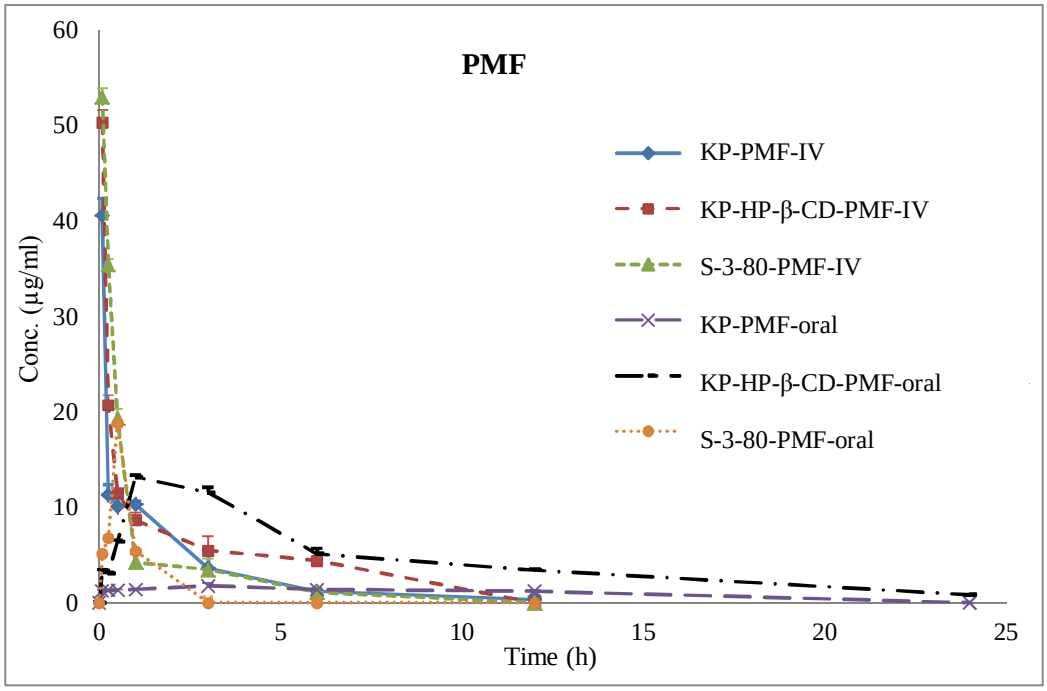

Figure 102 Blood concentration-time profile of PMF in rats after intravenous or oral administration of KP crude extract, KP-HP-β-CD complex, and S-3-80

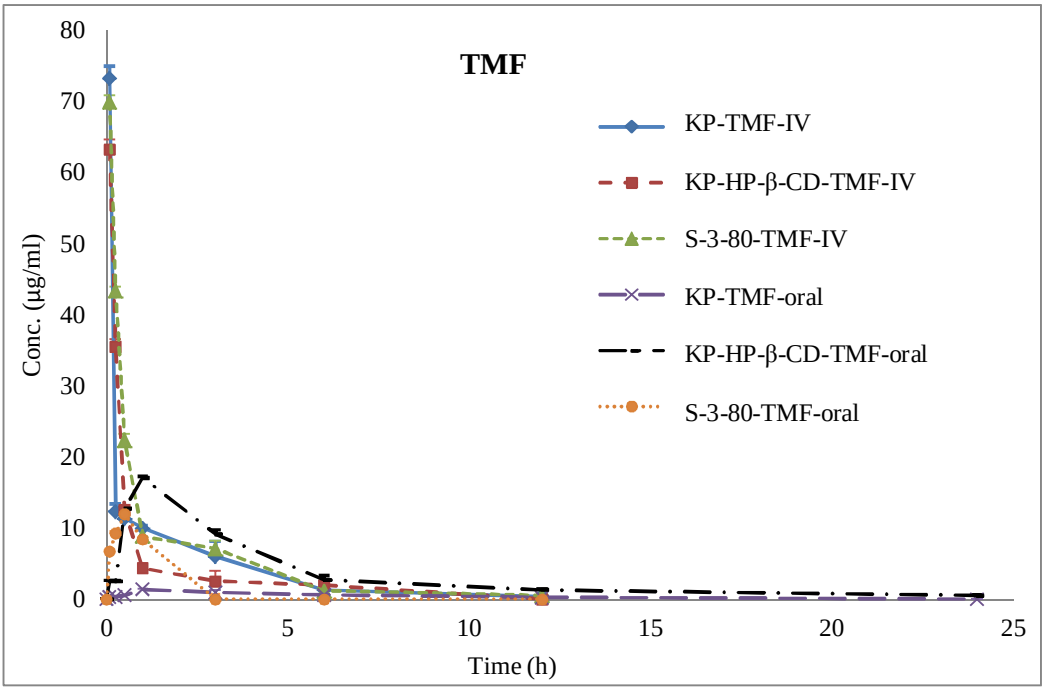

Figure 103 Blood concentration-time profile of TMF in rats after intravenous or oral administration of KP crude extract, KP-HP-β-CD complex, and S-3-80

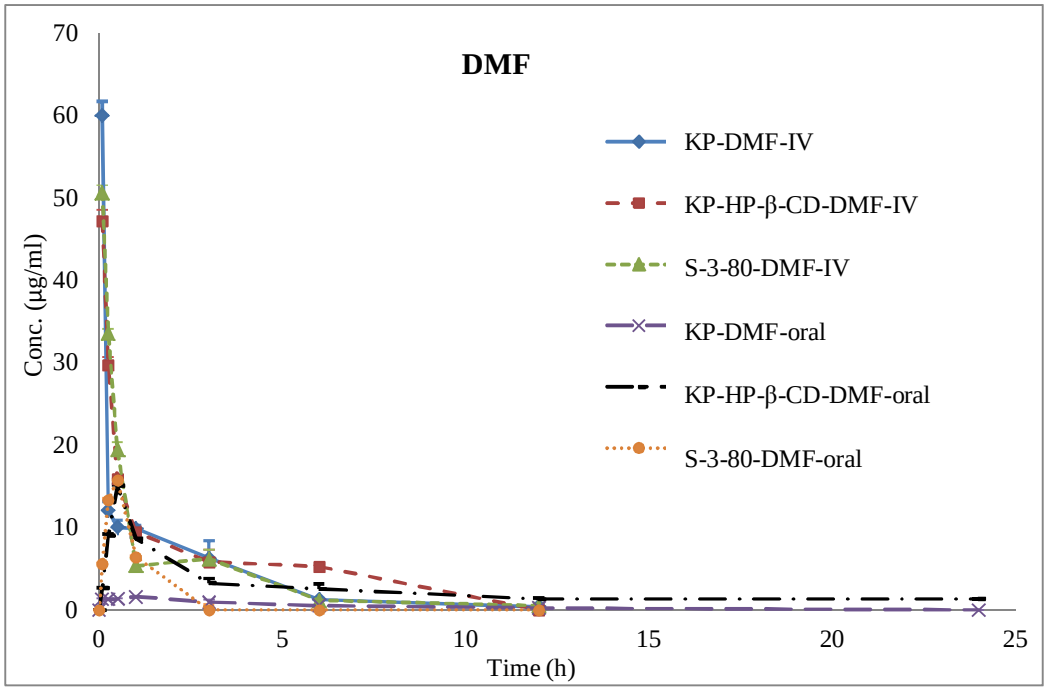

Figure 104 Blood concentration-time profile of DMF in rats after intravenous or oral administration of KP crude extract, KP-HP-β-CD complex, and S-3-80

Table 23 Pharmacokinetic parameters of PMF after intravenous administration of KP crude extract, KP-HP-β-CD complex, and S-3-80

PK parameters	KP crude extract	KP-HP-β-CD complex	S-3-80
AUC (h*ug/ml)	54.691 ± 11.867	75.674 ± 6.825*	68.800 ± 5.548
Dose (mg)	0.959 ± 0.024	1.025 ± 0.127	1.269 ± 0.113
$t_{1/2}$ (h)	2.332 ± 0.371	2.732 ± 1.026	1.799 ± 0.116
Cmax (ug/ml)	40.634 ± 6.689	50.118 ± 13.612	53.030 ± 2.267
Cl (ml/h)	35.084 ± 5.573	38.039 ± 8.471	33.060 ± 11.618
Vd (ml)	68.703 ± 10.391	77.094 ± 10.821	65.065 ± 10.248
Ke (1/h)	0.693 ± 0.165	0.620 ± 0.284	0.514 ± 0.198

*: significant difference from KP crude extract at P-value = 0.05.

Table 24 Pharmacokinetic parameters of TMF after intravenous administration of KP crude extract, KP-HP-β-CD complex, and S-3-80

PK parameters	KP crude extract	KP-HP-β-CD complex	S-3-80
AUC (h*ug/ml)	314.590 ± 74.801	179.702 ± 49.338*	285.533 ± 101.602
Dose (mg)	2.060 ± 0.008	0.964 ± 0.112	2.290 ± 0.227
$t_{1/2}$ (h)	2.228 ± 0.249	1.871 ± 0.120	2.267 ± 0.223
Cmax (ug/ml)	73.183 ± 11.356	67.307 ± 10.439	69.767 ± 7.988
Cl (ml/h)	9.314 ± 4.130	10.131 ± 6.359	9.089 ± 1.354
Vd (ml)	52.273 ± 8.137	68.572 ± 15.649	66.212 ± 20.258
Ke (1/h)	0.314 ± 0.037	0.358 ± 0.088	0.332 ± 0.030

*: significant difference from KP crude extract at P-value = 0.05.

Table 25 Pharmacokinetic parameters of DMF after intravenous administration of KP crude extract, KP-HP-β-CD complex, and S-3-80

PK parameters	KP crude extract	KP-HP-β-CD complex	S-3-80
AUC (h*ug/ml)	171.348 ± 8.964	178.597 ± 31.864	286.298 ± 56.574*
Dose (mg)	0.865 ± 0.018	0.692 ± 0.028	1.133 ± 0.111
$t_{1/2}$ (h)	2.617 ± 0.177	2.548 ± 0.901	2.430 ± 0.648
Cmax (ug/ml)	59.408 ± 11.895	47.208 ± 3.939	50.616 ± 4.615
Cl (ml/h)	6.475 ± 1.393	6.013 ± 2.127	6.314 ± 2.238
Vd (ml)	414.013 ± 149.369	307.031 ± 141.381	574.952 ± 82.251
Ke (1/h)	0.266 ± 0.018	0.244 ± 0.170	0.268 ± 0.104

*: significant difference from KP crude extract at P-value = 0.05.

Table 26 Pharmacokinetic parameters of PMF after oral administration of KP crude extract, KP-HP-β-CD complex, and S-3-80

PK parameters	KP crude extract	KP-HP-β-CD complex	S-3-80
AUC (h*ug/ml)	2.508 ± 0.639	49.692 ± 3.621*	57.311 ± 11.907*
Dose (mg)	1.465 ± 0.176	1.036 ± 0.150	1.389 ± 0.216
$t_{1/2}$ (h)	4.858 ± 1.578	4.766 ± 0.271	3.069 ± 0.412
Cl (ml/h)	434.264 ± 100.486	346.971 ± 37.052	604.166 ± 174.213
Tmax (h)	1.659 ± 0.185	1.571 ± 0.579	1.072 ± 0.173
Cmax (ug/ml)	1.763 ± 0.717	13.210 ± 4.228*	18.825 ± 2.896*
Vd (ml)	5873.587 ± 318.158	1537.231 ± 148.738*	3590.354 ± 1814.606*
Ke (1/h)	0.147 ± 0.023	0.155 ± 0.009	0.234 ± 0.030*
F (%)	2.97	64.25	75.38

*: significant difference from KP crude extract at P-value = 0.05, F: oral bioavailability.

Table 27 Pharmacokinetic parameters of TMF after oral administration of KP crude extract, KP-HP-β-CD complex, and S-3-80

PK parameters	KP crude extract	KP-HP-β-CD complex	S-3-80
AUC (h*ug/ml)	6.920 ± 1.932	117.223 ± 24.765*	228.182 ± 27.139*
Dose (mg)	2.470 ± 0.284	0.973 ± 0.132	2.319 ± 0.103
$t_{1/2}$ (h)	4.739 ± 0.443	4.359 ± 0.372	3.165 ± 0.748*
Cl (ml/h)	482.365 ± 97.887	358.507 ± 104.017	389.768 ± 25.694
Tmax (h)	1.038 ± 0.130	0.907 ± 0.068	1.338 ± 0.101*
Cmax (ug/ml)	1.376 ± 0.397	17.010 ± 5.429*	11.981 ± 2.993*
Vd (ml)	2803.527 ± 657.611	2204.555 ± 326.751	2699.903 ± 1385.795
Ke (1/h)	0.148 ± 0.007	0.175 ± 0.010	0.203 ± 0.070
F (%)	1.84	62.92	77.28

*: significant difference from KPcrude extract at P-value = 0.05, F: oral bioavailability.

Table 28 Pharmacokinetic parameters of DMF after oral administration of KP crude extract, KP-HP-β-CD complex, and S-3-80

PK parameters	**KP crude extract**	**KP-HP-β-CD complex**	**S-3-80**
AUC (h*ug/ml)	5.858 ± 1.402	114.064 ± 10.441*	208.815 ± 34.275*
Dose (mg)	1.068 ± 0.046	0.688 ± 0.024	1.141 ± 0.040
$t_{1/2}$ (h)	5.573 ± 0.808	4.521 ± 0.803	3.271 ± 0.487*
Cl (ml/h)	330.327 ± 51.928	350.944 ± 59.900	381.079 ± 40.758
Tmax (h)	0.790 ± 0.067	0.693 ± 0.135	0.833 ± 0.088
Cmax (ug/ml)	1.603 ± 0.297	15.075 ± 2.755*	15.791 ± 3.645*
Vd (ml)	3974.393 ± 1842.232	459.554 ± 102.165	3512.476 ± 1202.165
Ke (1/h)	0.132 ± 0.025	0.150 ± 0.046	0.199 ± 0.057
F (%)	2.79	63.88	72.56

*: significant difference from KP crude extract at P-value = 0.05, F: oral bioavailability.